ISSN: 2164-3164 Volume 4, Number 4, December 2014

Scientific Research

Open Journal of Civil Engineering

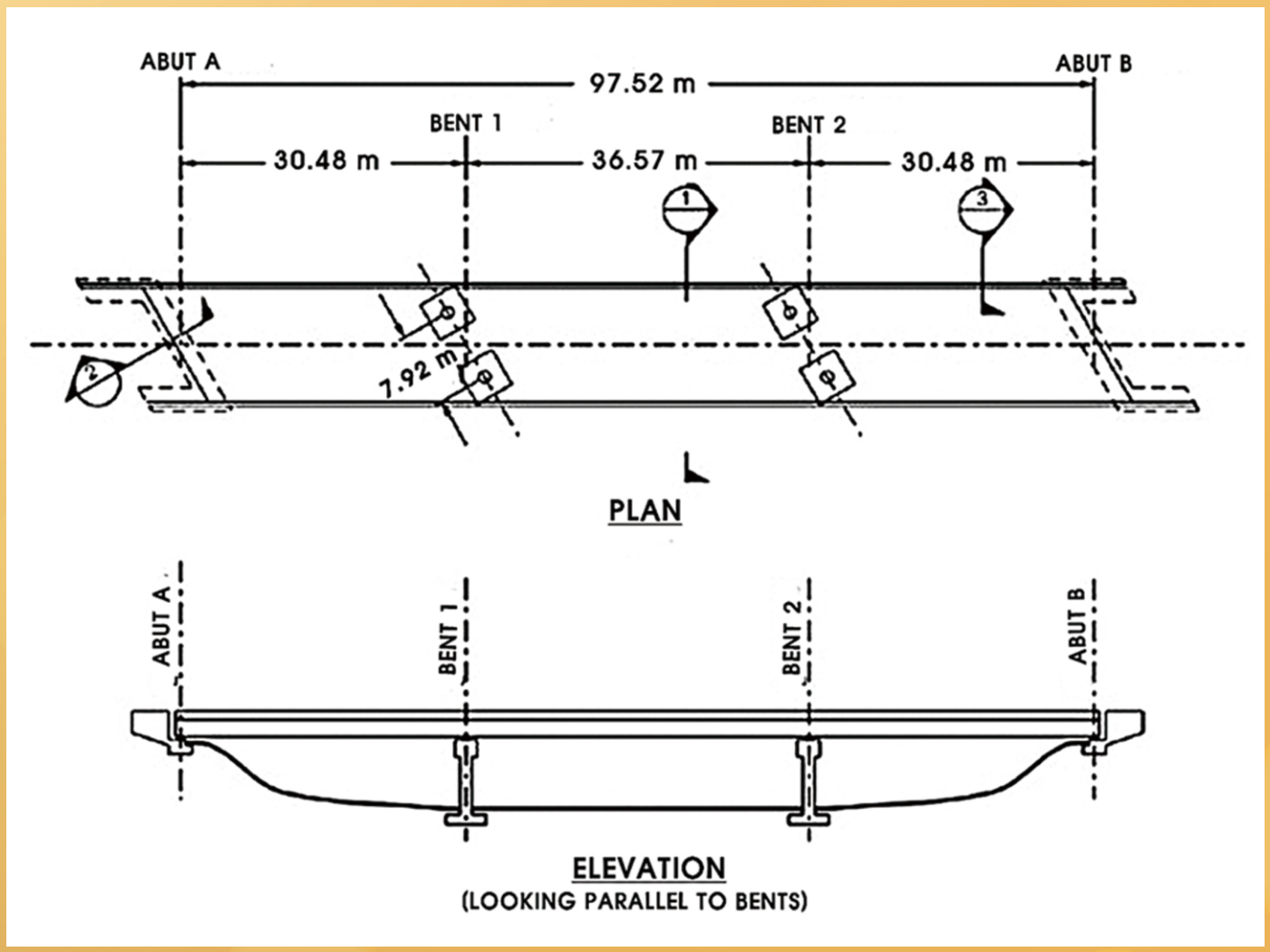

ISSN: 2164-3164

www.scirp.org/journal/ojce

Journal Editorial Board

ISSN Print: 2164-3164 ISSN Online: 2164-3172

http://www.scirp.org/journal/ojce/

Editor-in-Chief

Editorial Board

Guest Reviewers

Open Journal of Civil Engineering, 2014, 4, 301-405
Published Online December 2014 in SciRes. http://www.scirp.org/journal/ojce

Table of Contents

Volume 4 Number 4 December 2014

The figure on the front cover is from the article published in Open Journal of Civil Engineering, 2014, Vol. 4, No. 4, pp. 361-372 by Woo-Suk Kim, Dong-Joon Ahn and Jong-Kook Lee.

Open Journal of Civil Engineering (OJCE)

Journal Information

SUBSCRIPTIONS

The *Open Journal of Civil Engineering* (Online at Scientific Research Publishing, www.SciRP.org) is published quarterly by Scientific Research Publishing, Inc., USA.

Subscription rates:

Print: $79 per issue.
To subscribe, please contact Journals Subscriptions Department, E-mail: sub@scirp.org

SERVICES

Advertisements
Advertisement Sales Department, E-mail: service@scirp.org

Reprints (minimum quantity 100 copies)
Reprints Co-ordinator, Scientific Research Publishing, Inc., USA.
E-mail: sub@scirp.org

COPYRIGHT

PRODUCTION INFORMATION

For manuscripts that have been accepted for publication, please contact:
E-mail: ojce@scirp.org

Open Journal of Civil Engineering, 2014, 4, 301-310
Published Online December 2014 in SciRes. http://www.scirp.org/journal/ojce
http://dx.doi.org/10.4236/ojce.2014.44025

Indicators Benchmarking of Cement-Based Construction Technologies: Brazilian Case Study

Alberto Casado Lordsleem Júnior, Bárbara Eloá Gonçalves de Lima

Department of Civil Engineering, Polytechnic School of Pernambuco University, Recife, Brazil
Email: acasado@poli.br

Received 24 September 2014; revised 15 October 2014; accepted 1 November 2014

Abstract

The adoption of performance indicators promotes knowledge of quantitative and qualitative material wastes in businesses and, when inserted in a collaborative process, provides a comparative evaluation of results between companies and, thereafter, an identification of best practices (benchmarking). The purpose of this paper is to present the best practices identified by performance indicators, related to the measurement of wastes and associated to construction companies participation in the benchmarking research process "Implementation of a system of performance indicators of cement-based construction technologies of the Community of Construction of Recife city in Brazil-PROGRIDE", coordinated by the Brazilian Association of Portland Cement-ABCP. Therefore, it was sought to characterize best practices that led to the benchmarking of performance indicators related to the wastes of concrete, industrialized mortar for masonry settling and blocks/bricks. As a contribution, a set of factors that characterize the best practices for each technology and conducted to benchmarking were identified.

Keywords

Indicators, Concrete, Masonry, Construction, Technologies

1. Introduction

The Brazilian construction industry has experienced a moment of elevated growth and the existing competitiveness confirms the need for changes, according to Pinho [1], since it has generated concerns such as: meeting the deadlines for the delivery of constructions and the inability to fulfill the costs in the determined budget. In order to execute more agile services to have a better cost efficiency, adjustments are necessary so that the building

How to cite this paper: Lordsleem Jr., A.C. and de Lima, B.E.G. (2014) Indicators Benchmarking of Cement-Based Construction Technologies: Brazilian Case Study. *Open Journal of Civil Engineering*, **4**, 301-310.
http://dx.doi.org/10.4236/ojce.2014.44025

materials are used more efficiently.

Still, construction companies have to live with the criticism of belonging to a sector wasteful of resources [2]. In particular, the waste of materials at construction sites is something always discussed in the technical scope, demonstrating the need for frequent changes and to seek new perspectives to improve the production process of construction works.

Aiming to better manage the production process and reduce the waste of materials, construction companies have adhered to the performance measurement through indicators. Since this is a relatively recent practice, it has received impulse through the implementation and certification of quality management systems in construction companies [3].

The adoption of performance indicators promotes knowledge of corporate performance and when inserted in a collaborative process, it offers a comparative evaluation of results between construction companies and identification of the best practices [4].

Benchmarking is the name given to comparative evaluation for the search for the best practices in the industry that lead to superior performance. It is seen as a positive and proactive process through which the company examines how the other one performs a function in order to improve the same or a similar function [5].

Within this context, the importance of monitoring performance indicators within the construction site was registered, as a tool for monitoring production processes and thus, serves as a tool for continuous improvement.

This research aimed to identify the best practices verified by the performance indicators associated with the cement-based construction technologies from construction companies participating in a benchmarking experience. The reference was the program conducted with the participation of twelve construction companies located in the city of Recife, in Brazil, participants in the process of benchmarking of the research "Implementation of a system of performance indicators of cement-based construction technologies of the Community of Construction in Recife city in Brazil-PROGRIDE" coordinated by the Brazilian Association of Portland Cement-ABCP and conducted by the POLITECH research group of the Polytechnic School of Pernambuco University. Therefore, three operational elements (spreadsheets) were developed to conduct the research to characterize the factors that culminated in acquiring the benchmarking of performance indicators, namely: waste of concrete, waste of industrialized mortar for masonry settlement and waste of blocks/bricks. It was aimed to identify the practices that led companies that presented the best results to overcome in a specific indicator.

The factors identified in the research for each indicator will be presented and discussed as follows, since the methodology until the conception of the company's practices that obtained the benchmarking.

2. Methodology

The research consisted of a descriptive research, whose purpose includes literature review and case study. The descriptive facts are observed, recorded, analyzed and interpreted, without interference from the researchers. Standardized techniques for collecting data from operational element (spreadsheets questionnaires) and systematic observation were used.

The research was developed in the course of a year and was divided into four stages.

Stage 01: Definition of potential features relevant to obtain performance benchmarking. Accomplishment of literature review regarding the subject (standards, thesis and papers), as well as the study of PROGRIDE.

Stage 02: Development of the operational element under the form of spreadsheets and definition of participant companies in research.

Stage 03: Field research with the investigation of relevant factors and follow-up through the operational element.

Stage 04: Identification of relevant features and characterization of best practices with its detailed description, with the purpose of organizational improvement, providing competitive superiority.

The implantation of PROGRIDE contemplated three collection cycles, where construction companies involved in the program were able to collect monthly data on indicators of waste of materials and labor productivity of reinforced concrete structure, the elevation of the sealing masonry and plaster coating of the facade. Over 150 results were obtained, originated from 15 sites of 12 construction companies.

At this stage of the research, knowledge and definition of potential factors relevant for a company to reach benchmarking were sought. Initially, benchmarkings from PROGRIDE were identified regarding three analyzed indicators: waste of concrete, waste of industrialized settling mortar and waste of blocks/bricks.

2.1. Waste of Concrete

Reinforced concrete can be defined as "the union of plain concrete and a material resistant to traction (involved by concrete) so that both jointly resist the soliciting forces". The elements of the superstructure of reinforced concrete, responsible for resisting these efforts, are basically pillars, slabs and beams. For the production of these elements, services related to molds, assembly and concreting are performed [6].

Some factors can be considered as potential influencers in the waste of concrete, with the possibility of being present both in the preparation of the site to be concreted as well as in the place of the concrete application. The waste of concrete can be influenced mainly by solicitation planning of concrete according to what was originally designed; quantitative control during its delivery; awareness in choosing the transport equipment, in the event of a pump, predict the use of remaining concrete in the pipe and in the pump; geometric control of the structural elements before and during concreting, and the use of good quality molds [1] [7] [8].

2.2. Waste of Mortar for Settling

The mortar for masonry laying is used for the elevation of walls of bricks or blocks. Its main functions are to unite the masonry units in order to form a monolithic element, contributing to the resistance to lateral forces and distribute the loads acting on the wall evenly throughout the resistant area of the blocks.

Waste of mortar for laying, according to Tcpo [8], is mainly influenced by the use of rational tools and equipment for the settlement or transportation of mortar, the adoption of materials/components of good quality and use of the specific design for masonry.

The Tcpo-Table of Composition of Prices for Budgets corresponds to the largest credible database in the Brazilian Civil Construction Industry. Its functionality consists in guiding and referencing the elaboration of budgets of construction and civil works.

Construction companies can gain efficiency in the use of industrialized mortar, performing an analysis on the processes involved, which range from receiving to the application of the material [9].

2.3. Waste of Blocks/Bricks

The blocks or bricks are components used in the construction of sealing masonry, which bonded by mortar joints, form a rigid union that provides division of internal environments and peripheric coverage of a building [10].

The Tcpo [8] reports as influential factors in the waste of blocks/bricks, the use of complementary components for modulation accuracy, the use of tools and rational equipment for the execution of cuts the adoption of good quality materials, the use of pallets for the supply of blocks/bricks and specific utilization for the design of masonry.

3. Development of the Operational Element

Before you begin to format your paper, first write and save the content as a separate text file. Keep your text and graphic files separate until after the text has been formatted and styled. Do not use hard tabs, and limit use of hard returns to only one return at the end of a paragraph. Do not add any kind of pagination anywhere in the paper. Do not number text heads—the template will do that for you.

Finally, complete content and organizational editing before formatting. Please take note of the following items when proofreading spelling and grammar:

For the development of the research and determination of the companies participating in the process of analysis of performance indicators, it was sought to determine between twelve participating companies in the benchmarking process developed by PROGRIDE, those who had the best results.

It is noteworthy that the description of the implementation of PROGRIDE is contemplated in the Master's Degree Dissertation by Pinho [1], whose development will not be treated in this work, except when essential to the understanding of this research.

The responsibility of data collection in PROGRIDE was of the construction companies, which were properly trained for the application of standard methodology in their respective worksites. After the monthly period of collection, the companies forwarded the results to the researchers involved in order to obtain reference values of the benchmarking process. From these values, it was possible to determine the companies that have excelled in the indicators mentioned, and thus seek to identify the practices adopted that resulted in the benchmarkings.

For the identification of the practices adopted, from the reading of the bibliographies (some mentioned previously), benchmark spreadsheets of three indicators that are the aim of the research were prepared: waste of concrete, waste of industrialized mortar for settlement and waste of blocks/bricks and they will be presented with the checklist completed by the construction companies (**Tables 4-6** respectively). The worksheets were developed in the format of checklists, allowing the identification of practices adopted, applied through visits and interviews onsite with those responsible for the companies that generated the benchmarkings.

4. Results and Discussion

4.1. Characterization of Construction Companies and Worksites

For the analysis of the results over the 3 collection cycles of PROGRIDE, characterizations of worksites and companies participating in this study were performed. These characterizations were important for detailment and analysis of benchmarking (**Table 1**).

From **Table 1**, some features of the worksites were verified, such as: supervision staff, ranging from 03 to 06 members; forecast of the duration of the work, varying from 27 to 59 months; number of slabs of the enterprise, ranging from 08 to 22 slabs. Some characteristics are common to the three analyzed, as the type of design, being all residential.

The characterization of the companies participating in the program is presented in **Table 2**.

All participating companies in the program develop activities related to the construction of residential buildings, in addition to performing residential construction, all companies have participated in some type of institutional training program for quality.

Initially, the values were identified through PROGRIDE benchmarking, which also allowed to identify the companies that reached benchmarking in **Table 3**.

The results presented in **Table 3** were collected and managed by PROGRIDE. They represented the best values obtained, being analyzed then, by indicator, in order to identify the conditions that led a determined company to obtain certain results.

Table 1. Characterization of worksites.

	Worksite A	Worksite B	Worksite C
1) Staff (supervision)			
Interns/Foreman/Workers	01/01/-	04/01/05	01/01/-
Engineers	01	01	01
2) Types of companies	Residential	Residential	Residential
3) Pattern of companies	Popular	High	Medium
4) Type of design	Singular	Singular	Pattern
5) Forecast of work duration	27 months	49 months	50 months
6) Technical data			
Number of slabs	08	32	22
Total height of the building (m)	29.40	97.00	60.00
Floor height (m)	3.00	2.95	2.71
7) Typologies			
Structure	Reticulated with ribbed slab and edge beams		Reticulated with solid slab and edge beams
Sealing (block)	Concrete	Ceramic	Ceramic
Internal coating	Mortar/Texture	Ceramic	Ceramic
External coating	Plaster, painting and ceramic	Single mass and ceramic	Single mass and ceramic

Table 2. Characterization of construction companies.

	Construction companies		
	A	B	C
1) Constructed area in the last 5 years (m^2)	45.000	196.189	5247
2) Activities performed by the company in the last 2 years			
Incorporation and construction of residential edifications	X	X	
Residential worksites for private clients			X
Industrial worksites for private clients	X		
Commercial worksites for private clients		X	
Public worksites (social interest housing)		X	
3) Participation in an institutional program (training)			
Agreement with the university	X		
Consulting company	X	X	X
SENAI			X
SEBRAE		X	
SINDUSCON	X	X	X
4) Designs of improvement already developed			
Literacy	X	X	X
ISO 9001/Standardization in processes	X/X	X/X	X/X
Safety at work	X	X	X

Table 3. Benchmarking of construction companies.

Indicators	Benchmarking	Company	Site	Median*	Maximum*
		Concreting-pillar			
Waste of concrete (%)	5.18	A	A	6.66	17.29
		Concreting-Beam + slab + pillar complement			
Waste of concrete (%)	2.00	A	A	4.75	26.61
		Sealing masonry			
Waste of blocks/bricks (%)	0.83	B	B	3.50	15.00
Waste of mortar (%)	12.34**	C	C	114.13	429.29***

*Regarding the group of participating companies from PROGRIDE; **Reference consumption adopted = 20.0 kg/m^2; ***Reference consumption adopted = 6.6 kg/m^2.

4.2. Influential Factors of Benchmarking

4.2.1. Regarding Concrete Waste

Worksite A reached benchmarking in concrete pillar waste of 5.18% and of concrete beam + slab + pillar complement of 2.00%.

The interview was held with the engineer responsible for Worksite A and in it was completed the checklist shown in **Table 4**. The questionnaire was assembled as follows: The factors that may have led the company to achieve benchmarking were presented, being analyzed their existence and frequency at the worksite, besides other factors verified during the interview/visit.

In Worksite A, it was not possible to measure the amount of concrete in the trucks as there was no way to confirm whether the volume of concrete that was provided by concrete supplier was the same as that requested; so a

Table 4. Spreadsheet for the characterization of the concrete waste indicator from Site A.

Factor	Frequency of visualization of the factor at the worksite				
	Always	Often	Sometimes	Seldom	Never
Accurate estimate of the volume of concrete to be used		X			
Equal portions to concrete	X				
Well-structured molds	X				
Existence of control in the amount of concrete received	X				
Big concretings		X			
Pump does not retain concrete	X				
Use of remaining concrete on the transport element		X			
Request of remaining concrete consistent with the progress of concreting		X			
Utilization of tools needed to control the level of concrete	X				
There is no remaining concrete in the molds			X		
Area of regular access	X				
Little vibration of concrete in transportation	X				
The thickness of the slab is not increased	X				
Height of free fall of the concrete is less than 2 meters	X				
Good operating of the elements of concrete transport	X				
Encouragement of workers to minimize wastes					X

guaranteed surplus ranging around 3% to 5% was solicited. This additional amount of concrete that was requested as prevention, in most cases, was used in other concretings.

The last truck, to prevent waste, was requested with only the amount needed for the completion of concreting. On arrival of the truck to the construction site, quality control was always performed, the slump test, avoiding future problems with the consistency of concrete. The request for remaining concrete was always according to the progress of concreting to be held.

For the control and leveling of concrete, metal grids were used, which had bolts welded in its extension, where the bolt threads are adjusted according to the height desired to be controlled. At the end of each concreting, a mapping of the areas was done, identifying where each concrete truck was applied in order to avoid future problems, in case the concrete does not reach the specified resistance.

During the work, there was great concern as to the path where the concrete transporting equipments would go through, the accesses to the construction site were prepared so the waste due to spills were not reported and wheelbarrows were always in good condition. When in slabs and pillars, concreting was performed with the spear, and what was left in the truck, was carried in barrels (maintenance performed weekly), which had access to the place of loading and unloading, and generally covered with woods to avoid waste of concrete.

The remaining concrete on the transport equipment was not wasted, thus it was used in other concretings-beams and sidewalks. The release pumps were adjusted and were maintained so that they commonly did not retain concrete.

In the worksite of Worksite A, the slabs were equal, thus the slab adjustment was made only on the first concreting. On the others, the amount of concrete became standard, so that the volume was previously known, the request was consistent with the amount to be used, avoiding waste.

As for molds, they were very well structured so that no mold burst/opened during construction. Sometimes, there was remaining concrete in the molds, and this concrete in many times, could not be reused in other concretings, being one of the reasons for concrete waste. The thickness of the slab, in no concreting, was higher than that anticipated in the design, which could cause unnecessary waste.

The construction made no kind of incentive to employees so they could reduce wastes. Although, the engineer considered that they could be further reduced if the employees had full awareness of the importance for the total

cost of the work as well as the damage to the environment.

4.2.2. Regarding Waste of Settling Mortar

In Enterprise C, which showed a benchmarking value of 12.34%, the interview was held with the engineer responsible for the quality of the work and in it, the checklist shown in **Table 5** was answered.

As for molds, they were all well structured so that no mold burst/opened during the construction. Sometimes, there was a remainder of concrete in the molds, this concrete for many times could not be reused in other concretings, being this one of the reasons for the waste of concrete. The thickness of the slab, in no concreting, was higher than anticipated in the design, which could cause unnecessary waste.

During the interview and visit to the construction site, were observed factors that led this design to reach the benchmarking in waste of mortar.

Depending on the volume of mortar required by the bricklayer and for the person responsible for the mixture, it was produced by a mixer, ensuring to obtain a higher workability rather than when produced manually. This way, it was perceived that the mortar was settled over the ceramic block gaining more adherence.

For the production of mortar in the mixer, water measuring instruments such as graded buckets were used to ensure that the mortar contained the water quantity indicated by the manufacturer.

In order to ensure that the material could be transported in an easy and practical way, avoiding transport wastes by improper handling, the worksite was always organized, and the way the wheelbarrows would go through were prepared in advance.

There was a concern with the condition and operational quality of the transportation equipment and wheelbarrows. There was also the concern as to the preventive maintenance of hoists and lifts, respecting deadlines previously established by hiring mechanical engineers and specialized technicians.

The storage of mortar sacks was performed properly to avoid the action of humidity over the material. For such, the mortar was stored on pallets (**Figure 1**) and it was aimed to ensure that the warehouse was always ventilated.

The stock keeper controlled the departure of materials with spreadsheets which ensured that the amount of material that would be used was consistent with the planning. He was also responsible for making sure that the oldest sacks were used before the most recent, implying that the mortar was always used within the validity period.

At the worksite of Enterprise C, a design for the production of the masonry sealing was used, specifying the materials and conceiving the construction details such as the modulation of the blocks, causing the mortar to be

Table 5. Spreadsheet for the characterization of the mortar waste indicator from Site C.

Factor	Frequency of visualization of the factor at the worksite				
	Always	Often	Sometimes	Seldom	Never
Accurate estimate of the volume of concrete to be used	X				
Use of specific design for masonry	X				
Good accommodation of mortar in stock, no action of humidity	X				
Use of older sacks before the most recent	X				
Mortar not unloaded on the floor		X			
No over-thickness of the horizontal joints of the masonry		X			
No over width of the vertical joints of the masonry		X			
Use of specific tools for settlement, such as tubes and boards	X				
Transport of mortar by appropriate ways and/or equipment for such	X				
Reutilization of mortar that falls on the floor		X			
It is necessary to settle until the mortar is over	X				
Encouragement of workers to minimize wastes	X				
Good operation of the transport elements mortar	X				

improperly used to fill voids left by the absence of specific block for modulation (fillings increase the consumption of mortar). With the design, the electrical installations were designed to avoid rework and break of blocks that would leave spaces and would be filled with mortar.

The volume of mortar going up to the apartments was always compatible with the amount of blocks that would be settled at that moment, secured by the design for the production of masonry. According to specifications, the vertical and horizontal joints did not exceed one (01) centimeters (cm), avoiding unnecessary use of mortar (**Figure 2**).

The use of specific tools for settling the mortar on the block, such as the trowel is used in the worksite of construction C, and of great importance to minimize wastes. With the trowel, the mortar is spread on the walls of the blocks with horizontal and vertical movements, using only the recommended amount of mortar.

Constantly, bricklayers and helpers received training, ministered both by more experienced employees of the company, as well as engineers and technicians or by institutions and organizations, in order to improve productivity and settlement services. For the employees, it was recommended that they used instantly the mortar that fell on the floor, which remained invariably clean. Moreover, employees were given incentives to minimize the waste of mortar. They functioned so that the amount of mortar that was not wasted, was reversed in financial bonuses to the employees, considering the consumption and the goal set by the company.

Monthly, monitoring was carried out to evaluate wastes and productivity, and the results were presented in tables at the construction site, so that employees could compare and evaluate the progress of the work in respect to quality.

4.2.3. Regarding the Waste of Blocks/Bricks

Construction company B had the best result with the indicator of block/brick waste with a total of 0.83%. **Table 6** presents the results of the responses of the checklist.

Figure 1. Mortar stocked on pallets.

Figure 2. Joints within specifications.

Analyzing **Table 6**, it is also possible to observe which practices adopted by construction company B minimized waste of materials. Construction company B, due to a greater control of wastes, developed a program called "Work in hand", and in this program each bricklayer that was responsible for laying the blocks on the wall had a masonry design next to him. In the program, a system of communication between the floors where it was functioning, the inventory and labor management was developed. Communication was performed using an apparatus located on each floor of the worksite, where three kinds of emitted light signals: green (the service is in progress normally), yellow (service stop risks) and red (the service is stopped) were used.

With this system, based on the Japanese philosophy of Andon and Kanban, there was greater control over the amount of blocks/bricks that were being used and whether the planned amount was consistent with what was being used. If a yellow or red light was lit on the floor in question, it meant that the site needed attention or the adequate procedures should be taken as to the quantity of blocks.

Verifying the existent specific masonry design of the worksite, kits were assembled and arrived at the pavements with the amount of blocks necessary to lay on the respective floor, this way, avoiding remaining blocks. In this worksite, modular blocks (family of blocks with its own compensators) were used, that composed the kits in quantities correspondent to the floor. Still, along with the electrical design, blocks with suitable modulation for the use in the composition of the electrical kit (electrical blocks: openings already undertaken by the manufacturer for the bolting of the electricity boxes) were used.

Moreover, construction company B invested a lot in specialized training for each function performed by the employees, so, for example, when the cut of additional blocks became necessary, it was done by a professional and with the use of tools, such as a diamond disc suitable for such, thus preventing that the block was torn or fractured during the cutting.

The blocks that arrived at the construction site went through quality control and those that were not within specifications were returned to the supplier and the company received other blocks within the quality standard.

The blocks were stored on pallets and separated and classified by type in pens, according to the modulation of the block. They were transported in pallet carts by planned access paths and cemented to prevent it from falling.

5. Conclusion

The growth of the construction industry has increasingly demanded the need to build in an efficient and rational way, to meet the demands of the consumer market in quality and time planned as well as the budgeted cost. The construction and management practices presented by the construction companies in the survey demonstrated to

Table 6. Spreadsheet for the block/brick waste indicator characterization from Site B.

Factor	Frequency of the factor visualization at the worksite				
	Always	Often	Sometimes	Seldom	Never
Blocks/Bricks are not cut for modulation adjustment	X				
Blocks/Bricks of good quality	X				
Blocks/Bricks palletized	X				
Sending of a precise number of blocks/bricks to the work fronts	X				
Existence of a masonry design, the constructive solutions are not improvised	X				
Use of tools and techniques adequate for cutting the block/brick		X			
Factor	**Frequency of visualization of the factor at the worksite**				
	Always	Often	Sometimes	Seldom	Never
Existence of quality control and quantity at the reception of the block/brick	X				
After settling the walls are not sectioned for installations			X		
There is no considerable destruction of blocks/bricks in transportation or execution	X				
Organization of the worksite, facilitating material movement	X				

be consistent with the current context of improvement needed for the development of the construction of buildings. In the search for the rationalization of construction, it was found that it is necessary to control the work processes. Practices to be adopted must necessarily lead to waste minimization, still allowing taking steps to improve the management of materials. Thus, this research aimed to identify the best practices pointed out by the performance indicators, related to the measurement of wastes and associated to cement based constructive technologies of construction companies participating of the benchmarking process. Having the entire theoretical basis for such, operational elements which allowed characterizing the benchmarks obtained by the three companies selected from PROGRIDE were developed. The worksheets subsidized the collection of data at the construction sites and thus, it was possible to characterize and determine which of the main factors caused construction companies to obtain the best values for the indicators. From the results obtained during the research, it was possible to conclude that most of the best practices identified are associated with the design for production, construction site planning, resource management and prior definition of stock and equipment spaces.

References

[1] Pinho, S.A.C. (2013) Desenvolvimento de programa de indicadores de desempenho para tecnologias construtivas à base de cimento: Perdas, consumo e produtividade. Master Dissertation, Pernambuco University, Recife.

[2] Pinto, T.P. (1989) Perdas de materiais em processos construtivos tradicionais. Ph.D. Dissertation, Federal University of São Carlos, São Carlos.

[3] Duarte, C.M.M. (2011) Desenvolvimento de sistema de indicadores para benchmarking em empresas de construção civil. Master Dissertation, University of Pernambuco, Recife.

[4] Lordsleem Jr., A.C., Andrade, F.K.G. and Pinho, S.A.C. (2011) Benchmarking em construtoras: Caracterização das melhores práticas de 04 indicadores de execução de obras. In: *VIII Encontro Tecnológico da Engenharia Civil e Arquitetura—ENTECA*, Maringá, 1-12.

[5] Bakens, W., Viries, O. and Courtney, R. (2005) International Review of Benchmarking in Construction. PSIBOUW, Amsterdã.

[6] Bastos, P.S.S. (2008) Fundamentos do concreto armado. http://wwwp.feb.unesp.br/pbastos/concreto1/FUNDAMENTOS.pdf

[7] Araújo, L.O.C. (2000) Método para a previsão e controle da produtividade da mão de obra na execução de fôrmas, armação, concretagem e alvenaria. Master Dissertation, São Paulo University, São Paulo.

[8] Tcpo (2010) Tabelas de Composição de Preços para Orçamentos. Pini, São Paulo.

[9] Oliveira, F.A.L. (2006) Argamassa industrializada: Vantagens e desvantagens. Civil Engineer Degree Dissertation, Anhembi Morumbi University, São Paulo.

[10] Lordsleem Jr., A.C. (2000) Execução e inspeção de alvenaria racionalizada. Editora O Nome da Rosa, São Paulo.

Open Journal of Civil Engineering, 2014, 4, 311-317
Published Online December 2014 in SciRes. http://www.scirp.org/journal/ojce
http://dx.doi.org/10.4236/ojce.2014.44026

Studies on Strength and Related Properties of Concrete Incorporating Aggregates from Demolished Wastes: Part 1—A Global Perspective

Shodolapo Oluyemi Franklin[1], Mmasetlhomo Tommy Gumede[2]

[1]Department of Civil Engineering, Faculty of Engineering and Technology, University of Botswana, Gaborone, Botswana
[2]Norvels (Pty) Ltd T/A Engineers International, G. West Industrial, Gaborone, Botswana
Email: franklinso@mopipi.ub.bw, tgooms05@yahoo.com

Received 30 September 2014; revised 20 October 2014; accepted 4 November 2014

Abstract

The present study addresses the global concern of sustainability in building and construction engineering and how to an extent the use of demolished aggregate wastes in concrete production contributes towards ameliorating or minimizing the problem. The influence of demolished aggregate waste on the mechanical strength and stiffness of concrete are examined from the standpoint of the compressive, split tensile and flexural strengths as well as the modulus of elasticity of the concrete. In this respect the research carried out by previous investigators are noted. It is observed that in the Southern African region in general and Botswana in particular there is a paucity of studies on the subject, and consequently, it is concluded that further investigations need to be conducted utilizing aggregates derived from local wastes or sources.

Keywords

Sustainability, Demolished Aggregates, Wastes, Concrete, Strength

1. Introduction

Sustainability has been defined as the improvement in the quality of human life while living within the carrying capacity of supporting eco-systems. However, apart from its reference to human well-being, it has also been defined in terms of the global balance of production and consumption. It infers responsible and pro-active decision

How to cite this paper: Franklin, S.O. and Gumede, M.T. (2014) Studies on Strength and Related Properties of Concrete Incorporating Aggregates from Demolished Wastes: Part 1—A Global Perspective. *Open Journal of Civil Engineering*, **4**, 311-317. http://dx.doi.org/10.4236/ojce.2014.44026

making and innovation that significantly reduces any negative impact and maintains the balance between social, environmental and economic growth to ensure a desirable planet earth for all forms of life presently and well into the future (Milne *et al*. [1]). Another closely allied concept and equally fashionable is the term "sustainable development", defined by the Brundtland Commission of the United Nations [2] as the development that fulfills present needs without compromising the ability of future generations to satisfy their own requirements.

Of relevance to the issue of sustainability is the idea of environmental management which attempts to reduce negative human impact and enhance ecosystem delivery. In respect of the earth's raw materials, it is projected that by the year 2050, 140 billion tons of minerals, ores, fossil fuels and biomass per year (three times the present amount) could be consumed unless the economic growth rate is detached or de-coupled from the rate of natural resource consumption (UNEP [3]). As a consequence, dematerialization, or the switch from the linear path of materials (or from extraction to use to ultimate disposal in landfill) to a circular material flow that reuses materials as much as practicable, has been embraced. From a life cycle perspective, it is obvious that the use of sustainable biomaterials obtained through renewable means or recycling offers significant advantages compared to the utilization of non-renewable resources.

The above considerations are of crucial importance in building and civil engineering. In support of this assertion the American Society of Civil Engineers [4] in its Policy Statement 418 entitled "The Role of the Civil Engineer in Sustainable Development" has stressed the leadership role of engineers in sustainable development and the necessity to provide effective and innovative solutions in addressing the problems or challenges of sustainability. The reality of limited natural resources should be recognized and hence the need for sustainable practices involving life cycle analysis and sustainable design approaches cannot be over-estimated. In a similar vein the Royal Academy of Engineering UK [5] in its report "Engineering for Sustainable Development: Guiding Principles" has described sustainable development as the process of development or evolution where the socio-economic and techno-centric concerns are kept within the eco-centric concerns, or the human expectations and aspirations are satisfied by developing skills of engineers and an economic system in a manner that the eco-centric concerns are fulfilled, in other words, in a way that the earth can sustain humanity. It is argued that since it is civil engineers who lead the decision making process about materials usage, energy resources, infrastructure development etc., they must feature prominently and take the lead in sustainable development, constantly proposing available alternatives that satisfy the needs of clients in a sustainable manner.

Building and civil engineering activities such as clearing of land, excavation, construction, remodeling, repair and demolition of such infrastructures like buildings, bridges, roads and other utilities result in solid wastes of which a significant proportion is Construction and Demolition (CD) waste. Most of the latter is used in landfills and include bricks, concrete and other masonry materials, soil mixed with other CD debris, rock, wood, wall covering, plaster, drywall reclaimed asphalt pavement, glass, etc. However continuous industrial development coupled with the ever increasing world population and the consequent reduction in availability of landfill space poses serious problems, not only in respect of availability of natural aggregate for the production of new concrete, but also with reference to CD waste disposal (Chandra [6] [7]). It is obvious that in the conservation of natural resources with respect to the construction sector, the recycling and reuse of CD wastes represent a logical way of solving the afore-mentioned problem (Khalaf and de Venny [8]). With proper planning the amount of waste earmarked or destined for landfills from the construction industry could be minimized, thus helping to conserve scarce natural resources, lowering waste disposal costs and ultimately protecting the environment.

2. Use of Demolished Aggregates

Since they constitute a major portion of total solid waste production in the world, CD waste could be recycled and the resulting aggregates used in everyday concrete production. CD waste is produced when roads, buildings, bridges and other engineering works are demolished or maintained. Recycling is the act of processing the previously used material for use in creating new products, and involves breaking, removing and crushing existing concrete into a material with a specified size and quality. Hence recycled aggregate (RA) is derived from demolition of buildings, bridges, roads, and other civil engineering infrastructures. The concrete manufactured using such aggregates is termed as recycled aggregate concrete (RAC). Ismam and Ismail [9] in reviewing the approach adopted in strategic management for waste management in China and Hong Kong amongst others have noted that recycled aggregate is accepted as a sustainable construction material.

Generally speaking, unprocessed recycled aggregates are used for bulk fill, bank protection, for drainage

structures as base or fill, construction of roads, noise barriers and embankments. The majority of the unprocessed crushed concrete aggregate is sold as 37.5 mm or 50 mm fraction for pavement sub-bases. After contaminants are removed by selective demolition, screening, air separation and size reduction in a crusher to aggregate sizes, the crushed concrete aggregates can be used in new concrete. This RAC is commonly utilized in pavements, curbs and gutters, bridge foundations, structural grade concrete and bituminous concrete, amongst others (Portland Cement Association [10]).

Several investigators have carried out studies on the use of demolished aggregates in concrete. Notable amongst previous researches are the studies of Rao *et al*. [11], Rakshvir and Barai [12], Wagih *et al*. [13], etc. A very comprehensive summary of the various investigations to date on the subject is presented by de Brito and Saikia [14]. However, in the current paper the emphasis is not on usage of RAC, but rather, on the assessment of the influence of demolished aggregates on the mechanical strength and stiffness of concrete, or more particularly, the compressive and flexural strengths as well as the modulus of elasticity of the concrete. The exercise has been executed primarily through a succinct review of the work carried out by past investigators to date on the subject. Some attention has been paid to investigations or findings in the South African sub-continent where there has been less awareness of the need for sustainability management or sustainable development, compared to other technologically more advanced societies.

3. Compressive Strength of Recycled Aggregate Concrete

In their studies in Kharagpur, India on RAC, Rakshvir and Barai [12] found that the properties of the original concrete influenced the mechanical properties of RAC. They noted that the compressive strength of RAC is generally lower than that of conventional concrete made from similar mix proportions. The amount of reduction in strength depended on parameters such as grade of demolished concrete, replacement ratio, water-cement ratio, processing of recycled aggregate, etc. The compressive strength decreased with increasing amounts of recycled aggregates, the variation being in the range 5% - 15%, with the upper limit representing a replacement of natural aggregates by recycled aggregates in the proportion 75% by weight.

Richardson *et al*. [15] reported that ungraded recycled demolition waste resulted in a 54% strength reduction when compared to the control sample. However grading the recycled aggregate and washing out the fine material reduced the strength loss of the recycled demolition waste aggregate concrete to 28% in comparison with the plain control specimen manufactured from virgin aggregates. It was suggested that although this strength reduction was quite significant, it was influenced by the type of recycled aggregate as well as the aggregate condition in terms of shape, porosity and fine material present.

Guan [16] conducted compressive strength tests in Singapore on concrete of three different water-cement ratios 0.57, 0.50 and 0.43. He replaced natural aggregates with Grade 20 recycled concrete aggregate (RCA) in the proportions 25%, 50%, 75% and 100%. He found that all three mixes were able to achieve approximately a minimum of 98% of the natural aggregate concrete strength when replacement percentages were kept below 25%. The cube strength reduced with an increasing RCA content.

Ahmad *et al*. [17] investigated the properties of concrete made with North Carolina recycled coarse and fine aggregates. The results showed that concrete strength decreases approximately linearly with increasing percentage of recycled fine aggregate in lieu of natural fine aggregate. The overall strength reduction was relatively insensitive to the age of the concrete as well as the amount of recycled fine aggregate used in the mixture. For concretes with 60% recycled concrete aggregate and older than 14 days, the decrease in compressive strength for the mixtures with 100% recycled fines was approximately 25% to 30% of the mixtures with all natural fine aggregates.

The results of a study conducted on behalf of RILEM by Hansen [18] revealed that the compressive strength of RAC was between 14% and 32% lower than that of conventional concrete. Furthermore RAC consisting of coarse recycled aggregate and natural sand but possessing the same compressive strength as comparable conventional concrete made with natural aggregate for similar water-cement ratios could be produced. It was argued that the compressive strength of recycled aggregates is governed by the strength of the original concrete and is largely dependent on the combination of the water-cement ratios of the original and the recycled concrete where all other factors are basically identical. For situations where the water-cement ratio of the original concrete is the same or lower than that of the recycled concrete, then the strength of the latter can be equivalent or exceed that of the original concrete.

4. Splitting Tensile and Flexural Strengths

The average splitting tensile and flexural strengths of RAC are lower than that for natural aggregate concrete. Their reduction ranges from 5% to 12% for splitting tensile strengths, and 4% to 15% for flexural strengths, according to Singh and Sharma [19]. A study by Kumutha and Javai [20] indicated that for recycled aggregates obtained from crushed concrete, as the percentage of recycled aggregates increased from 20% to 80%, the reduction in splitting tensile strength was in the range 5% - 31%. The corresponding reduction for flexural strength was 20% - 47%.

Ahmad *et al*. [17] observed a linear decrease in splitting tensile strengths with increasing percentages of recycled fine aggregates. At 28 days for concrete with 100% recycled fine aggregate, the overall decrease in splitting tensile strength was 18% - 27% in comparison with concrete made 100% natural fine aggregate. The corresponding value in respect of flexural strength was 15% - 20%.

Hansen [18] indicated that the flexural strength of recycled concrete is approximately 12.5% - 20% of the compressive strength. These values are comparable to that for conventional concrete. Notwithstanding, Rakshvir and Barai [12] found that both the splitting tensile and flexural strengths of recycled gravel aggregate concrete were up to 10% lower than the natural aggregate concrete for the range 0% - 50% replacement.

Katz [21] has noted that the ratios of flexural and splitting tensile strengths to the compressive strength were in the ranges of 16% - 23% and 9% - 13%, respectively for recycled ordinary Portland cement and white Portland cement concretes taken together. He opined that these values are relatively high in comparison with the recommendations of ACI 363R for the recycled ordinary Portland cement concrete in particular.

A study by Rao [22] suggests a reduction in strength of 15% - 20% in relation to natural concrete for 100% replacement. In another investigation where high strength and high performance concretes were of primary interest, it was noted that the tensile strengths of recycled aggregate and natural aggregate concretes differed by less than 10% (Ajdukiewicz and Kliszczewicz [23]).

Guan [16] reported that there is about 25% - 30% decrease in tensile strength for concrete made with recycled aggregate produced from 30 MPa concrete or recycled coarse aggregate obtained by crushing concrete from unknown sources such as a dump site.

5. Modulus of Elasticity

Singh and Sharma [19] found that the static modulus of elasticity for the recycled aggregate concrete is lower than that of natural aggregate by a maximum margin of 15%. They suggest that this was on account of the higher proportion of hardened cement paste in the RAC. Ahmad *et al*. [17] reported that all the concrete made with 60% RCA showed an overall decrease in modulus of elasticity as the percentage of recycled fine aggregate was increased. However, similar to the case of compressive strength, such reductions were sensitive to the age of the concrete. It was concluded that for concrete with 60% RCA the decrease in elastic modulus for mixtures with 100% recycled fines was approximately 28% - 40% of that for mixtures with 100% natural fine aggregates. According to Hansen [18] due to the large amount of old mortar with a relatively low modulus of elasticity which adheres to original aggregate particles in recycled aggregates, the modulus of elasticity of RAC should be expected to be lower than that of the reference concrete made with natural aggregates.

Rao *et al*. [11] have pointed out that the modulus of elasticity for RAC has been found by several investigators to be in the range 50% - 70% of conventional concrete. However the value is dependent on the water-cement ratio and the replacement proportion of recycled aggregate. Guan [16] has noted that the modulus of elasticity of both parent and recycled aggregate concretes is related to the compressive strength; for a given strength of concrete, the modulus of elasticity of RAC is lower than that for the parent concrete.

6. General Discussion

Although researchers have reported a reduction in strength of recycled aggregate when compared to conventional concrete, it appears that the extent of the reduction is dependent on factors such as the type of concrete used for obtaining the recycled aggregate whether high, medium or low strength, the replacement ratio, water-cement ratio and the moisture condition of the recycled aggregate (Rao *et al*. [11]). It is also noted that the strength of RAC and reference concrete may be comparable even at 100% replacement, provided that the water-cement ratio is not higher than 0.55. However, as the water-cement ratio is reduced to 0.40, the strength of RAC may generally be no more than 75% of the reference mix. Kumutha and Vijai [20] have noted that concrete specimens

with greater replacement proportion of recycled aggregate have lower compressive strength when compared to concrete samples with less recycled aggregates. This was the case whether crushed concrete or crushed brick was used to produce the recycled coarse aggregate. Tempest *et al*. [24] have concluded that structural compressive strength can be developed in concretes incorporating up to 100% recycled aggregate using standard mixing procedures and economical mix designs.

In a similar manner to compressive strength, the splitting tensile and flexural strengths of RAC have been found to be generally lower than that for reference concrete. At 28 days, as the percentage of recycled aggregate fell in the range 80% - 100%, the reduction in splitting tensile or flexural strengths appeared to be in excess of 20% in most cases. On average it is noted that the ratio of flexural strength to compressive strength for RAC was 15% - 22% while the corresponding value for splitting tensile strength was about 9% - 13%. The flexural strength ratios are comparable to that of conventional concrete according to Hansen [18]. However, when viewed in relation to the ACI 363R recommendations for recycled ordinary Portland cement concrete, these values are relatively high.

In respect of modulus of elasticity, all investigations indicate that concretes with natural coarse aggregates have the highest values while concretes with 100% recycled aggregates have the lowest modulus of elasticity. Reductions of the order of 40% have been noted in several instances. This reduction is attributed to the large proportion of old mortar with a comparatively low modulus of elasticity adhering to the original aggregate particles in recycled concrete (Hansen [18]).

It has not been possible to find investigations in the literature of a similar manner reported herein with reference to the Southern African region. Most of the investigations appear to be in respect of waste management practices. For instance Macozoma [25] reported that in South Africa there are over 1 million tonnes of building rubble reaching landfill sites every year throughout the country with the construction industry generating about 5 to 8 million tonnes of waste yearly. However, the recycling of rubble is limited to single operations in Western Cape, Kwa-Zulu Natal and Gauteng. In addition he noted that there is much CD material waste reuse for aspects such as landfills and informal housing. Nevertheless a lot of these applications are for low-level usage. In respect of Botswana, Kgosiesele and Zhaohui [26] report that there is no national database on quality of waste generated. Furthermore they assert that there is insufficient waste management; the wastes from construction and demolition are not recycled, but rather a high proportion is illegally dumped in the outskirts of cities and towns. Bolaane [27] has observed that although the benefits of recycling are known in Botswana, the attitude of local government personnel is not to embrace waste management developments like recycling. Rather, conventional waste collection and disposal is favoured while recycling is left to private sector initiatives. Hence it can be safely concluded that apart from CD waste management procedures and practices, little or no investigation on strength or related properties of concrete incorporating aggregates from demolished wastes has been carried out in the Southern African sub-continent.

7. Conclusion

The present work, albeit a comprehensive review, represents a preliminary portion of an on-going investigation by the authors on the assessment of the strength of concrete incorporating aggregates from demolished wastes. The investigation is expected to include experimental studies involving demolished concrete wastes collected from some major dump sites in Gaborone the capital city of Botswana. From the study carried out herein, a number of conclusions may be drawn. It is obvious that structural compressive strengths may be developed in concretes incorporating up to 100% recycled aggregates based on standard mix design procedures. We note also that the compressive, split tensile and flexural strengths, as well as the modulus of elasticity of recycled aggregate concretes, are generally lower than that of conventional concretes made entirely from natural aggregates. The reduction in strength is dependent on several factors such as the type of concrete used in obtaining the recycled aggregates, the replacement ratio, the water-cement ratio and the moisture condition of the recycled aggregates. Additionally we observe that in the Southern African sub-continent including Botswana, apart from investigations on construction waste management practices, there has been practically no study to the best of the authors' knowledge on the relative strength of concrete incorporating aggregates from demolished wastes.

References

[1] Milne, M.J., Kearins, K. and Walton, S. (2006) Creating Adventures in Wonderland: The Journey Metaphor and Envi-

ronmental Sustainability. *Organization*, **13**, 801-839. http://dx.doi.org/10.1177/1350508406068506

[2] United Nations General Assembly (1987) Report of the Working Commission on Environment and Development: Our Common Future. Transmitted to the General Assembly as an Annex to Document A/42/427—Development and International Co-Operation: Environment, Our Common Future, Chapter 2. http://en.wikipedia.org/wiki/Sustainability

[3] UNEP (2011) De-Coupling Natural Resource Use and Environmental Impacts from Economic Growth. Report of the Working Group on De-Coupling to the International Resource Panel, United Nations Environment Programme, Nairobi.

[4] American Society of Civil Engineers (2013) Policy Statement 418—The Role of the Civil Engineer in Sustainable Development. Adopted by the Board of Direction on October 8, 2013. http://www.asce.org/Public-Policies-and-Priorities/Public-Policy-Statements/Policy-Statement-418---The-Role-of-the-Civil-Engineer-in-Sustainable-Development/

[5] The Royal Academy of Engineering (2005) Engineering for Sustainable Development: Guiding Principles. The Royal Academy of Engineering, London.

[6] Chandra, S. (2004) Implications of Using Recycled Construction and Demolition Waste as Aggregate in Concrete. Session Lead Paper. *Proceedings of the International Conference on Sustainable Waste Management and Recycling*, Kingston University, London, 14-15 September 2004. In: Limbachiya, M.C. and Roberts, J.J., Eds., *Sustainable Waste Management and Recycling*: *Challenges and Opportunities. Volume* 2—*Construction Demolition Waste*, Thomas Telford Publishing, London, 105-114.

[7] Chandra, S. (2005) Conference Report. *Cement and Concrete Composites*, **27**, 738-741. http://dx.doi.org/10.1016/j.cemconcomp.2005.01.001

[8] Khalaf, F.M. and DeVenny, A.S. (2004) Recycling of Demolished Masonry Rubble as Coarse Aggregate in Concrete: Review. *ASCE Journal of Materials in Civil Engineering*, **16**, 331-340. http://dx.doi.org/10.1061/(ASCE)0899-1561(2004)16:4(331)

[9] Ismam, J.N. and Ismail, Z. (2014) Sustainable Construction Waste Management Strategic Implementation Model. *WSEAS Transactions on Environment and Development*, **10**, 48-59.

[10] Portland Cement Association (2011) Recycled Aggregates. Materials Concrete Technology. http://cement.org/tech/index.asp

[11] Rao, A., Jha, K.N. and Misra, S. (2007) Use of Aggregates from Recycled Construction and Demolition Waste Concrete. *Resources, Conservation and Recycling*, **50**, 71-81. http://dx.doi.org/10.1016/j.resconrec.2006.05.010

[12] Rakshvir, M. and Barai, S.V. (2006) Studies on Recycled Aggregate-Based Concrete. *Waste Management & Research*, **24**, 225-233. http://dx.doi.org/10.1177/0734242X06064820

[13] Wagih, A.M., El-Karmoty, H.Z., Ebid, M. and Okba, S.H. (2012) Recycled Construction and Demolition Waste as Aggregate for Structural Concrete. *HBRC Journal*, **9**, 193-200. http://dx.doi.org/10.1016/j.hbrcj.2013.08.007

[14] De Brito, J. and Saikia, N. (2013) Recycled Aggregate in Concrete: Use of Industrial, Construction and Demolition Waste. Green Energy and Technology, Springer-Verlag, London. http://dx.doi.org/10.1007/978-1-4471-4540-0

[15] Richardson, A., Allain, P. and Veuille, M. (2010) Concrete with Crushed, Graded and Washed Recycled Construction Demolition Waste as a Coarse Aggregate Replacement. *Structural Survey*, **28**, 142-148. http://dx.doi.org/10.1108/02630801011044244

[16] Guan, J.L.L. (2011) Effects of Recycled Aggregates on Concrete Properties. Master of Engineering Thesis, National University of Singapore, Singapore.

[17] Ahmad, S.H., Fisher, D.G. and Sackett, K.W. (1996) Properties of Concrete Made with North Carolina Recycled Coarse and Fine Aggregates. Centre for Transportation Engineering Studies, North Carolina State University, Raleigh.

[18] Hansen, T.C. (1992) Recycling of Demolished Concrete and Masonry. Report of Technical Committee 37-DRC Demolition and Reuse of Concrete, RILEM, E & FN Spon, London.

[19] Singh, S.K. and Sharma, P.C. (2007) Use of Recycled Aggregates in Concrete—A Paradigm Shift. *Journal of New Building Materials and Construction World*, **13**, 173-183. http://www.nbmcw.com/articles/concrete/576-

[20] Kumutha, R. and Vijai, K. (2010) Strength of Concrete Incorporating Aggregates Recycled from Demolition Waste. *ARPN Journal of Engineering and Applied Sciences*, **5**, 64-71.

[21] Katz, A. (2003) Properties of Concrete Made with Recycled Aggregate from Partially Hydrated Old Concrete. *Cement and Concrete Research*, **33**, 703-711. http://dx.doi.org/10.1016/S0008-8846(02)01033-5

[22] Rao, A. (2005) Experimental Investigation on Use of Recycled Aggregates in Mortar and Concrete. Thesis Submitted to the Department of Civil Engineering, Indian Institute of Technology Kanpur, Kanpur.

[23] Ajdukiewicz, A. and Kliszczewicz, A. (2002) Influence of Recycled Aggregates on Mechanical Properties of HS/HPC. *Cement and Concrete Composites*, **24**, 269-279. http://dx.doi.org/10.1016/S0958-9465(01)00012-9

[24] Tempest, B., Cavalline, T., Gergely, J. and Weggel, D. (2010) Construction and Demolition Waste Used as Recycled

Aggregates in Concrete: Solutions for Increasing the Marketability of Recycled Aggregate Concrete. *Concrete Suitability Conference*, University of North Carolina, Charlotte, Tempe, 13-15 April 2010, 1-15.

[25] Macozoma, D.S. (2006) Developing a Self-Sustaining Secondary Construction Materials Market in South Africa. Master of Science Dissertation, University of the Witwatersrand, Johannesburg.

[26] Kgosiesele, E. and Zhaohui, L. (2010) An Evaluation of Waste Management in Botswana: Achievements and Challenges. *Journal of American Sciences*, **6**, 144-150.

[27] Bolaane, B. (2006) Constraints to Promoting People Centred Approaches in Recycling. *Habitat International*, **30**, 731-740. http://dx.doi.org/10.1016/j.habitatint.2005.10.002

Open Journal of Civil Engineering, 2014, 4, 318-327
Published Online December 2014 in SciRes. http://www.scirp.org/journal/ojce
http://dx.doi.org/10.4236/ojce.2014.44027

Study on the Style of Urban Development as a Center of Kitakyushu Monorail

—About the User Actual Situation and the Demographic around the Station

Yuanwen Zhang[1], Hiroatsu Fukuda[1], Tianyi Yu[2]

[1]Faculty of Environmental Engineering, University of Kitakyushu, Kitakyushu, Japan
[2]School of Architecture and Fine Art, Dalian University of Technology, Dalian, China
Email: *zhangyuanwen1982@163.com

Received 21 September 2014; revised 18 October 2014; accepted 2 November 2014

Abstract

The ageing of the population in Japan has become a problem. According to the research of different regions, where the ratio of the ageing population is above 25%, it is found that the Japanese society is gradually turned to hyper-aged society. The population along Kitakyushu monorail is also in such a situation. This study is based on the background, with excessive reliance on their own vehicles and public transport problems arising from the abolition of public transportation in Kitakyushu as the area of this study. Under the full consideration of people who can't drive, the elderly who had to take buses as well as people who lack of transport ability where population decrease and the aging problem have been worsening, their surrounding environment should be further improved. In addition, it should be taken into consideration to increase the population in the walking distance around the stations.

Keywords

Monorail, Population, Hyper-Aged Society, Aging Ratios

1. Introduction

Ageing of the population in Japan has become a problem and Kitakyushu is no exception. From the year 1995 (during the year 1995, people over 65 accounts for 15.7% of the population) and in the year 2010, the number revealed an increasing tendency. (Till the September of the year 2010, people aged 65 or above accounts for 19% of the population) According to different regionally statistical data, regions with the ratio of the ageing popula-

How to cite this paper: Zhang, Y.W., Fukuda, H. and Yu, T.Y. (2014) Study on the Style of Urban Development as a Center of Kitakyushu Monorail. *Open Journal of Civil Engineering*, **4**, 318-327. http://dx.doi.org/10.4236/ojce.2014.44027

tion above 25% are gradually turned to hyper-aged society. The population along the Kitakyushu monorail [1] is also in such a situation. As the ratio of working people (from the age 15 to 64 years old) is reduced, the traffic is correspondingly reduced.

This study is based on the background that is people excessively rely on their own vehicles, and much public transportation [2] [3] has been abolished. Kitakyushu, the areas of this study, is facing the same problem. Under the full consideration of people who can't drive, the elderly who had to take buses as well as people who lack of transport ability, we conduct a survey in form of questionnaire investigation on the people who lived and used the monorail. From the questionnaire we can find and solve the problem to enhance the capacity of public transit.

2. Literature Review

Tachikawa Minoru and Nisiura Sadatuqu studied on the influences of public transportation on land and building uses: The case of Tama Monorail Line [4]. In that study, author investigate the land building use of the consideration area for and the change as a case study in the Tama area that assumed Tama Monorail Line of Tokyo an axis in detail and build the result as a database. The authors investigate the terms of reference for a range of distance 500 m from the sation where it is thought that a person uses Tama Monorail Line.

Kohei Matsumoto and Shuichi Murakami studied on re-evaluation of the Abandoned Monorail Structures as Urban Landscape Elements. That paper through a case of the abandoned monorail structures in the city of Himeji [5]. The remaining structures were measured of their height, width, location, and visibility from the streets around the located areas [6] [7]. Owners and uses of the lots accessibility from the surroundings and evidences and traces showing and uses of the structures were also investigated. The result shows the ruins' two sides of potential values, to be seen and to be used, as one of the urban landscape elements.

Junyi Shen *et al*. studied the influence of environmental deterioration and network improvement on transport modal choice [8]. That paper examines how these impacts affect individuals' decisions on selecting transport mode under an extension plan for the Osaka Monorail Loop-line. To estimate these impacts, they perform a Stated Choice experiment for collecting data in the neighborhood along the monorail's extended line. They estimate their model with the Heteroskedastic Extreme Value specification in order to avoid the Independence of Irrelevant Alternatives assumption in the Multinomial Logit model [9]. Both the results of full-sample and subsample data imply that residents prefer public transport modes (monorail or bus) to private cars when either the natural environment becomes worse or the transport network improves.

The difference between the present research and the above-mentioned study is that they were studied the land building use of the consideration area and the re-evaluation of the abandoned monorail structure as urban landscape. Tachikawa Minoru *et al.* investigate the terms of reference for a range of distance 500 m from the station. The present research is based on the long-distance range (500 m) and short-distance range (200 m) with the monorail station as the centre. It investigates the aging problem of the population in the areas surrounding the Kitakyushu monorail and the utilization situation of the monorail.

3. Population Characteristics of People along the Monorail in Kitakyushu

Figure 1 shows the variation trend of public transportation in Kitakyushu. According to the graph, after reaching the climax in the first half of the year in 1965 [10], the number of people taking the public transport has been in a general decline in Kitakyushu. Influenced by the suspension of Kyushu Line of Nishitetsu (streetcar), the number of people taking buses has declined dramatically from 2000 to 2006. The number of people taking JR, monorail and Chikuho rail has also shown a declining trend in recent years. Besides, the number of private cars has increased to a certain extent.

3.1. The Population Predictions along the Monorail in Kitakyushu

Seen from the population structures in the areas along the monorail in 2005 (**Figure 2**), the number of people aged between 30 and 40 was 7400 as the most. From the population distribution in 2010 (**Figure 3**), the number of people between 35 and 39 was 6831, which is also the most. From 2005 to 2010, the population in the surrounding areas along the monorail declined from 86,933 to 86,311, and the ratio of people aged more than 65 increased from 17% to 19%. Since the population change of various age groups from 2005 to 2010 is known,

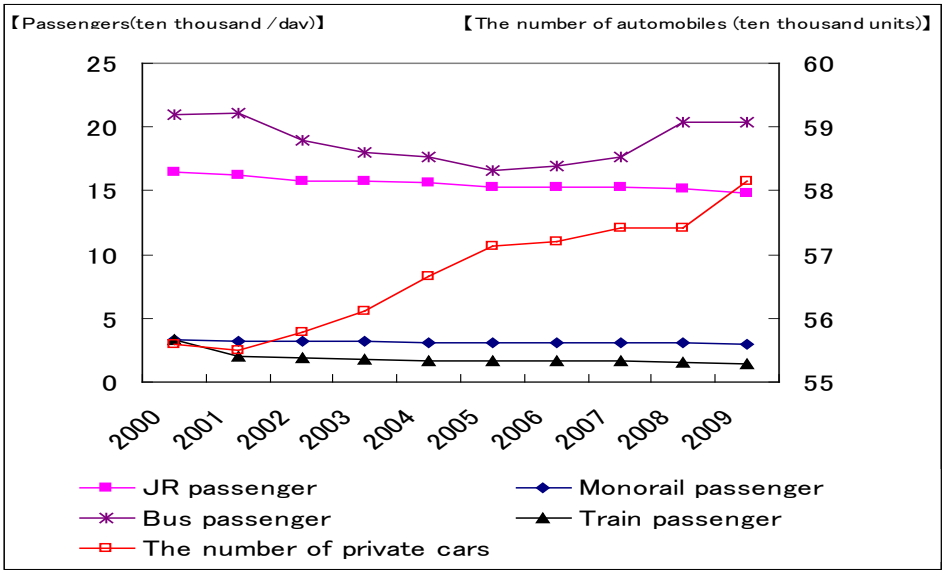

Figure 1. The situation of public transportation in Kitakyushu.

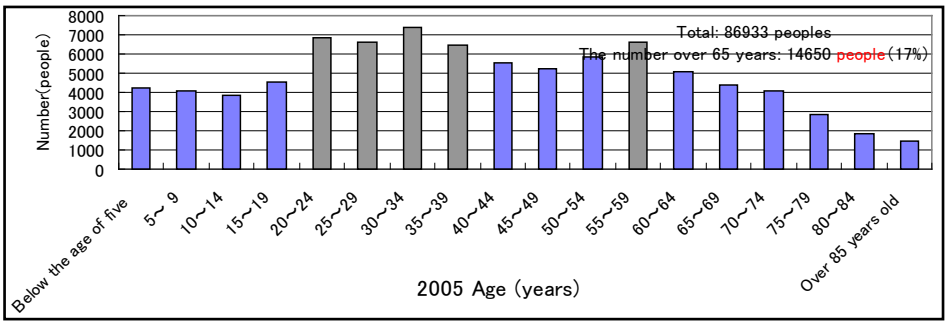

Figure 2. The population structures in 2005.

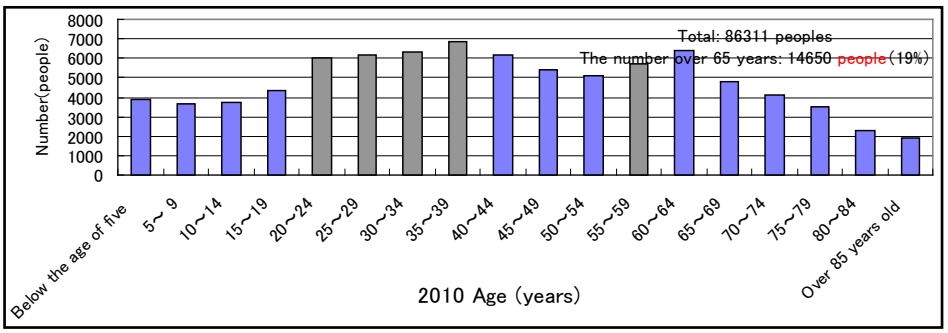

Figure 3. The population structures in 2010.

assuming that the population change from 2010 to 2015 is in the same increase or decrease as that from 2005 to 2010, the population of 2015 (**Figure 4**) and 2020 (**Figure 5**) can be forecasted by analogy.

According to the speculations, from the year 2010 to 2020, the population in the surrounding areas along the monorail will decline from 86,311 to 83,130, and the ratio of people aged more than 65 will increase from 19% to 25%. Then the aging society will come.

3.2. Changes of the Aging Ratios in the Areas along the Monorail

This study is based on the long-distance range (**Figure 6**) (each station as a centre, 500 meters as the radius) and

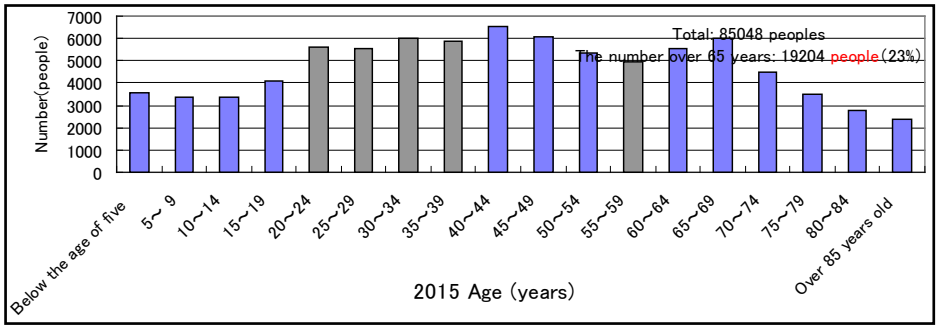

Figure 4. The population structures in 2015.

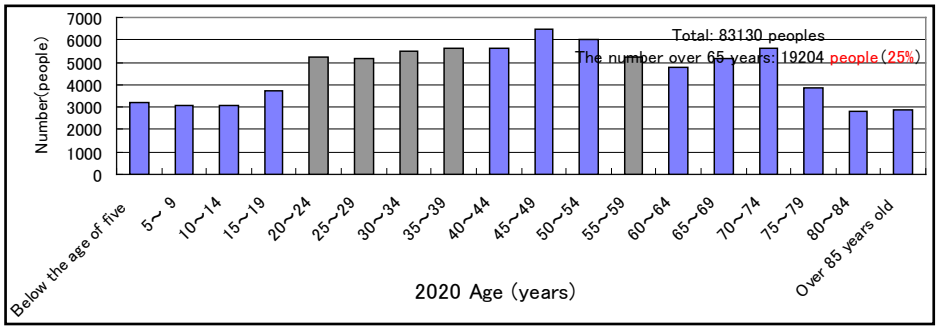

Figure 5. The population structures in 2020.

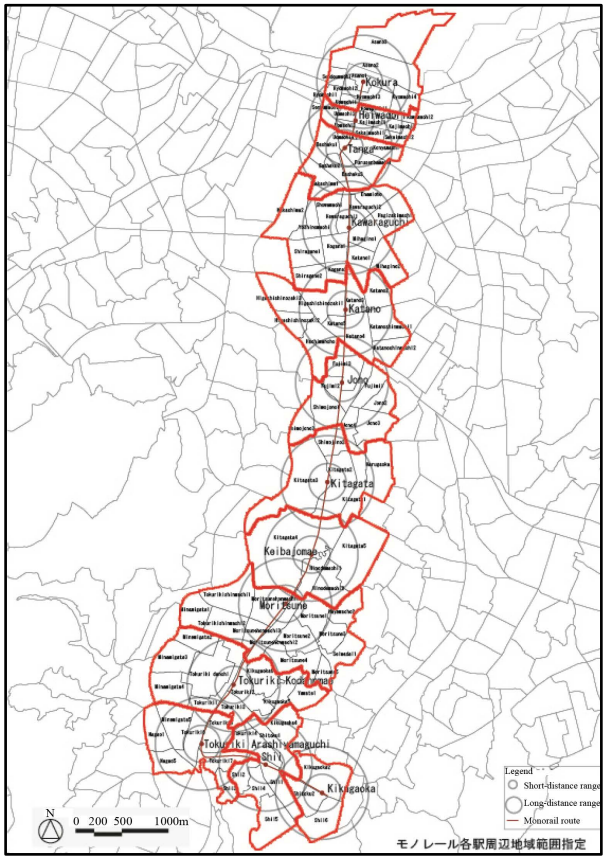

Figure 6. Population density of the areas along the monorail.

short-distance range (each station as a centre, 200 meters as the radius) with the monorail station as the centre. The aging ratio of each station will increase year by year. By 2020, the ratio of the people aged more than 65 of each station will have reached the climax, which will be especially true for the Shii Station and Kawaraguchi Station, with the ratio of 31% and 28% respectively. Besides, the ratio of Katano Station and Tokuriki Kodanmae Station will be reached 27% (**Figure 7**).

3.3. Population Density of the Areas along the Monorail

According to the speculations, the situation of population density [11]-[13] in 2025 is shown as follows. The population density at Kokura Station, Heiwadōri Station and Keibajomae Station will decline. Therein, the population density at Kokura Station will reduce from 25 people/ha in 1995 to 15 people/ha in 2025, the population density at Keibajomae Station will reduce from 24 people/ha in 1995 to 18 people/ha, and at Heiwadōri Station from 30 people/ha in 1995 to 24 people/ha. The population will be in a very low density. In addition, in 2025, the stations with the population density of more than 80 people/ha will be Kawaraguchi Station, Katano Station, Moritsune Station, Tokuriki Kodanmae Station, Tokuriki Arashiyamaguchi Station, Shii Station and Kikugaoka Station. Especially at Kikugaoka Station, its population density will reach 149 people/ha in 2025 (**Figure 8**).

3.4. Numbers of Wholesale Stores in the Areas along the Monorail

Figure 9 shows the number of wholesale stores in the areas along the monorail. As the business centre of Kitakyushu, Kokura has the most wholesale stores. Near Kokura, at Heiwadōri Station, Tanga Station, and Kawaraguchi Station, there are also a lot of such stores. At Kikugaoka Station, the number of wholesale stores is the least. Since there are not many residents at Keibajomae Station, the number of wholesale stores is also small.

3.5. The Annual Sales and the Sales per Unit Area of Stores in the Areas along the Monorail

Figure 10 shows the annual sales and the sales per unit area of stores in the areas along the monorail. In terms of the annual sales, Kokura Station ranks the first, followed by its nearby station, Heiwadōri Station. In terms of the sales per unit area, Heiwadōri Station ranks the top, of 4,568,250,000 yen per ha.

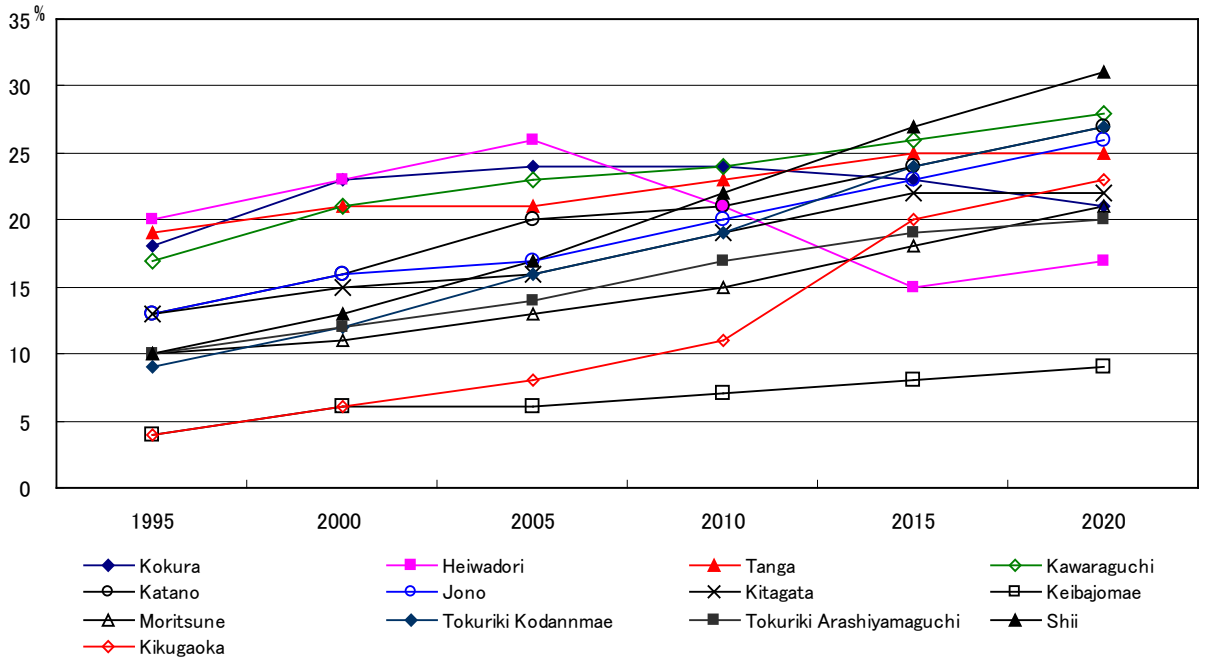

Figure 7. Changes of the aging ratios in the areas along the monorail.

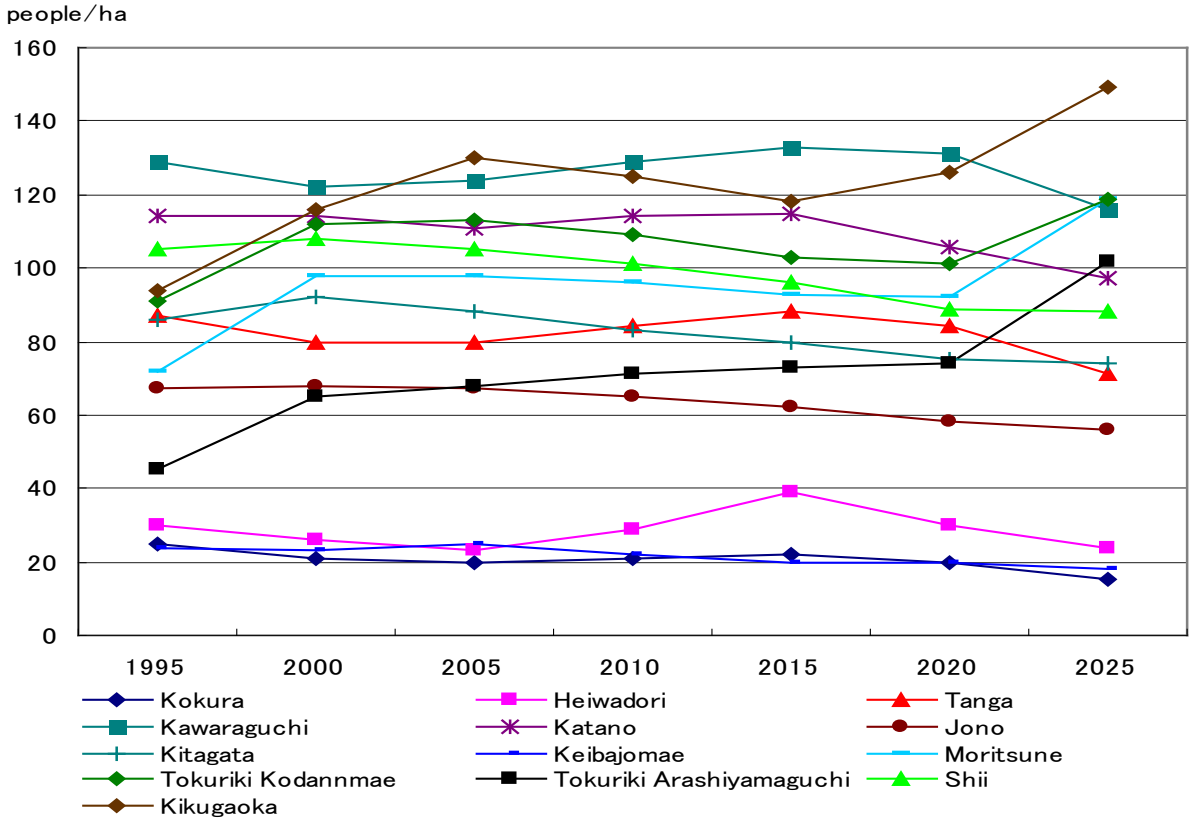

Figure 8. Population density of the areas along the monorail.

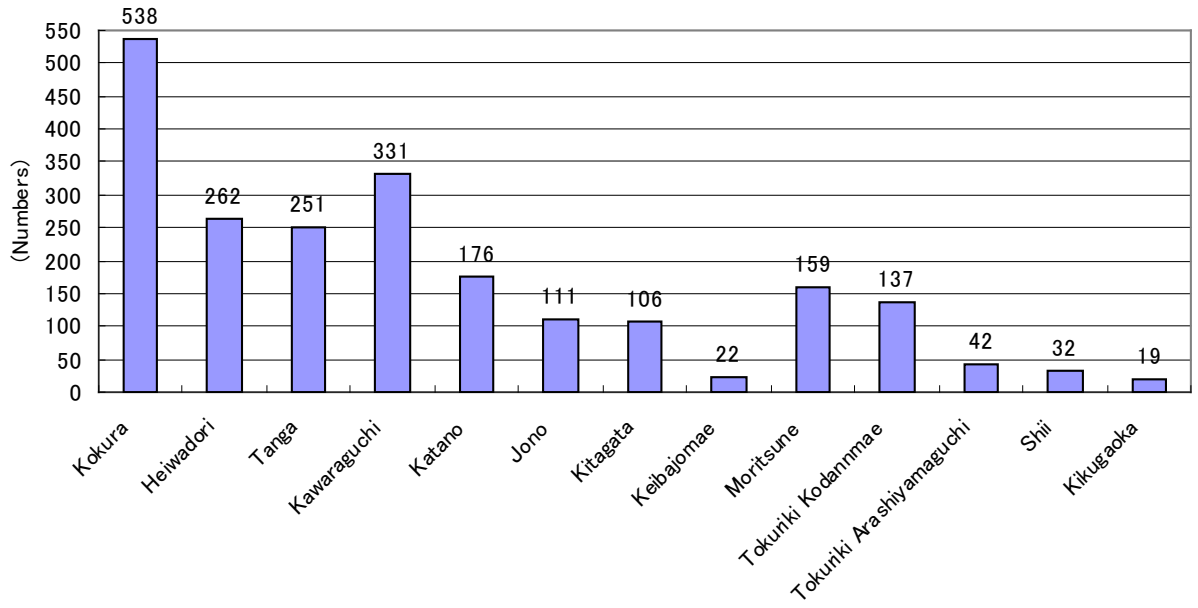

Figure 9. Numbers of wholesale stores in the areas along the monorail.

4. Investigation on the Residents along the Monorail in Kitakyushu and the Analysis of the Questionnaire Results

In order to know the utilizing situation of the monorail by the residents in the surrounding areas and their will of

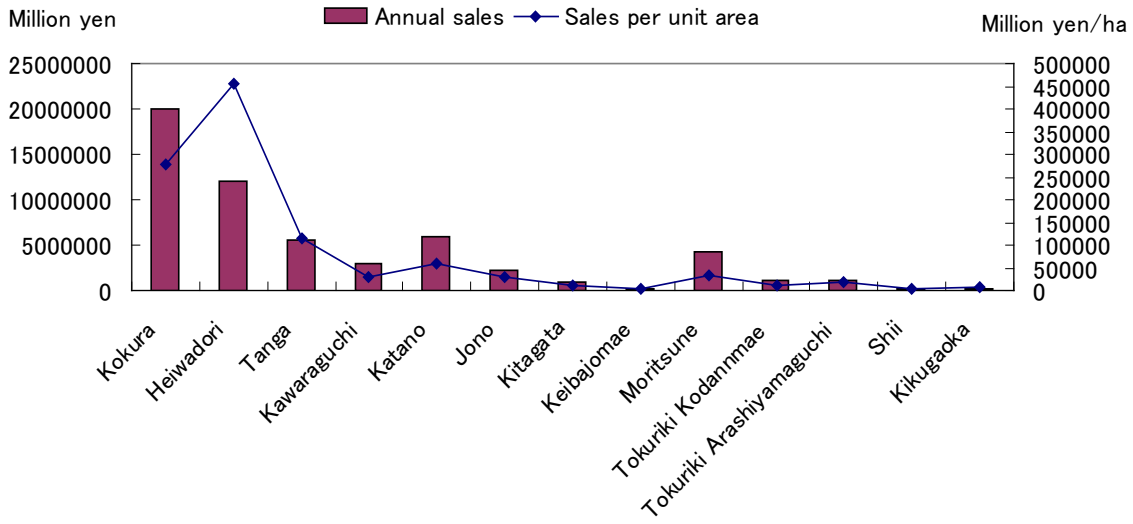

Figure 10. The annual sales and the sales per unit area of stores in the areas along the monorail.

future utilization of the monorail, questionnaire researches were made in 2002 and 2010 to collect the basic data for enlarging the need of the residents along the monorail.

Table 1 is the summary of the research. Subjects of the questionnaire were the males and females aged more than 15 in 2002. In 2010, the subjects were all the users of the monorail. Approaches of delivering the questionnaire, in 2002, it was delivered to the families of residents along the monorail and collected back two weeks later. In 2010, the questionnaires were delivered in each station and collected back at the next station. Collection results: 2867 questionnaires were collected back in 2002 and 6850 questionnaires were collected back in 2010.

4.1. Comparison of the Purpose of the Users of the Monorail

In terms of users' purpose, "commute" accounted for 38.1% in 2010, which was more than twice of 16.3% in 2002. The ratio of "school commutes" in 2010 increased by 10% compared with that in 2002 (6.6% in 2002 and 16.6% in 2010). With regard to shopping as the objective, the ratio in 2010 declined dramatically to 15.1% compared with 37.4% in 2002. The number of private car users increases and people do not have time limitation for using private cars. Therefore the ratio of shopping is in decline. The ratios of "entertainment" and "others" in 2010 reduced by half compared with that in 2002. Besides, the ratios of "business" and "going to the hospital" had no obvious change (**Figure 11**).

4.2. Comparison of the Transportation from Home to Monorail Station

In terms of vehicles taken to the monorail station, "Walking" accounted for 70.1% in 2002 and 59.3% in 2010, with a decrease of about 10%. The ratio of using bicycles in 2010 was almost half of that in 2002 (13% in 2002 and 6.6% in 2010). The ratio of "Shuttle service" was near 6.4% in 2002 and 1% in 2010, which showed a dramatic decrease compared with that in 2002. The ratio of "Private car" increased from 2.3% in 2002 to 3.5% in 2010, with a growth of 1.2%. The ratios of "Bus", "Bicycle" and "Taxi" had almost no change (**Figure 12**).

4.3. Comparison of the Age Groups of Monorail Users

In terms of the age groups of monorail users, the ratio of users aged less than 19 accounted for 6.4% in 2002 and 13.6% in 2010. The ratios of users aged 20, 30, 40 and 50 had almost no obvious change. The ratio of users aged 60 decreased by 3.3% compared with that in 2002. The ratio of users aged more than 70 decreased by 5.2%. When the ratio of users aged 60 is combined with that of users aged more than 70, the total decrease is 8.5%. The increase of private cars led to the result that the ratio of users aged 20, 30, 40 and 50 decreased by 5.6%. When people are more than 65 years old, it will be difficult for them to go out by themselves and the using frequency of public transport in the future will be decreased accordingly. Therefore the shuttle service should be improved to benefit them (**Figure 13**).

Table 1. The summary of the research.

	2002	2010
Subjects	Males and females aged more than 15	All the users
Period	2002/02/02~19	2010/05/20 (From AM8 to PM7)
Method	Visit placement	Distributes on the day and collects
Collection results	2867	6850

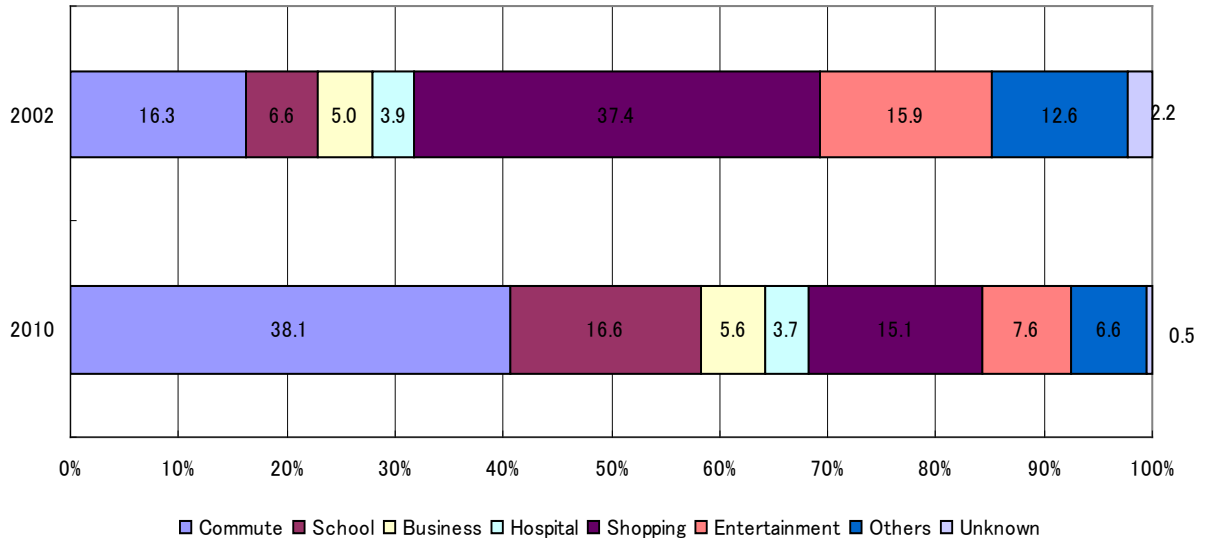

Figure 11. The purpose of the users of the monorail.

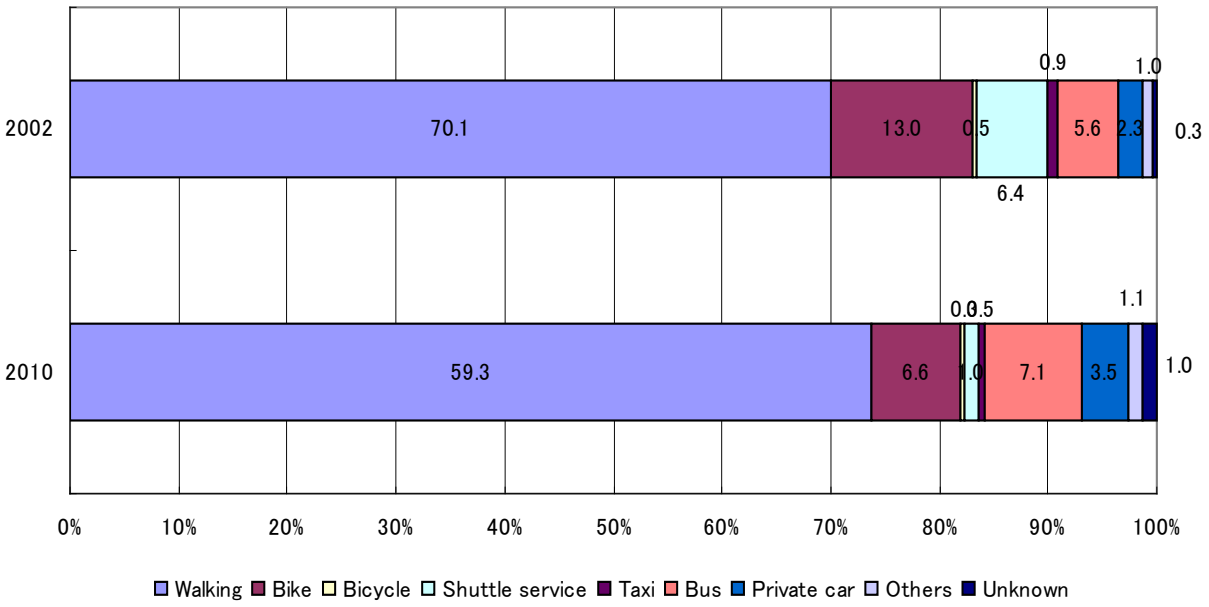

Figure 12. The transportation from home to monorail station.

5. Discussion

5.1. Analysis and Forecast of the Population in the Areas along the Monorail

According to the analysis and speculations of the population in the areas along the monorail, in 2020, the sta-

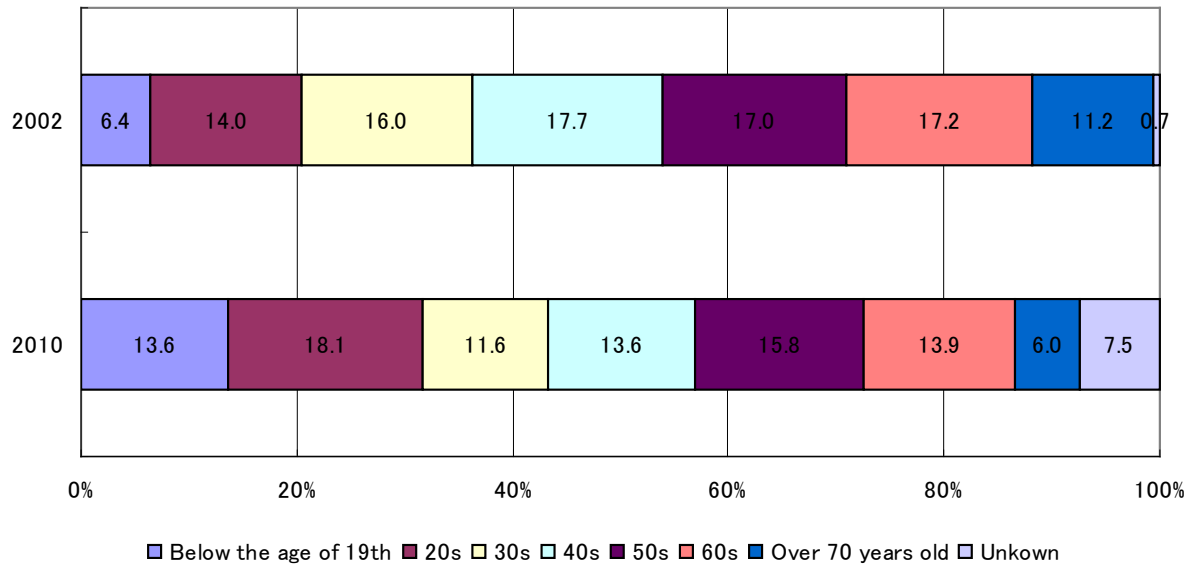

Figure 13. The age groups of monorail users.

tions with the aging ratio of 25% will be Tanga Station, Kawaraguchi Station, Katano Station, Jōno Station, Tokuriki Kodanmae Station and Shii Station. The stations with the reducing population will be Katano Station, Kitagata Station, Keibajomae Station, Moritsune Station, Tokuriki Kodanmae Station and Shii Station. The stations with the aging ratio of more than 25% and the reducing population will be Katano Station, Tokuriki Kodanmae Station and Shii Station. The areas surrounding these stations will enter hyper-aged from nowadays aging society.

5.2. Investigation and Analysis of the Current Use of the Monorail

The research questionnaire showed that the ratio of the monorail users for shopping almost decreased by half, which may be related to the increase of private cars.

In terms of the annual sales of each station, the stations with the most annual sales are Heiwadōri Station, Tanga Station and Katano Station, which are near the Kokura business circle. Shii Station, which is the farthest from the business center, has the least year sales among the total 13 stations. The population reduction will also have influence on the sales of stores surrounding the stations in future.

With regard to the ratios of vehicles taken to the monorail, the ratio of people walking and taking buses and private cars altogether has increased by 11.5%; instead, the ratio of people taking bicycles and shuttle has decreased by 11.8% totally. With the increase of people walking and taking buses, it should be considered to make urban planning and infrastructure construction of public transport [14]-[16] based on the condition of going out on foot.

The ratio of people aged more than 60 in the areas along the line is in decline, while the ratio of the monorail users aged more than 60 has decreased. Since the population has increased, it is necessary to improve the surrounding environment of the aged people, for instance, to offer shuttle service to the monorail station.

6. Conclusions

This study takes the Kitakyushu monorail as the subject. It did research on the current population in the areas surrounding the monorail and made the forecast of their future population. Questionnaires were delivered to investigate the utilization situation of the monorail. The results show that in 2020, the stations with the aging ratio of more than 25% will be Tanga Station, Kawaraguchi Station, Katano Station, Jōno Station, Tokuriki Kodanmae Station and Shii Station. The areas surrounding those stations will enter a super aging society from an aging society. Besides, with the increase of the aging population, thus the number of people who can not take private cars will increase.

Especially for Katano Station, Tokuriki Kodanmae Station and Shii Station, where population decrease and the aging problem have been worsening, their surrounding environment should be further improved. In addition, it should be taken into consideration to increase the population in the walking distance around the stations.

References

[1] Wikipedia. http://en.wikipedia.org/wiki/Kitaky%C5%ABsh%C5%AB_Monorail

[2] Satoh, K. and Lan, L.W. (2007) Development and Deployment of Sustainable Transportation. *Sustainable Transportation*, **5**, 67-69.

[3] Cervero, R. and Golub, A. (2011) Information Public Transport: A Global Perspective. Urban Transport in the Developing World.

[4] Sadatuqu, T.M.N. and Toshio, K. (2010) Study on the Influences of Public Transportation on Land and Building Use: The Case of Tama Monorail Line. http://ci.nii.ac.jp/naid/130004587724

[5] Matsumoto, K. and Murakami, S. (2006) A Study on Re-Evaluation of the Abandoned Monorail Structures as Urban Landscape Elements. www.cpij.or.jp/com/ac/reports/4-4_95.pdf

[6] Banerjee, R.K., Peelukhana, S.V. and Goswami, I. (2014) Influence of Newly Designed Monorail Pressure Sensor Catheter on Coronary Diagnostic Parameters: An *in Vitro* Study. *Journal of Biomechanics*, **47**, 617-624. http://dx.doi.org/10.1016/j.jbiomech.2013.12.005

[7] Lee, C.H., Kawatani, M., Kim, C.W., Nishimura, N. and Kobayashi, Y. (2006) Dynamic Response of a Monorail Steel Bridge under a Moving Train. *Journal of Sound and Vibration*, **294**, 562-579. http://dx.doi.org/10.1016/j.jsv.2005.12.028

[8] Shen, J.Y., Sakata, Y. and Hashimoto, Y. (2009) The Influence of Environmental Deterioration and Network Improvement on Transport Modal Choice. *Environmental Science & Policy*, **12**, 338-346. http://dx.doi.org/10.1016/j.envsci.2009.01.003

[9] Arrington, G.B. (2004) Portland's TOD Evolution: From Planning to Lifestyle. In: Curtis, C., *et al.*, Eds., *Transit Oriented Development*: *Making It Happen*, 109-123.

[10] Statistical Yearbook of Kitakyushu. http://www.city.kitakyushu.lg.jp/shisei/menu05_0125.html

[11] Mu, R. and de Jong, M. (2012) Establishing the Conditions for Effective Transit-Oriented Development in China: The Case of Dalian. *Journal of Transport Geography*, **9**, 234-249. http://dx.doi.org/10.1016/j.jtrangeo.2012.02.010

[12] Sung, H. and Oh, J.-T. (2011) Transit-Oriented Development in a High-Density City: Identifying Its Association with Transit Ridership in Seoul, Korea. *CITIES*, **2**, 70-82. http://dx.doi.org/10.1016/j.cities.2010.09.004

[13] Dittmar, H. and Ohland, G. (2004) The New Transit Town Best Practice in Transit-Oriented Development. http://community-wealth.org/content/new-transit-town-best-practices-transit-oriented-development

[14] Anthony, M. (2009) Improving Decision-Making for Sustainable Urban Transport: An Introduction to the DISTILLATE Research Programme. *European Journal of Transport and Infrastructure Research*, **9**, 184-201.

[15] Potgieter, L.J. (1996) Transportation and Land Use Guidelines for Developing Urban Areas. *Transportation Research Part A*: *Policy and Practice*, **1**.

[16] Pollemans, J.E.M. (Hans) (2001) GRP Gives Monorail a New Lease of Life. *Reinforced Plastics*, **45**, 46-47. http://dx.doi.org/10.1016/S0034-3617(01)80135-1

Open Journal of Civil Engineering, 2014, 4, 328-337
Published Online December 2014 in SciRes. http://www.scirp.org/journal/ojce
http://dx.doi.org/10.4236/ojce.2014.44028

Scientific Research

Effects of Pit-Sand on Resistance Capacities of Reinforced Concrete Space Framed Structures

Lekan Makanju Olanitori, Joseph Olaseinde Afolayan

Department of Civil Engineering, Federal University of Technology, Akure, Nigeria
Email: lekanolanitori@gmail.com

Received 22 October 2014; revised 18 November 2014; accepted 29 November 2014

Abstract

This paper used the existing formulae in estimating resistance parameter of reinforced concrete structure to assess the effect of concrete produced from pit-sand in Akure metropolis, on the resistance parameters of a collapsed building in Oba-Ile, Akure. Site inspections were carried out on the collapsed building, and concrete samples were taken. Both destructive and non-destructive methods were used to determine the structure's concrete strength. The number of reinforcements in each structural element was determined by exposing them. Resistance parameters such as moments of resistance for slab (M_{RS}), for beam (M_{RB}) and shear capacity (V_C) of the structural elements were estimated using existing formulae and, compare the results with the structure's actual resistance parameters. The average concrete strength was 8.5 N/mm² which was less than 20 N/mm², the prescribed concrete strength for construction of the building. The estimated resistance parameters M_{RS}, M_{RB} and V_C based on 8.5 N/mm² concrete strength are 18.2 kN·m, 46.3 kN·m and 64.4 kN respectively. Also the estimated resistance parameters M_{RS}, M_{RB} and V_C based on 20 N/mm² concrete strength are 20.6 kN·m, 54.1 kN·m and 90.73 kN respectively. The actual M_{RS}, M_{RB} and V_C at collapse were 6.67 kN·m, 13.6 kN·m and 18.88 kN respectively. The existing formulae for predicting resistance parameters did not give accurate resistance parameters for the building at collapse. The collapse of the building was by shear failure, since shear failure capacity will be reached first before any of the other resistance parameters.

Keywords

Structure, Collapse, Load Capacity, Shear Capacity, Concrete

How to cite this paper: Olanitori, L.M. and Afolayan, J.O. (2014) Effects of Pit-Sand on Resistance Capacities of Reinforced Concrete Space Framed Structures. *Open Journal of Civil Engineering*, **4**, 328-337.
http://dx.doi.org/10.4236/ojce.2014.44028

1. Introduction

In the past few years a considerable improvement has taken place in the understanding of structural concrete and has been incorporated in the revised codes of practice. The British Standard CP110: Code of Practice for the Structural Use of Concrete [1], has superseded the British Standard Codes of Practice CP114 [2], for reinforced concrete. Similarly, in America the ACI Standard ACI 318-71 [3] has replaced the previous standard ACI 318-63 [4]. The major aspects of the revised codes are the limit state approach for designing reinforced concrete structures and the separation of methods of concrete mix design procedures from that of concrete design considerations. However, in Nigeria, consultant structural engineers still make concrete specifications based on CP 114 [2], which states concrete mixes of 1:2:4, 1:1½:3 and 1:1:2 produces concrete with compressive strength of 21 N/mm^2, 25.5 N/mm^2 and 30 N/mm^2 respectively at 28 days. However, Olanitori and Olotuah [5] show that these compressive strengths might not be attained due to the clay/silt content of sand, which negatively affects the compressive strength of concrete produced from them.

In CP110 [1] and BS8110 [6], this portion of CP114 [2] that dealt with concrete mix prescription was expunge from the code and standard. This is to the superior knowledge that concrete produced from different types of sand but of same mix proportion will produce concrete with different strengths. With the publication of BS8110 in 1985 [6], CP110 [1] was withdrawn. The publication of CP110 [1] and BS8110 [6] were accompanied with several BS standards which dealt with different aspects of concrete production [7].

The quality of concrete produced depends on the quality of its constituent materials and their mix ratios, the higher the percentage of clay/silt contents of sand, the lower the characteristic strength [5]. To mitigate the effect of clay/silt content of sand on the strength of concrete produced from it, there is a need to increase the cement content of the concrete, depending on the clay/silt percentage [8]. Olanitori, 2012 [9] determines the cost implication of mitigating the effect of clay/silt content of sand using mathematical models. In order to improve the quality of concrete produced from locally available aggregates, there is the need to have indigenous codes of practice, which will take the quality of the available aggregates into consideration [7].

The collapse of most reinforced concrete structures is by shear failure at the beam-column joint and sudden in nature [10]. In 1962, Joint ACI-ASCE Committee 326 [11] published a report regarding the design and behavior of beams failing due to shear and diagonal tension. To develop safe design recommendations, a database of 194 beam tests without shear reinforcement was compiled. The database consisted of 130 laboratory specimens tested under single-and double point loads and 64 beams subjected to uniformly distributed loads. Based on those data, design equation was formulated and is included in ACI 318-05 [12] and presented as Equation (1).

$$V_c = \left(\sqrt{f_c^1} + 120\rho_w \frac{V_u d}{M_u}\right)\frac{b_w d}{7} \le 0.3\left(f_c^1\right) b_w d \tag{1}$$

where V_c is the nominal shear strength provided by concrete; f_c^1 is the specified compressive strength of concrete; ρ_w is the ratio $\frac{A_s}{b_w d}$; V_u is the factored shear force at section; M_u is the factored moment at section; b_w is the web width; d is the effective depth of section; and A_s is the area of tension reinforcement.

By neglecting the term $\frac{Vd}{M}$ in Equation (1) a simplified but conservative version could be derived and presented as Equation (2).

$$V_c = \frac{1}{6}\sqrt{f_c^1} b_w d \tag{2}$$

To include the effects of loading type and shear span to depth ratio into current code provisions, for members in which more than 1/3 of the factored shear at the critical section results from concentrated load located between 2d and 6d of the face of the support, Brown *et al.* [13], proposes:

$$V_c = \frac{1}{12}\left(f_c^1\right) b_w d \tag{3}$$

Such a reduction in shear strength as indicated in Equation (3) will substantially reduce the number of tests that fall below code values.

According to Arslan [14], the nominal shear strength provided by concrete can be estimated using Equation (4).

$$V_{cr} = V_{crt} + V_{crd} = 0.15\left(f_c\right)^{0.5} b_w d + 0.02\left(f_c\right)^{0.65} b_w d \tag{4}$$

where: V_{cr} is the cracking shear strength, V_{crt} is the diagonal tension cracking strength and V_{crd} is the dowel strength.

Based on the principal shear strength V_o carried in the compression zone, considering the influence of parameters; the slenderness ratio (a/d) and size effect ($1/d$), Arslan, 2012 [15] expresses the diagonal cracking strength of RC slender beams without stirrups as given in Equation (5).

$$V_c = \left[0.2 f_c^{2/3}\left(\frac{c}{d}\right)\left(1+0.032 f_c^{1/6}\right)\left(\frac{4}{a/d}\right)^{0.15}\left(\frac{400}{d}\right)\right] b_w d \tag{5}$$

where c is the depth of the neutral axis.

Other existing shear strength models for slender beams without stirrups, by Kim and Park, 1996 [16], Khuntia and Stojadinovic, 2001 [17], and Rebeiz, 1999 [18] are presented in **Table 1**.

The ACI 318-08 [19] design shear strength is a simple superposition of transverse reinforcement and concrete strength. The design strength is independent of whether flexural yield has occurred prior to shear failure. For members, design shear strength is calculated using Equation (6).

$$V_n = V_c + V_s = \frac{\sqrt{f_c}}{6} b_w d + \frac{A_w f_y d}{s} \tag{6}$$

where V_c is the contribution of concrete to shear strength; V_s is the contribution of shear reinforcement to shear strength; f_c is the compressive strength of concrete; A_w is the area of shear reinforcement within a distance s and f_y is the shear reinforcement yield strength. The contribution of shear reinforcement is derived from basic equilibrium considerations on a 45-degree truss model with constant shear reinforcement spacing and an effective depth.

In their work,Arslan and Polat [20], show that there exists a significant amount of contribution of concrete to the shear strength (18% - 69%), however, noted further experiments should be conducted with a wider range of shear reinforcement ratio, shear span-to-depth ratio, concrete strength and various loading schemes in order to obtain more reliable assessments.

Since the mid-1980s, there is an increasing amount of experimental evidence showing that the underlying concepts of the provisions of current codes (for example, BS 8110-1985 [6] and ACI 318-05 [12]) for the shear in particular and, to a certain extent for the flexural design of reinforced concrete (RC) structures are in conflict with fundamental properties of concrete at both the material and the structural levels [21]. Also, only few of the existing shear strength models give reasonable shear strength capacity for reinforced concrete structures constructed from concrete produced from locally available aggregates.

Table 1. Some of the existing shear strength models for slender beams without stirrups.

Investigator	Shear strength models
Kim and Park (1996)	$V_u = \left[3.5 f_c^{\alpha/3} \rho^{3/8}\left(0.4+\frac{d}{a}\right)\left(\frac{1}{\sqrt{1+0.008d}}+0.18\right)\right] b_w d$ $\alpha = 2-(a/d)/3$ for $1.0 \le \frac{a}{d} \prec 3.0$; $\alpha = 1$ for $\frac{a}{d} \ge 3.0$
Rebeiz (1999)	$V_c = \left[0.4+\sqrt{f_c \rho \frac{a}{d}}\left(2.7-0.4A_d\right)\right] b_w d$ $A_d = \frac{a}{d}$ for $\left(\frac{a}{d}\right) \prec 2.5$ and $A_d = 2.5$ for $(a/d) \ge 2.5$
Khuntia and Stojadinovic (2001)	$V_c = \left[0.54\sqrt[3]{\rho\left(f_c \frac{Vd}{M_u}\right)^{0.5}}\right] b_w d$; $\frac{M_u}{Vd} = \frac{a}{d} - 1$

A lot of work has been carried out to determine the effect of the various types of pit-sand on the cube strength of concrete, however very little work from literature has been carried out to determine the effect of the various types of pit-sand on the resistance capacities of reinforced concrete space framed structures. This paper, using existing formulae from the codes, the estimated and actual resistance capacities of the collapsed building at Oba-Ile were determined, in order to determine the effect of the pit-sand used on the resistance capacities.

2. Materials and Methods

2.1. Materials

The materials used for this study are structural detailing, portable rotary drilling machine, 15 samples of 75 mm diameter cores of concrete, PUNDIT6 equipment, and a manually operated universal testing machine. The client of the collapsed building was not willing to provide the architectural plan and structural detailing. Consequentially, as-built architectural plan and the structural detailing were produced from site inspection and by exposing the structural components such as slab, beams and columns. Result of the site inspection given in **Table 2** and **Figure 1** shows some part of the collapsed building.

2.2. Procedure

Fifteen samples of 75 mm diameter cylindrical cores of concrete were taken from slabs, beams and columns. Five samples were taken from each structural element. The cores were vertically and horizontally drilled with a portable rotary drilling equipment using water as the drilling fluid and diamond impregnated bit. The retrieved cores were taken to the laboratory for examination and tested for strength using Universal Testing Machine (UTM) in accordance with BS 1881-120, 1983 [22]. Also non-destructive tests were carried out on parts of the building that are yet to collapse using PUNDIT 6 in accordance with BS 1881 [23] [24]. The compressive strengths from UTM and the PUNDIT6 are presented in **Table 3**, while the characteristic strengths from UTM and the PUNDIT6 are presented in **Table 4**.

2.3. Method of Analysis

From the as-built structural drawing, using equations in the code, moment of resistance of the slab and beam as

Figure 1. Collapsed part of the building.

Table 2. The summary of the areas of tension reinforcement provided for the structural elements of the collapsed building and the structural re-assessment.

Structural Element (mm)	Provided Flexural Reinforcement	Provided Shear Reinforcement	Comments of Re-Assessment
Slab (150)	Y12-250 B/S and T/S		Reinf. prov ok.
Beams (250 × 400)	2Y16 B/S and T/S	Y10@300	Y10@300 not ok
Columns (250 × 250)	4Y16		Reinf. prov ok.

Table 3. Results from universal testing machine and the PUNDIT 6.

SM	Slab							Beam				Column			
PD6	11.5	10.2	11.0	9.8	10.2	10.5	9.3	9.5	10.2	9.8	10.4	10.6	9.1	9.9	8.5
UTM	10.0	9.8	9.4	9.0	9.7	9.2	10.5	7.9	8.8	10.8	9.4	9.6	10.2	10.4	8.2

Table 4. Characteristic strengths from universal testing machine and the PUNDIT6.

Formulae	Pundit 6 (N/mm^2)	Universal Testing Machine (N/mm^2)
ε	10.03	9.53
$\sum(x-\varepsilon)^2$	8.01	9.47
$\sigma=\sqrt{\left[\sum(x-\varepsilon)^2/(n-1)\right]}$	0.76	0.82
$F_k=\varepsilon-1.64\sigma$	8.80	8.20

well as the shear capacity of the beam were estimated and presented in **Table 5**. The estimated moment of resistance and the shear capacity were compared with actual moment of resistance and the shear capacity. Also shear capacity of the collapse building was evaluated based on the existing shear strength models for slender beams without stirrups (and presented in **Table 6**), and compared with that of the estimated and actual shear capacities.

3. Moment of Resistance (M_r) and Shear Capacity (V_c)

3.1. Estimated Moment of Resistance for Slab and Beam (M_{ER})

The moment of resistance of the slab and beam is estimated using Equation (7) below:

$$M_{ER}=F_{cc}*z=F_{st}*z \tag{7}$$

$M_{ERS}=20.6\,\text{kN}\cdot\text{m}$ and $M_{ERB}=54.1\,\text{kN}\cdot\text{m}$.

Equations (14) and (15) of BS 8110-1, 1997 [25] can be written in a compressed form, thus having;

$$m=\beta_s n l_x^2 \tag{8}$$

m is the maximum design ultimate moments either over supports or at mid-span on strips of unit width and span (l_x or l_y).

β_s is the sagging (or hogging) moment in the spans (or over the edges), per unit width, in the direction of shorter spans/edges (or longer spans/edges), divided by nl_x^2.

n is the slab load and, l_x is the shorter span.

Using Equation (8)

$20.6=0.056\times n\times 4^2$; $n=23\,\text{kN}/\text{m}^2$; where n is the estimated collapse load for slab.

For a continuous beam, the maximum moment occurs at the middle of end span, hence

$$M_{RB}=0.09FL \quad \text{(Table 3.5 BS 8110-1: 1997 [25])}. \tag{9}$$

where F is the total design ultimate load and, L is the effective span.

Table 5. Resistance parameters of the collapsed building.

Type of resistance (R)	Resistance from prescribed concrete strength (R_{PCS})	Resistance from actual collapse load (R_{ACL})	Resistance from actual concrete characteristic strength (R_{ACCS})
M_{RS} (kN·m)	20.6	6.67	18.2
M_{RB} (kN·m)	54.1	13.6	46.3
N_{PCL} (kN/m^2)	23	7.44	12.6
N_{TCL} (kN/m^2)	37.5	7.44	32.2
V_C (kN)	90.73	18.88	64.4

M_{RS}—moment of resistance of slab; M_{RB}—moment of resistance of slab; N_{PCL}—partial collapse load; N_{TC}—total collapse load; V_C—shear capacity.

Table 6. Shear capacities determined from existing shear strength models.

Investig/ Con Shear Capacity	ACI (2005)	Brown *et al* (2006)	Arslan (2008)	Arslan (2012)	Kim and Park (1996)	Rebeiz (1999)	Khuntia and Stojadinovic (2001)
V_{CACS} (kN)	45.2	22.6	48.2	13.2	20.4	84.6	12.56
V_{CPCS} (kN)	69.4	34.7	75.4	35.3	28.3	109.9	14.56

V_{CACS}—shear capacity, determined using actual concrete strength; V_{CPCS}—shear capacity, determined using prescribed concrete strength.

Using Equation (9), we have:

$F = wl$, hence $M = 0.09wl^2$

Equating M_{ERB} and M_{RB}, w can be determined. Where w is the beam load in kN/m.

$54.1 = 0.09wl^2$, from where $w = 37.57$ kN/m.

Using equation 10, the equivalent slab load on beam can be estimated.

$$w = 1/4nl_x \tag{10}$$

where n is the slab load and, l_x is the shorter span of the slab supported by the beam.

$$37.5 = 1/4 \times n \times 4$$

$$n = n_{esl} = 37.5 \text{ kN/m}^2$$

where n_{esl} is the estimated equivalent slab collapse load on beam (Total Collapse Load).

These results are presented in **Table 5**.

3.2. Estimated Shear Capacity of Beam (V_{EB})

The shear capacity of a section for a given stirrup size and spacing can be estimated by Equation (11):

$$V_{EB} = \left(\frac{A_{sv}}{S_v} 0.95 f_{yv} + bv_c \right) d \tag{11}$$

Using Equation (11) above, we have:

$$V_{EB} = \left(0.523 \times 0.95 \times 250 + 250 \times 0.472\right) \times 372 \times 10^{-3}$$

$$V_{EB} = V_s + V_c = 46.83 + 43.90 = 90.73 \text{ kN}.$$

This result is presented in **Table 5**.

3.3. Moments of Resistance, Load and Shear Capacities, of the Collapsed Space Framed Building

3.3.1. Collapse Load of the Space Framed Building

At collapse, the load acting on the structure is estimated as follows:

Slab load = 0.15 × 24 = 3.6 kN/m^2. Live load during construction = 1.5 kN/m^2. Collapse slab load n_s = 1.4 × 3.6 + 1.6 × 1.5 = 7.44 kN/m^2.

Load due to beam weight = $0.25\times(0.4-0.15)\times 24\times 1.4$ = 2.1 kN/m. Hence collapse beam load

$$w_c = \frac{1}{4}nl_x + 2.1 = \frac{1}{4}\times 7.44\times 4 + 2.1 = 7.44 + 2.1 = 9.44 \text{ kN/m}$$

Using above loadings, Equations (8) and (9) can be used to determine the maximum span moments for slab and beam respectively.

$$M_{RS} = \beta_x n l_x^2 = 0.056\times 7.44\times 4^2 = 6.67 \text{ kN}\cdot\text{m}$$

$$M_{RB} = 0.09FL = 0.09\times 37.76\times 4 = 13.6 \text{ kN}\cdot\text{m}$$

The maximum shear force acting on a beam can be estimated using Equation (12).

$$V = \frac{wl}{2} \tag{12}$$

where w is the uniformly distributed load on beam and, l is the beam span. Hence using Equation (12):

$$V = \frac{wl}{2} = \frac{9.44\times 4}{2} = 18.88 \text{ kN}.$$

These results are presented in **Table 5**.

3.3.2. Moment of Resistance Using Analysis of Section Method

Average characteristic strength $= (8.8+8.2)/2 = 8.5 \text{N/mm}^2$. Taking the cube strength of concrete to be 8.5 N/mm^2, Equation (7) can be used to determine the moments of resistance of slab and beam, Equations (8) and (9) can be used to determine the slab and beam load and, Equation (10) can be used to determine equivalent slab load on beam, while Equation (12) can be used to determine the shear capacity. The results are presented in **Table 5**.

4. Analysis and Discussion of Results

From **Table 2**, the results of the structural re-assessment show that tension reinforcements provided for the slab were adequate. Also, the longitudinal reinforcements provided for the beams were equally adequate, while that of shear reinforcement was not adequate. The reinforcements provided for the columns were adequate.

Table 3 shows the results of universal testing machine and the PUNDIT6, while **Table 4** gives the characteristic strength of the concrete from which the collapsed building was built as 8.8 N/mm^2 and 8.2 N/mm^2 for PUNDIT6 and Universal Machine respectively, resulting in an average characteristic strength of 8.5 N/mm^2. The prescribed design concrete strength for the building was 20 N/mm^2. This shows a 57.5% reduction in the concrete strength caused by the low quality of pit-sand used for the construction.

The estimated resistance parameters, such as moment of resistance (M_R), shear capacity (V_C) and collapse load (N_C) of the building were estimated using equilibrium equation of a reinforced concrete section with the prescribed and actual characteristic strengths of concrete which equal 20 N/mm^2 and 8.5 N/mm^2 respectively. The analysis equations of the BS 8110-1, 1997 [25] were used to determine the actual resistance parameters of the collapsed building using the actual collapse load. The estimated and actual resistance parameters of the collapsed building were presented in **Table 5**.

From **Table 5**, the moments of resistance of slab (M_{RS}) estimated from equilibrium equation of a reinforced concrete section, using the prescribed strength of concrete (R_{PCS}), actual collapse load (R_{ACL}) and, actual concrete characteristic strength (R_{ACCS}) are 20.6 kN·m, 6.67 kN·m and 18.2 kN·m respectively. Also, the moment of resistance of beam (M_{RB}) determined using (R_{PCS}), (R_{ACL}) and, (R_{ACCS}) are 54.1 kN·m, 13.6 kN·m and 46.3 kN·m respectively.

Also, from **Table 5**, partial collapse load (N_{PCL}) determined from the values of (R_{PCS}), (R_{ACL}) and, (R_{ACCS}) are 23.0 kN/m^2, 7.44 kN/m^2 and 12.6 kN/m^2 respectively. Also, the total collapse load (N_{TCL}) from (R_{PCS}), (R_{ACL}) and, (R_{ACCS}) values are 37.5 kN/m^2, 7.44 kN/m^2 and 32.2 kN/m^2 respectively, while the shear capacity (V_C) from (R_{PCS}), (R_{ACL}) and, (R_{ACCS}) values are 90.73 kN, 18.88 kN and 64.4 kN respectively.

From the above, the estimated moments of resistance of slab (M_{RS}) determined from R_{PCS}, and R_{ACCS} are 20.6 kN·m and 18.2 kN·m respectively, and greater than that determined from R_{ACL}, which equals 6.67 kN·m by 209% and 173% respectively. Equally, the estimated moments of resistance for beam (M_{RB}), determined from R_{PCS} and R_{ACCS} are 54.1 kN·m and 46.3 kN·m respectively, and greater than that determined from R_{ACL}, which equals 13.6 kN·m by 298% and 240% respectively.

The partial collapse loads (N_{PCL}) determined from R_{PCS} and R_{ACCS} are 23.0 kN/m^2 and 12.6 kN/m^2 respectively, and greater than that determined from R_{ACL}, which equals 7.44 kN/m^2 by 209% and 69% respectively. The total collapse loads (N_{TCL}) determined from R_{PCS} and R_{ACCS} are 37.5 kN/m^2, and 32.2 kN/m^2 respectively, and greater than R_{ACL}, which equals 7.44 kN/m^2 by 404% and 333% respectively. Also, the shear capacity, determined from R_{PCS} and R_{ACCS} are 90.73 kN and 64.4 kN respectively, and greater than that determined from R_{ACL}, which equals 18.88 kN, by 381% and 241% respectively.

The estimated moments of resistance of slab (M_{RS}) determined from R_{PCS} and R_{ACCS} are 20.6 kN·m and 18.2 kN·m respectively. This shows that, when the strength of concrete decreases by 57.5% (20 N/mm^2 to 8.5 N/mm^2), M_{RS} only decreases by 12%. Also decrease by 57.5% in concrete strength, only have decrease effect of 14.4% on M_{RB}. Decrease in concrete strength by 57.7% only has decease effect of 14.1% on the total collapse load (N_{TCL}). The shear capacity determined from R_{PCS} and R_{ACCS} are 90.73 kN and 64.4 kN respectively, hence the decrease effect of 57.7% of concrete strength is 29%.

Table 6 shows shear capacities determined from existing shear strength models. Only the shear strength models of Brown *et al.* [13] and Kim and Park [16] give shear capacities of 22.6 kN and 20.4 kN respectively, which compares favorably with the actual shear capacity of the collapsed building which equals 18.88 kN. The shear capacities from Brown *et al.* [13] and Kim and Park [16], defer from that of the actual shear capacity by 8.1% and 19.7% respectively.

Table 7 shows the percentage increment of resistance parameters over that due to the actual collapse load. From **Table 7**, shear capacity V_C has the highest percentage of increment; hence shear failure capacity will be reached first before any others in resistance parameters of the collapsed building. Therefore, the collapse of the building is by shear failure which is sudden in nature.

5. Conclusions

From the discussion above, the following conclusions can be drawn:

1) The collapse of the building was caused by shear failure which is sudden in nature.

2) Method of analysis of section, for reinforced concrete structures, gives overestimated values of the resistance parameters.

3) Coefficient method gives more accurate values of the resistance parameter.

4) Shear strength models of Brown *et al.* (2006) and Kim and Park (1996) give the most accurate value of shear capacity of reinforced concrete at failure.

5) The estimated resistance capacities, determined using the actual concrete characteristic strengths, gives an overestimated resistance capacities when compared with the actual resistance capacities. This shows that there is the need to investigate the effect characteristic concrete strength on resistance capacities of reinforced concrete space framed structures.

Table 7. Percentage increment of resistance parameters over that due to collapse load.

R/α	$\alpha_E = \frac{R_{PCS} - R_{ACL}}{R_{ACL}} \times 100\%$	$\alpha_E = \frac{R_{ACCS} - R_{ACL}}{R_{ACL}} \times 100\%$
M_{RS} (kN·m)	208.8	172.9
M_{RB} (kN·m)	297.8	240.4
N_{PCL} (kN/m^2)	209.1	69.4
N_{TCL} (kN/m^2)	404.0	332.8
V_C (kN)	380.6	241.1

6. Recommendations

1) Local Codes of Practice should be developed so as take into consideration, the quality of the locally available aggregates in formulating design formulae, which will be capable of given more realistic resistance parameters.

2) Effect of the reduction of the characteristic strength of concrete should be investigated, and appropriate measures should be put in place so as to produce safe reinforced concrete structures.

References

[1] CP 110 (1972) Code of Practice for Structural Use of Concrete: Part I—Design, Materials and Workmanship. British Standards Institution, London.

[2] CP 114 (1957) The Structural Use of Reinforced Concrete in Buildings (Amended in 1965). British Standards Institution, London.

[3] ACI Committee 318 (1971) Buildings Code Requirement for Reinforced Concrete. American Concrete Institute, Detroit.

[4] ACI Committee 318 (1963) Buildings Code Requirement for Reinforced Concrete. American Concrete Institute, Detroit.

[5] Olanitori, L.M. and Olotuah, A.O. (2005) The Effect of Clayey Impurities in Sand on the Crushing Strength of Concrete (a Case Study of Sand in Akure Metropolis, Ondo State, Nigeria). *Proceedings of* 30*th Conference on "Our World in Concrete and Structures*", Singapore City, 23-24 August 2005, 373-376.

[6] BS 8110 (1985) Structural Use of Concrete: Part—I: Code of Practice for Design and Construction. British Standards Institution, London.

[7] Olanitori, L.M. (2013) Codes of Practice: Prerequisite for Quality Structural Design and Management of Buildings in Nigeria. 5*th West Africa Built Environment Research* (*WABER*) *Conference*, Accra, 12-14 August 2013, 283-291.

[8] Olanitori, L.M. (2006) Mitigating the Effect of Clay Content of Sand on Concrete Strength. *Proceedings of* 31*st Conference on Our World in Concrete and Structures*, Kaula Lumpur, 15-17 August 2006, 344-352.

[9] Olanitori, L.M. (2012) Cost Implication of Mitigating the Effect of Clay/Silt Content of Sand on Concrete Compressive Strength. *Journal of Civil Engineering and Urbanism*, **2**, 143-148.

[10] Olanitori, L.M. (2011) Causes of Structural Failures of a Building: Case Study of a Building at Oba—Ile Akure. *Journal of Building Appraisal*, **6**, 277-284.

[11] Joint ACI-ASCE Committee 326 (1962) Shear and Diagonal Tension. *A CI Journal Proceedings*, **59**, 1-30.

[12] ACI Committee 318 (2005) Building Code Requirements for Structural Concrete and Commentary (ACI 318R-05). American Concrete Institute, Farmington Hills.

[13] Brown, M.D., Bayrak, O. and Jirsa, J.O. (2006) Design for Shear Based on Loading Conditions. *ACI Structural Journal*, **103**, 541-550.

[14] Arslan, G. (2008) Cracking Shear Strength of RC Slender Beams without Stirrups. *Journal of Civil Engineering and Management*, **14**, 177-182. http://dx.doi.org/10.3846/1392-3730.2008.14.14

[15] Arslan, G. (2012) Diagonal Tension Failure of RC Beams without Stirrups. *Journal of Civil Engineering and Management*, **18**, 217-226. http://dx.doi.org/10.3846/13923730.2012.671264

[16] Kim, J.K. and Park, Y.D. (1996) Prediction of Shear Strength of Reinforced Concrete Beams without Web Reinforcement. *ACI Materials Journal*, **93**, 213-222.

[17] Rebeiz, K.S. (1999) Shear Strength Prediction for Concrete Member. *Journal of Structural Engineering ASCE*, **125**, 301-308. http://dx.doi.org/10.1061/(ASCE)0733-9445(1999)125:3(301)

[18] Khuntia, M. and Stojadinovic, B. (2001) Shear Strength of Reinforced Concrete Beams without Transverse Reinforcement. *ACI Structural Journal*, **98**, 648-656.

[19] ACI Committee 318 (2008) Building Code Requirements for Structural Concrete and Commentary (ACI 318R-08). American Concrete Institute, Farmington Hills.

[20] Arslan, G. and Polat, Z. (2013) Contribution of Concrete to Shear Strength of RC Beams Failing in Shear. *Journal of Civil Engineering and Management*, **19**, 400-408. http://dx.doi.org/10.3846/13923730.2012.757560

[21] Kotsovs, M.D. (2007) Concepts Underlying Reinforced Concrete Design: Time for Reappraisal. *ACI Structural Journal*, **104**, 675-684.

[22] BS 1881 (1983) Testing Concrete—Part 120: Method for Determination of the Compressive Strength of Concrete

Cores. British Standards Institution, London.

[23] BS 1881 (1986) Testing Concrete—Part 201: Guide to the Use of Non-Destructive Methods of Test for Hardened Concrete. British Standards Institution, London.

[24] BS 1881 (1986) Testing Concrete—Part 203: Recommendations for the Measurement of Velocity of Ultrasonic Pulses in Concrete. British Standards Institution, London.

[25] BS 8110 (1997) Structural Use of Concrete—Part 1: Code of Practice for Design and Construction. British Standards Institution, London.

Open Journal of Civil Engineering, 2014, 4, 338-352
Published Online December 2014 in SciRes. http://www.scirp.org/journal/ojce
http://dx.doi.org/10.4236/ojce.2014.44029

Scientific Research

Sensitivity Analysis of Key Parameters in Decision Making of Two-Stage Evolutionary Optimization Maintenance Strategies

Elia A. Tantele*, Renos A. Votsis, Toula Onoufriou

Department of Civil Engineering and Geomatics, Cyprus University of Technology, Lemesos, Cyprus
Email: *elia.tantele@cut.ac.cy

Received 6 October 2014; revised 2 November 2014; accepted 18 November 2014

Abstract

Preventative maintenance (PM) measures for bridges are proactive maintenance actions which aim to prevent or delay a deterioration process that may lead to failure. This type of maintenance can be justified on economic grounds since it can extend the life of the bridge and avoid the need for unplanned essential/corrective maintenance. Due to the high importance of the effective integration of PM measures in the maintenance strategies of bridges, the authors have developed a two-stage evolutionary optimization methodology based on genetic algorithm (GA) principles which links the probabilistic effectiveness of various PM measures with their costs in order to develop optimum PM strategies. In this paper, the sensitivity of the methodology to various key input parameters of the optimization methodology is examined in order to quantify their effects and identify possible trends in the optimum PM intervention profiles. The results of the sensitivity studies highlight the combined use of both proactive and reactive PM measures in deriving optimum strategy solutions. The precise mix and sequence of PM measures is clearly a function of the relative effectiveness and cost of the different available PM options as well as the various key parameters such as discount rate, target probability of failure, initial probability of failure and service life period examined. While the results highlight the need for more reliable data they also demonstrate the robustness and usefulness of the methodology; in the case where data is limited it can be used as a comparative tool to improve understanding of the effects of various strategies and enhance the decision making process.

Keywords

Preventative Maintenance, Corrosion, Genetic Algorithm, Optimization, Reinforced Concrete Bridges, Sensitivity Analysis

*Corresponding author.

How to cite this paper: Tantele, E.A., Votsis, R.A. and Onoufriou, T. (2014) Sensitivity Analysis of Key Parameters in Decision Making of Two-Stage Evolutionary Optimization Maintenance Strategies. *Open Journal of Civil Engineering*, **4**, 338-352.
http://dx.doi.org/10.4236/ojce.2014.44029

1. Introduction

Maintenance measures can be applied to ensure that the bridge reliability remains below an acceptable probability of failure, *i.e*. the probability that the bridge will reach a specific limit state during its service life.

The constantly growing demand for reliable bridges, with low maintenance cost has highlighted the need to investigate the use of PM measures, as part of a proactive approach since "prevention is better than cure". This proactive management approach may not be essential now but it can be justified on economic grounds since it can enable the postponement of essential rehabilitation work, extend the service life and reduce the whole life cost of bridge structures [1].

However, there are significant uncertainties associated with the effectiveness of various PM measures which calls for a probabilistic approach. To this end a probabilistic methodology is developed by the authors, to address the effectiveness of PM measures. This is combined with an optimization methodology based on GA principles to create a tool which is capable of identifying optimum PM strategies against the specific forms of deterioration encountered in structures.

For the current study deterioration due to chloride induced corrosion is considered and the PM measures are actions designated to alleviate the corrosion process.

In this development a proactive approach is adopted in which PM measures are considered for maintaining the probability of corrosion initiation within an acceptable target level. The effectiveness of PM is modelled probabilistically. The various PMs fall in three categories depending on their effect on the probability of corrosion initiation through their ability to: 1) keep the reinforcing bar (rebar) free from chlorides ions (Cl^-); 2) reduce the total diffusion coefficient; 3) prevent further chloride ingress by removing the chloride ions from the rebar.

A probabilistic methodology developed in [2] incorporate the uncertainties that influence the PM degree of effectiveness (such as the amount of diffusivity of chloride when concrete is treated with PM), and predict the effectiveness of different PM actions.

By applying PM measures at different time intervals, corrosion initiation can be postponed and/or inhibited. As a result, the probability of failure (p_f) can be maintained within an acceptable target level. In the context of this study, the initiation of corrosion is adopted as the critical failure incident. In particular, failure (*i.e*. initiation of corrosion) occurs when the concentration of chlorides at the surface of the steel rebar exceeds a predefined threshold value. Mathematically, this can be expressed through the following limit state:

$$G(x) = C(th) - C(x,t) \tag{1}$$

where $C(th)$ is the threshold chloride concentration (kg/m^3); $C(x,t)$ is the chloride concentration at steel rebar (kg/m^3) calculated using Fick's second law of diffusion and $G(x)$ is the limit state.

The p_f is estimated using the Monte Carlo simulation method [2] [3]. Different PM measures will clearly result in different p_f profiles depending on their ability to reduce the diffusivity of chloride ions or to remove them from the reinforcement surface.

In the following sections, the probabilistic methodology is outlined and its sensitivity to key parameters is examined. Furthermore various trends in the optimum PM intervention profiles and whole life costs emerging from the results are presented.

2. GA Based Methodology for Optimum PM Strategies

The GA principles are adopted for optimization of the PM strategies. The GA method was invented by John Holland [4] while Goldberg was the first to solve engineering optimization problems using GA [5]. Miyamoto *et al*., [6] described the GA as a power tool for obtaining optimal maintenance plans. Other work using this approach for maintenance optimization is carried out by Liu and Frangopol [7], Furuta *et al*. [8] and Morcous and Lounis [9]. In the present application the developed GA based optimization methodology combines probabilistic effectiveness modelling of PM with the cost of different PM measures to identify optimum strategies that will combat the corrosion deterioration of RC structures. The GA methodology which is developed for this application [2] [3] is briefly outlined in this section and is depicted in **Figure 1**.

2.1. Objective of the Methodology

The aim of this study is to identify a PM strategy that will maintain the p_f of an examined bridge element under

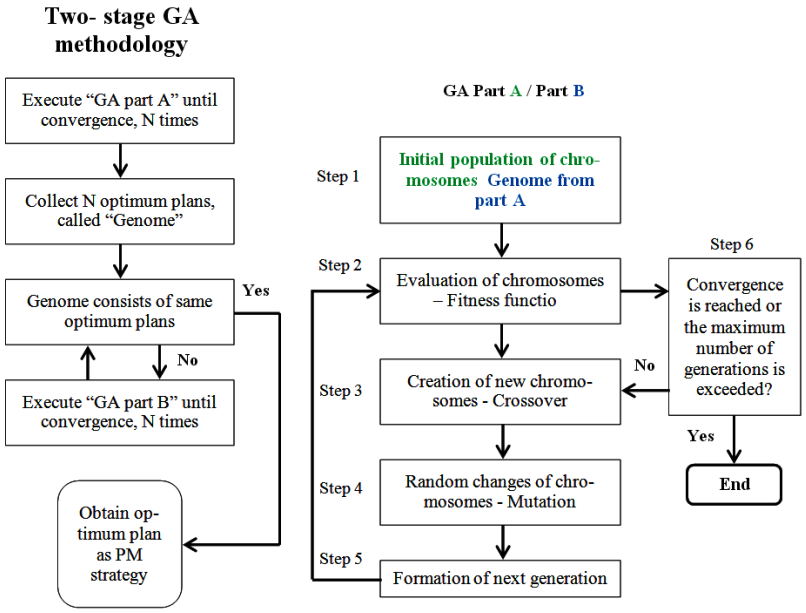

Figure 1. Proposed two stage GA methodology.

the actions of different PM measures, with the minimum possible cost (Equation (2)) lower than a target lifetime p_f (Equation (3)). Within the context of this study, the p_f represents the probability of corrosion initiation on the top level of the steel rebar.

$$F = \sum_{t=t'}^{T-1} C_{\mathrm{PM}_{t,j}} \rightarrow \text{Minimum cost} \tag{2}$$

$$\sum_{t=t'}^{T-1} p_f\left(\mathrm{PM}_{t,j}\right) < p_f\left(\text{target}\right) \tag{3}$$

where F is the total cost of PM measures; $C_{\mathrm{PM}_{t,j}}$ is the cost of PM measure j carried out in year t; j is the type of PM measure chosen for year t; $p_f\left(\mathrm{PM}_{t,j}\right)$ is the probability of failure for PM measure j carried out in year t; p_f (target) is the maximum acceptable value of p_f; T is the expected service life of the bridge element (set here equal to 120 years); t is the bridge element age (years) and t' is the present age of the bridge element (set here equal to 0).

2.2. Development and Implementation of GA Based Methodology

The key elements of the developed GA based methodology are outlined in this section (**Figure 1**) while a more detailed description can be found in [2]. The interpretation of **Figure 1** shows that initially GA produces a population of chromosomes; all are representing a possible solution to a given problem (Step 1). During each successive generation every member is tested according to a fitness function (Step 2). Highly "fit" chromosomes are ranked at the top of the pool and can be selected to mate with other highly fit members (form the parents) to produce new chromosomes (offsprings) [10] (Step 3). The offsprings contain characteristics from both of the parent chromosomes. Furthermore, in a few randomly selected individuals some arbitrary changes are made in their characteristics through mutation to add some diversity to the population (Step 4). However, it does provide accountable improvement to perform mutation to already good solutions. For this reason elitism selection is often embedded [6] [8] to enforce the preservation of the best individual chromosomes of the current generation to the next. With elitism, a number of good solutions are designated as elite solutions and are destined to propagate unchanged. At this point a new population is formed with chromosomes closer to the optimum solution (Step 5). Therefore, although GA is randomized, it efficiently incorporates information from previous generations to create new search points and explores the most promising areas.

The entire process is repeated for a number of generations until the chromosomes will evolve and ultimately converge to an optimum solution. The convergence in this study is reached when in the parent population the

chromosomes are the same. Hence, in this case even after crossover, there is no change in the genes and therefore one optimum solution is proposed (Step 6 in GA Part A, **Figure 1**). The entire "GA Part A" process shown in **Figure 1** is repeated to obtain a number of optimum solutions and to select the solution that fits best the objective/fitness functions.

Unfortunately, the "GA Part A" may fail because of a convergence to an unacceptable local optimum. To overcome this limitation, an improved two-stage GA methodology (Part A + Part B), outlined in **Figure 1**, is proposed. The purpose of the "GA Part B" is twofold: firstly, to aid the finding of the optimum solution and secondly, to ascertain whether there are flaws in the selection of key parameters of the GA process in order to revise them and achieve convergence more efficiently.

As **Figure 1** illustrates, "GA Part A" is executed and the collected optimum solutions form the genome which is treated as the initial population in "GA Part B" (Step 1 in GA Part B). The simulations in "GA Part B" stop when all the chromosomes of the genome are the same, thus one optimum solution (optimum PM strategy) is proposed. The termination of the simulations is based on the logic that "optimum" parents (optimum solutions) cannot produce "more optimum" offspring (optimum solutions). For the implementation of the proposed methodology a computer program was developed using Visual Basic environment.

3. Sensitivity Study

In total, 19 case studies are reported here. In each case a number of PM actions are defined as options and the methodology is used to identify the most optimum whole life strategy. The PM actions include proactive measures such as surface treatment measures (silane, sealer, and coating) and reactive measures such as cathodic protection (CP), electrochemical chloride extraction (ECE) and concrete replacement (CR). The interval for PM maintenance action is assumed to be 5 years.

The parameters examined within the sensitivity study are summarized in **Table 1**. The case studies examined a bridge beam with average quality Portland cement (PC) and a 40 mm cover (Cases 1-19 in **Table 1**) while Case 19 investigates a bridge deck with similar quality concrete, and depth of cover. An initial pilot case (*i.e.* Case 1) is presented first in the following section, which forms the basis of comparison with all the other cases to identify trends and to study the sensitivity of different input data of the GA methodology.

The encoding representation and the genetic operators used for the GA based optimization methodology are presented in **Table 2** and **Table 3** respectively. A more detailed discussion of the basis of these parameters is given in [2]. For the parameter representation real value encoding is used so the actions are represented as integers. The parameters of the generic operators of the GA methodology were taken from literature while the population size and the mutation rate are based on sensitivity studies carried out by the authors. The service life and cost of PM measures are summarized in **Table 4**. These values are based on reports from Weyers *et al.* [11], HA [12], Pearson and Cuninghame [13], Kepler *et al.* [14] and Krauss *et al.* [15]. Whole life costing (WLC) is used to enable the economical appraisal of different PM strategies where expenditure is discounted over time and normalized to a common base year. The cost is discounted to the present value (PV) according to [16]:

$$\mathrm{PV} = \frac{C}{(1+r)^t} \tag{4}$$

where C is the cost at current price levels, r is the discount rate and t is the time period expressed in years.

The effectiveness of PM actions is based on the probabilistic models developed by the authors and presented elsewhere [17].

3.1. Pilot Case: Effectiveness of Different Proactive and Reactive Measures

A Pilot case is examined first in which all the proactive and reactive measures shown in **Table 2** are included as options. In this application it is assumed that the discount rate is 3% [18], the target p_f is 0.1 [19]-[21], the initial p_f is 0 (representing either a new element or one where chloride ingress has not commenced) and the service life of the element is 120 years.

A WLC of €100.7/m^2 is obtained for the optimum strategy. **Table 5** presents the different actions selected at 5-year intervals as established by the GA methodology. A combination of surface treatments and "do nothing" option are selected initially until p_f reaches the target value at which point a reactive measure is used. Based on

Table 1. Parameters examined in sensitivity study.

Key parameters	Case studies					
	Pilot case	2-5	6-13	14-16	17-18	19
Discount rate	3	0 3.5 6 8	3	3	3	3
Target p_f	0.1	0.1	0.08 0.085 0.09 0.095 0.105 0.11 0.115 0.12	0.1	0.1	0.1
Initial p_f	0	0	0	0.025 0.05 0.10	0	0
Service life of the bridge element	120	120	120	120	60 100	120

Table 2. Parameter representation.

Application of genetic code PM action	Genetic code
Do nothing	1
Silane	2
Polyurethane sealer	3
P-m coating	4
Cathodic protection	5
Chloride extraction	6
Concrete replacement	7

Table 3. Parameters of the genetic operator.

Parameter	Parameter value	References
Initial population size	48	[2]
Population size in every generation	48	[2]
Selection method	Roulette wheel selection and elitism selection (two chromosomes with the least overall PM cost are not subjected to mutation)	[6] [8] [10]
Crossover method	Single point crossover	[6]
Crossover rate, X_{rate}	Constant 100%	[6]
Mutation rate, M_{rate}	Constant 6%	[2]
Maximum generation	Until convergence or 300 generations	

Table 4. Service life and cost of PM measures [11]-[15].

Maintenance action	Time (years)	Cost (€/m^2)
Silane	5	5
Polyurethane sealer	5	6.4
P-m coating	10	38
Cathodic protection	As long is in service	Installation cost: 220 Maintenance cost*: 70
Chloride extraction	≈6 weeks	64
Concrete replacement	N/A	2464
Waterproofing system	25	32

*The maintenance cost includes maintenance of the anodes, application of sealer and inspection costs for every 5 years.

Table 5. Optimum PM plan of pilot case.

Year	0	5	10	15	20	25	30	35	40	45	50	55	60	65	70	75	80	85	90	95	100	105	110	115	120
Encoded actions in GA	3	1	1	1	4	-	6	1	3	6	1	4	-	4	-	6	1	3	6	1	4	-	4	-	1

Decoded Actions: 1: Do nothing; 2: Silane; 3: Sealer; 4: P-m Coating; 6: ECE; -: P-m coating still effective due to its service life (10 years).

the input data for this case ECE is identified as the best reactive PM measure to use as opposed to CP or CR when critical concentration of chloride is predicted on the rebar. This makes sense since the use of ECE has a dramatic impact on the p_f profile at little cost compared to the other reactive options. The cycle of proactive PM followed by a reactive PM is repeated throughout the lifetime. The combination of proactive measures is not the same throughout the lifetime of the element since the costs are discounted and cheaper solutions are sought at the beginning of the strategy (0 - 20 years)

The element performance when this recommended optimum PM plan is applied can be seen in **Figure 2** which shows the p_f profile with time. At no time frame the p_f exceeds the target p_f failure.

3.2. Effect of Different Discount Rates

The use of appropriate discount rate is important as this affects the sequence of application of PM and therefore the WLC profoundly (Equation (4)). The discount rates are quite variable between different agencies and are normally within the range of 2% - 8% [22]. Here, in addition to the Pilot case in which the discount rate is taken as 3%, other cases with 0%, 3.5%, 6% and 8% are investigated.

Cases 2-5 examine the sensitivity of the optimum strategy outcome to changes in the discount rate. As shown in **Figure 3** the highest WLC is obtained when the discount rate is 0% while the lowest cost is obtained when the rate is 8%. It is also clear that the sensitivity of the WLC results to the discount rate is significantly higher within the lower range of values.

The optimum maintenance plans proposed for different discount rates can be seen in **Table 6**, which shows that when the discount rate is 0% P-m coating is utilized for most PM intervals. However, **Table 5** and **Table 6** show that when the discount rate is higher than 0% (e.g. 3%, 3.5%, 6%, 8%) the optimization method selects less costly actions for the first 20 years, such as "do nothing", followed by the use of ECE and surface treatment at different PM intervals for the remaining life of the element. Where the higher discount rates are used (6% and 8%) there is a bigger reduction in costs with time (through discounting) compared to the lower discount rates (Equation (4)). This result in the increased use of ECE which is employed almost twice as many times compared to the lower discount rate cases (0%, 3%, 3.5%). The same optimum strategy is obtained for the two higher discount rates (6%, 8%) as shown in **Table 6** and **Figure 5**. While there is some difference in the discounting between these two cases this is not sufficiently high to change the optimum strategy solution. This is due to the number of available PM options investigated. A wider range of PM measures may result in different PM strategies between the higher discount rates. **Figure 4** and **Figure 5** illustrate the p_f profile under the action of the proposed PM plans. At no point in time does the p_f exceed the target p_f.

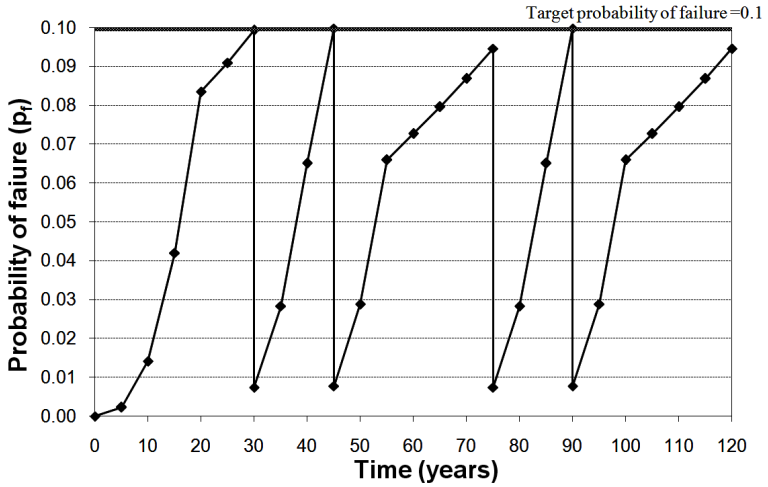

Figure 2. Probability of failure profile after the application of proposed strategy.

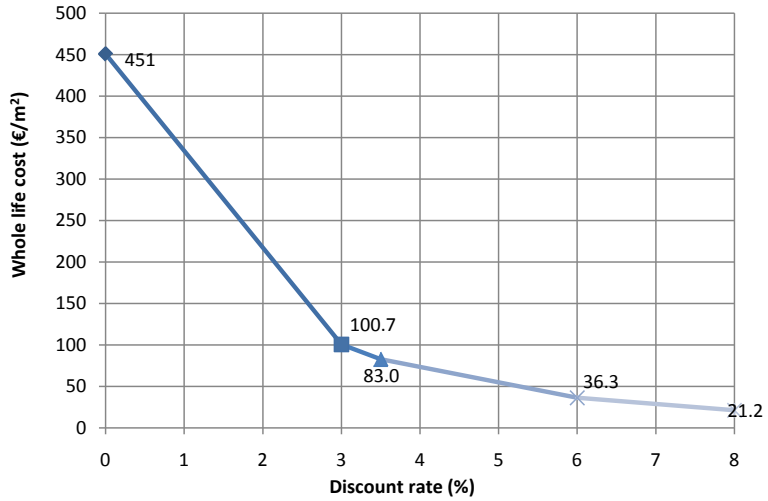

Figure 3. Effect of discount rate on the WLC.

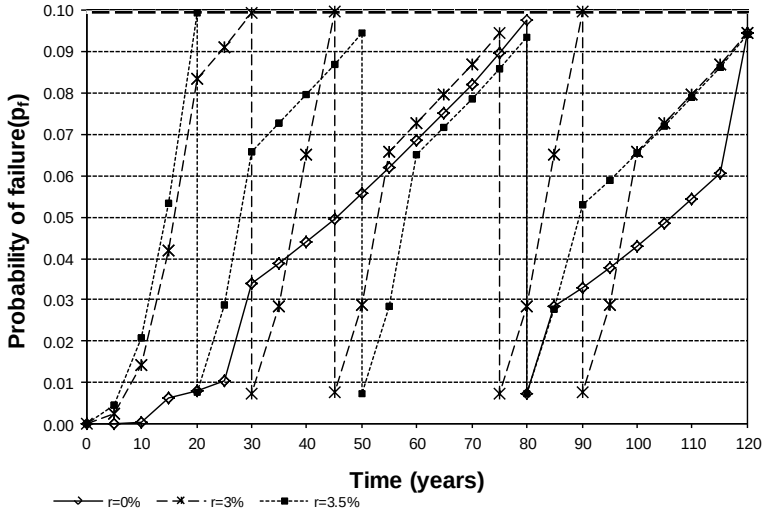

Figure 4. Probability of failure profile: Case studies (2-3) & pilot case.

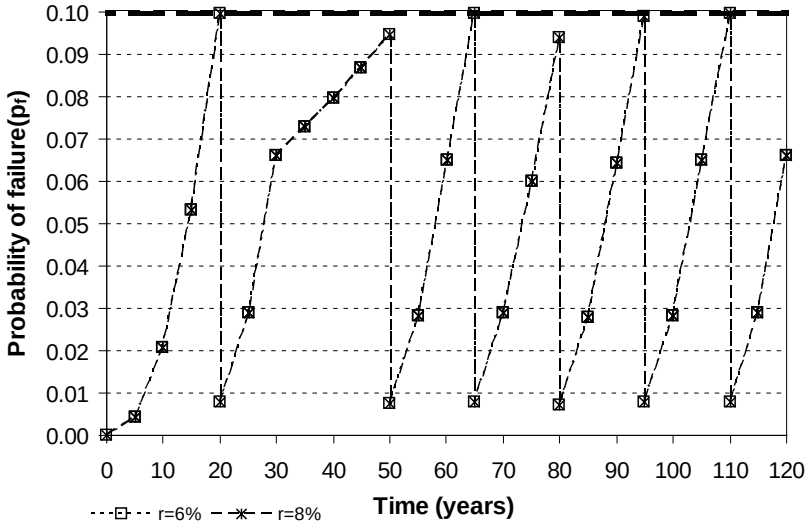

Figure 5. Probability of failure profile: Case studies (4-5).

Table 6. Optimum PM plan with different discount rate: Case studies (2-5).

Year	0	5	10	15	20	25	30	35	40	45	50	55	60	65	70	75	80	85	90	95	100	105	110	115	120
Actions r = 0%	4	-	1	4	-	1	4	-	4	-	4	-	4	-	4	-	6	4	-	4	-	4	-	3	1
Actions r= 3%	3	1	1	1	4	-	6	1	3	6	1	4	-	4	-	6	1	3	6	1	4	-	4	-	1
Actions r= 3.5%	1	1	1	1	6	1	4	-	4	-	6	1	4	-	4	-	6	3	4	-	4	-	4	-	1
Actions r= 6% & 8%	1	1	1	1	6	1	4	-	4	-	6	1	3	6	2	3	6	1	3	6	1	3	6	1	1

Decoded Actions: 1: Do nothing; 2: Silane; 3: Sealer; 4: P-m Coating; 6: ECE; -: P-m coating still effective due to its service life (10 years).

3.3. Effect of Different Target p_f

The target probability of failure is an important parameter in any probabilistic approach, within the context of integrity management of structures. Acceptable levels of probability of failure are not easy to define and depend on complex issues such as acceptable levels of risk and social impact. Some guidelines are provided in this area within Eurocode BS EN 1990 (2002) Annex B [20].

While a value of 0.1 was assumed for the Pilot study based on recommendations from codes of practice BS EN 1990 [20] and JCSS [21] a range of p_f values are examined within the sensitivity study to quantify the effect of this parameter. Case studies 6-13 adopt values within ±5%, ±10%, ±15% and ±20% of the assumed target p_f used in the pilot case. From the results of these cases it is clear that the target p_f influences highly the outcome of the WLC. **Figure 6** shows that when the target p_f increases the cost decreases. This is to be expected since increased reliability (lower p_f) would require more frequent use of PM measures and hence higher overall cost.

It is interesting to note that while on the whole the WLC decreases with increased target p_f the reduction in WLC is not continuous. This is due to the availability of the options to fit a strategy to ensure that the p_f remains below a target p_f. As more options are available the difference in WLC between the cases is expected to be more uniform. While the WLC is sensitive to changes in p_f the percentage change in WLC is lower than the corresponding change in p_f. A ±20% change in p_f results in only +8.1% and −8.3% change in WLC.

The optimum plans obtained from the GA methodology for a selection of case studies which their target p_f value provides minimum, maximum and average WLC are given in **Table 7**.

The p_f profiles of these cases are shown in **Figure 7**. Despite some differences in the choice of PM actions, a similar general pattern can be identified from these figures. The element is left to deteriorate with no action taken, approximately for the first 20 years. Then some surface treatments are selected for a period of 20 - 30 years

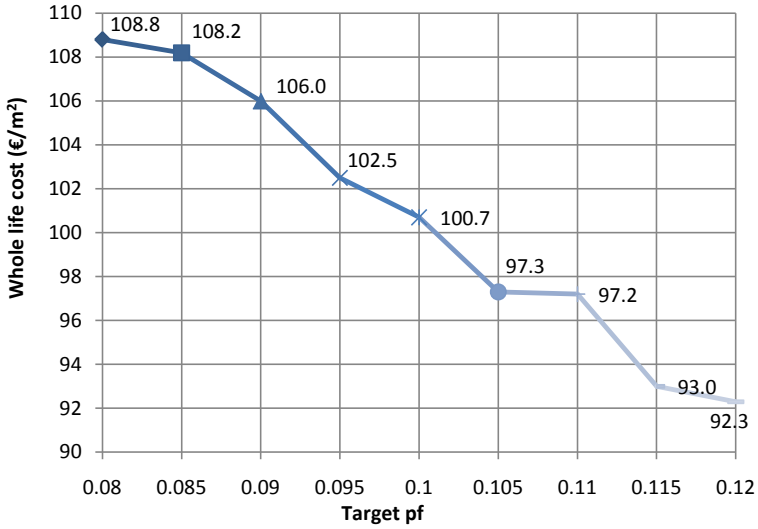

Figure 6. Effect of target p_f on the WLC.

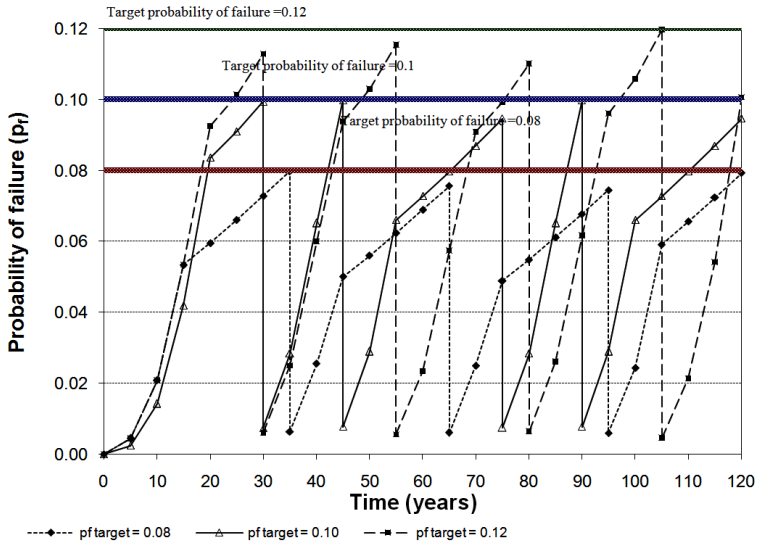

Figure 7. Probability of failure profile: Case studies 6; pilot case 13.

Table 7. Optimum PM plan with different target p_f: Case studies 6; pilot case 13.

Year	0	5	10	15	20	25	30	35	40	45	50	55	60	65	70	75	80	85	90	95	100	105	110	115	120
Actions p_f = 0.08	1	1	1	4	-	4	-	6	3	4	-	4	-	6	3	4	-	4	-	6	1	4	-	4	-
Actions p_f = 0.10	3	1	1	1	4	-	6	1	3	6	1	4	-	4	-	6	1	3	6	1	4	-	4	-	1
Actions p_f = 0.12	1	1	1	2	4	-	6	1	3	4	-	6	1	3	4	-	6	1	3	4	-	6	1	1	1

Decoded Actions: 1: Do nothing; 2: Silane; 3: Sealer; 4: P-m Coating; 6: ECE; -: P-m coating still effective due to its service life (10 years).

followed by the use of ECE. The latter pattern is repeated throughout the lifetime of the bridge element.

3.4. Effect of Initial p_f

Another important parameter is the initial p_f of the examined element. This parameter represents the probability

of corrosion initiation on the reinforcement of the element at the time examined. For example, if the initial p_f is zero then it means that the element is either new or chloride propagation has not commenced. The sequence of application of PM will be influenced by the initial p_f value.

Therefore the following case studies are examining the effect of initial p_f on the WLC. As expected with higher initial p_f the WLC also increases (**Figure 8**). This is due to the fact that more money is needed to restore the initial condition of the bridge element to safe levels (concerning its probability of failure) at an early stage. It can be seen that there is a significant increase in cost (85%) with an increase of the p_f from 0% to 10%. This relatively large increase in the WLC is due the cost of the PM actions required to restore the initial condition of the element. As these actions are applied at the beginning of its life they are not discounted, hence they have a marked effect on the overall cost of the strategy.

As shown in **Table 8** the first use of a reactive PM measure within each strategy is brought forward as the initial p_f increases. This is then followed by various cycles which combine either "do nothing" with sealer and ECE or "do nothing" with P-m coating and ECE. The use of P-m coating generally seems to increase in later years due to the discounting.

The optimum plans for different initial p_f are given in **Table 8**.

3.5. Effect of Different Service Life

The service life of an element is defined as the period of time during which it meets the standards and/or the target specified [23]. In the Pilot case the time period is set to 120 years to comply with the service life span of

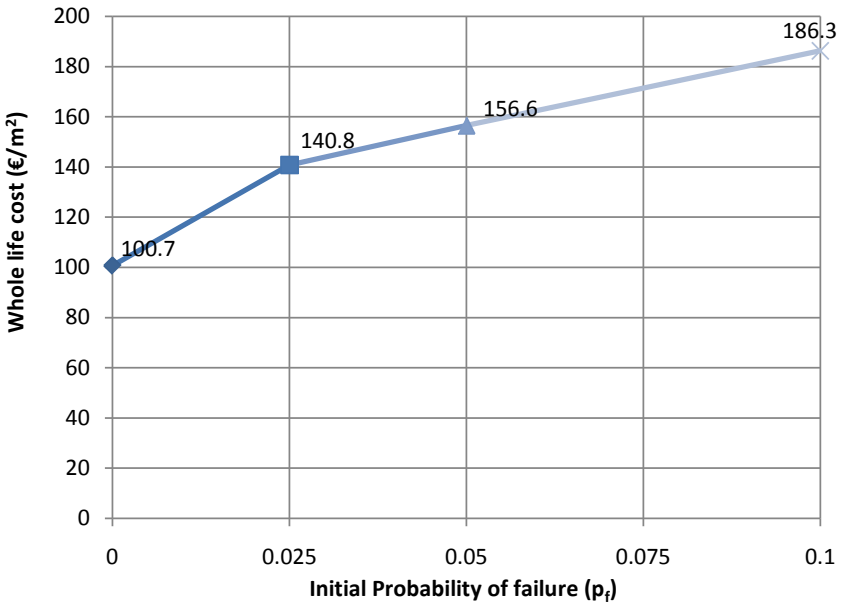

Figure 8. Effect of initial p_f on the WLC.

Table 8. Optimum PM plan with different initial p_f: Case studies (14-16) & pilot case.

Year	0	5	10	15	20	25	30	35	40	45	50	55	60	65	70	75	80	85	90	95	100	105	110	115	120
Actions p_f = 0	3	1	1	1	4	-	6	1	3	6	1	4	-	4	-	6	1	3	6	1	4	-	4	-	1
Actions p_f = 0.025	3	3	4	-	6	1	4	-	4	-	6	1	3	6	1	3	6	3	4	-	4	-	4	-	1
Actions p_f = 0.05	3	4	-	6	1	3	6	1	4	-	4	-	6	1	4	-	4	-	6	1	4	-	4	-	1
Actions p_f = 0.10	6	1	4	-	4	-	6	1	3	6	1	4	-	4	-	6	1	3	6	1	4	-	4	-	1

Decoded Actions: 1: Do nothing; 2: Silane; 3: Sealer; 4: P-m Coating; 6: ECE; -: P-m coating still effective due to its service life (10 years).

bridges designed before Eurocode requirements [24]. Additional analyses are performed to examine the effect of the service life on the optimum strategy selection. The service life values examined in Cases 17-18 are 60 years and 100 years [19].

Figure 9 illustrates the corresponding p_f profiles of these cases. The outcome of the analyses, which are the optimum strategies, the WLC and the corresponding p_f profile are presented in **Table 9** and **Figure 10**. The PM strategy is the same for all three cases for the first 30 years and combines the use of surface treatments and "do nothing" until the target p_f is reached when the reactive measure ECE is applied. In the subsequent cycles the P-m coating which is the most effective and expensive proactive measure becomes more beneficial and is selected more often. This is justified due to the combination of the longer life considered and the effect of the discounted cost. For the cases considering 60 and 100 years service life, two applications of ECE are required while in the case of 120 years, four applications are scheduled. When considering the WLCs for the three cases (**Figure 11**) it can be seen that as expected the WLC increases as the service life period increases although the rate of increase reduces with larger service life periods. The average cost per year reduces approximately linearly with increasing service life. The latter is partly due to the effect of discounting and also due to the fact that a longer service life plan provides more flexibility with the combination of options which can result in reduced overall cost.

3.6. Application of GA Methodology to Different Bridge Elements

So far the optimization methodology and its sensitivity were demonstrated with respect to a bridge beam. The methodology, however, is generic and can be applied to different bridge elements or even different deteriorating structures. In this example the methodology is demonstrated for a bridge deck instead of a beam. In the case of bridge decks the use of waterproofing system (WS) is mandatory in the UK since 1965 [13] therefore the WS is applied at year zero (0). Other actions that can be applied to bridge decks are the cathodic protection (CP) and concrete replacement (CR) hence these are also included as PM options in the analysis. Surface treatments with inadequate depth of penetration are not recommended since they can quickly wear when exposed to traffic abrasion [11] therefore they are excluded from this example.

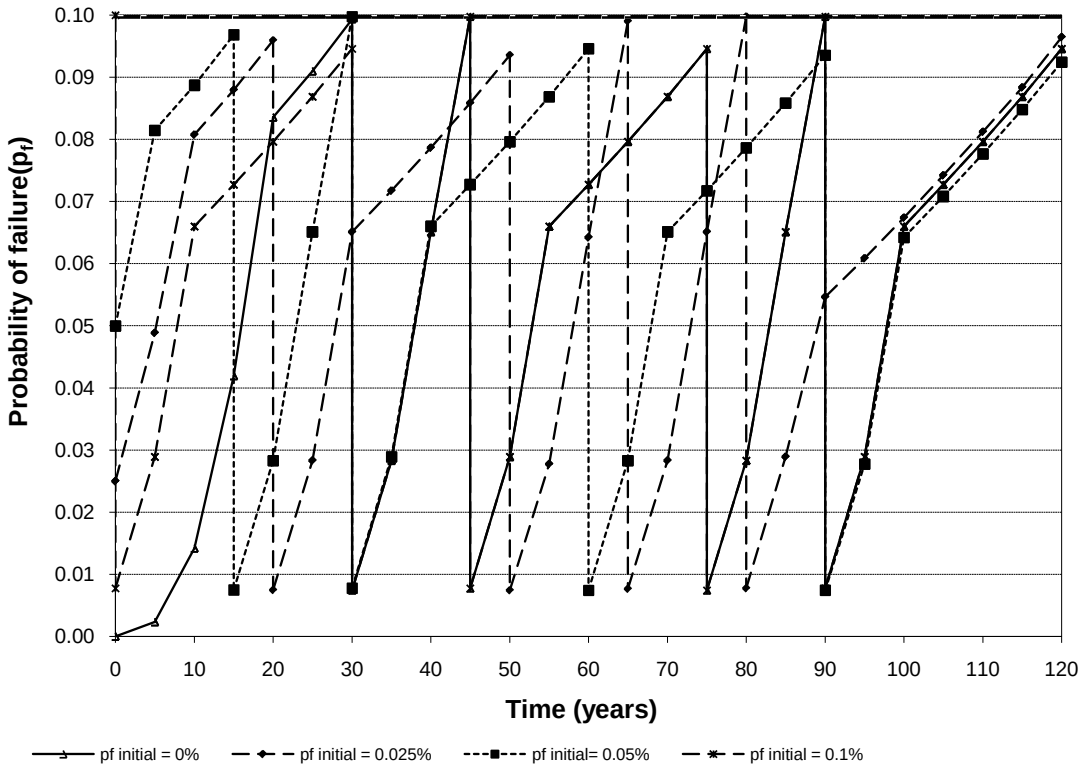

Figure 9. Probability of failure profile: Case studies (14-16) & pilot case.

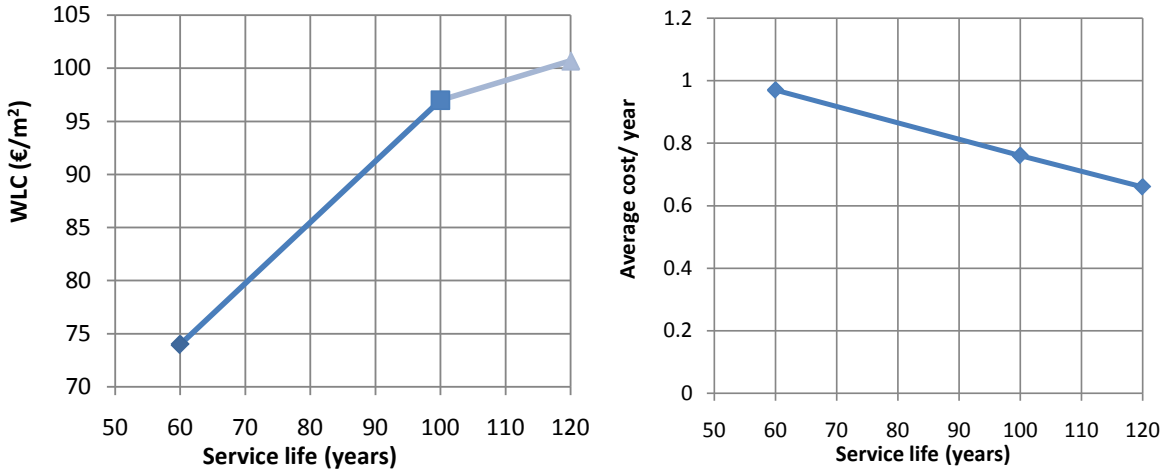

(a) (b)

Figure 10. Effect of service life on (a) WLC; (b) Average cost per year.

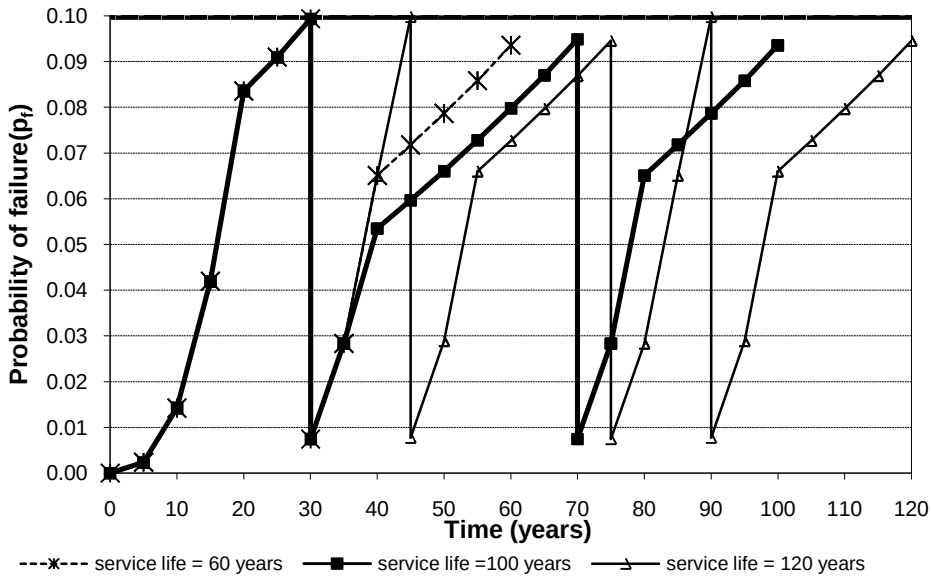

Figure 11. Probability of failure profile: Case studies (17-18) & pilot case.

Table 9. Optimum PM Plan with different service life: Case studies (17-18) & pilot case.

Year	0	5	10	15	20	25	30	35	40	45	50	55	60	65	70	75	80	85	90	95	100	105	110	115	120
Actions Ser. life = 60 yr	3	1	1	1	4	-	6	1	4	-	4	-	1												
Actions Ser. life = 100 yr	3	1	1	1	4	-	6	3	4	-	4	-	4	-	6	1	4	-	4	-	1				
Actions Ser. life = 120 yr	3	1	1	1	4	-	6	1	3	6	1	4	-	4	-	6	1	3	6	1	4	-	4	-	1

Decoded Actions: 1: Do nothing; 2: Silane; 3: Sealer; 4: P-m Coating; 6: ECE; -: P-m coating still effective due to its service life (10 years).

The WS is assumed to have a service life of 25 years [13] and the cost is taken as €31/m^2 [12]. Following the initial application of WS which is effective for 25 years the methodology is free to select any of the PM options included to maintain the p_f profile within acceptable limits and minimize the WLC.

In this case the use of WS is selected throughout the 120 years instead of CP or CR (**Table 10**). The WS is applied every 25 years (service life of WS) with the exception of a 5-year gap (at the 25th year) during which the deck can be left to deteriorate with no action taken (**Figure 12**). The repeated application of WS is sufficient to ensure that p_f remains below the critical p_f of 0.1 for the entire 120 years period without the need for any of the reactive PM measures CP and CR. The WLC is equal to €55.5/m^2 which is significantly less than the beam element WLC of €100.7/m^2. This suggests that the WS applied on bridge decks is a very effective PM measure.

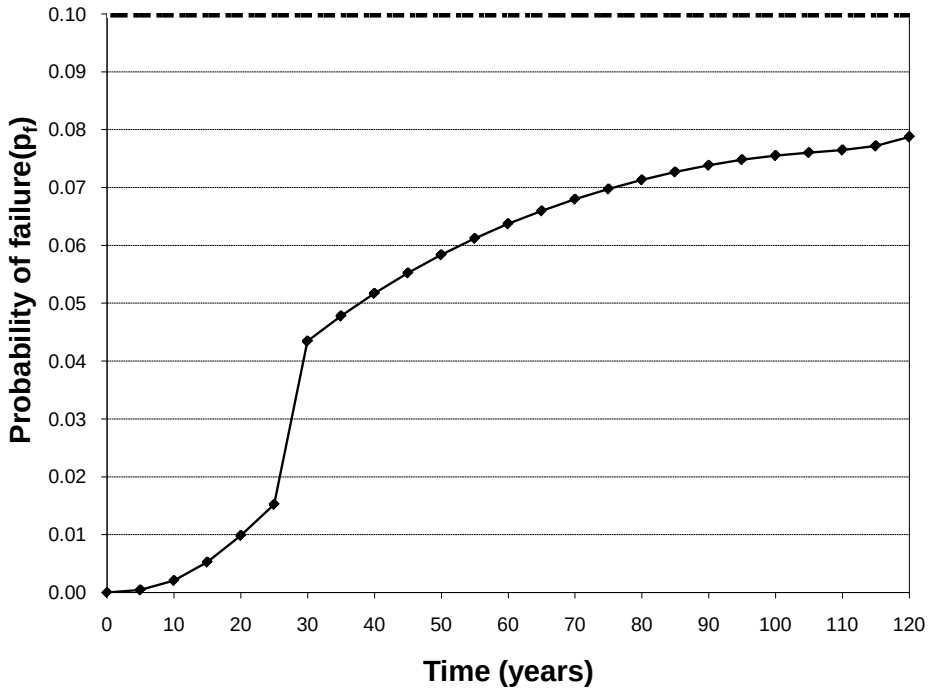

Figure 12. Probability of failure profile—Case study 19.

Table 10. Optimum PM plan of case study 19.

Year	0	5	10	15	20	25	30	35	40	45	50	55	60	65	70	75	80	85	90	95	100	105	110	115	120
Actions $p_f = 0$	8	-	-	-	-	1	8	-	-	-	-	8	-	-	-	-	8	-	-	-	-	8	-	-	-

Decoded Actions: 1: Do nothing; 8: waterproofing system; -: waterproofing system still effective during its service life (25 years).

4. Conclusions

A methodology is developed which combines probabilistic modelling of PM effectiveness with a GA based optimization methodology for identifying optimum PM strategies for reinforced concrete bridges. The PM strategies target one of the dominant deterioration problems in reinforced concrete bridges. The aim of the PM strategies is to delay/prevent the reinforcement corrosion of RC elements through contamination from chloride ions present in de-icing salts. The sensitivity of the methodology to various key input parameters is examined in order to quantify their effects and identify possible trends in the optimum PM intervention profiles. The results of the sensitivity studies highlight the combined use of both proactive and reactive PM measures in deriving optimum strategy solutions. When changes are introduced in the various parameters the methodology is capable of identifying optimum strategies which satisfy the p_f constraints and deliver minimum WLC. The precise mix and sequence of PM measures is clearly a function of the relative effectiveness and cost of the different available PM options as well as the various key parameters such as discount rate, target probability of failure, initial probability of failure and service life period examined.

As the discount rate increases the WLC reduces and becomes less sensitive towards the higher and of the range of 6% - 8%. In this range there is no change in the intervention sequence although the WLC is reduced

due to increased discounting. Higher discount rate cases make increasingly more use of expensive options towards the end of life.

As expected the methodology is sensitive to the target p_f, with WLC increasing as the target p_f increases. There appears to be approximately a linear dependence with some small step changes observed between different strategy combinations. Within the range examined the percentage rate of change in WLC of the optimum strategy is about half that of the change in target p_f.

The initial condition of the element (p_f value) has a large effect on the WLC of the optimum strategy. This is due to the PM actions required to restore the initial condition of the element. As these initial actions are applied at the beginning of the life, when the discounting effect is small, they have a marked effect on the overall strategy cost.

As the service life increases the WLC increases, however the sensitivity reduces with higher service life periods. This is mainly due the discounting but also due to the possibility of identifying more optimum PM combinations with a longer service life. This trend is also observed in the average cost per year which reduces linearly with the service life period.

Overall, the various case studies presented demonstrate the applicability of the methodology and highlight the efficiency and consistency in the results while showing some interesting trends. While the results highlight the need for more reliable data they also demonstrate the robustness and usefulness of the methodology. Where data is limited it can be used as a comparative tool to improve understanding of the effects of various strategies and enhance the decision making process. The methodology presented here although demonstrated for reinforced concrete bridge elements is generic and can be adapted to other type of deteriorating structures, systems or networks.

Acknowledgements

The support of this research by the UK Highways Agency (HA) and Transport Research Laboratory (TRL) is gratefully acknowledged. The opinions and conclusion presented in this paper are those of the authors and do not necessarily reflect the view of the sponsoring organizations.

References

[1] FHWA (2011) Bridge Preservation Guide, Maintaining a State of Good Repair Using Cost Effective Investment Strategies. Federal Highway Administration, US Department of Transportation, FHWA Publication Number, FHWA-HIF-11042.

[2] Tantele, E.A. and Onoufriou, T. (2010) Optimization of Life-Cycle Preventative Maintenance Strategies Using Genetic Algorithm and Bayesian Updating. *Proceedings of the* 5*th International Conference on Bridge Maintenance, Safety and Management*, *IABMAS*'10, *Smart EN ITN Mini-Symposium*, Philadelphia, 11-15 July, 2010.

[3] Tantele, E.A. and Onoufriou, T. (2009) Optimum Preventative Maintenance Strategies Using Genetic Algorithm and Bayesian Updating. *Ships and Offshore Journal*, **4**, 299-306. http://dx.doi.org/10.1080/17445300903247162

[4] Holland, J.H. (1975) Adaptation in Natural and Artificial Systems. University of Michigan Press, Ann Arbor.

[5] Goldberg, D.E. (1983) Computer-Aided Gas Pipeline Operation Using Genetic Algorithms and Rule Learning. Ph.D. Thesis, University of Michigan, Ann Arbor.

[6] Miyamoto, A., Kawamura, K. and Nakamura, H. (2000) Bridge Management System and Maintenance Optimization for Existing Bridges. *Computer Aided Civil and Infrastructure Engineering*, **15**, 45-55. http://dx.doi.org/10.1111/0885-9507.00170

[7] Liu, M. and Frangopol, D.M. (2004) Optimal Bridge Maintenance Planning Based on Probabilistic Performance Prediction. *Engineering Structures*, **26**, 991-1002. http://dx.doi.org/10.1016/j.engstruct.2004.03.003

[8] Furuta, H., Nakatsu, K., Ishibashi, K. and Miyoshi, N. (2014) Optimal Bridge Maintenance of Large Number of Bridges Using Robust Genetic Algorithm. *Structures Congress*, Boston, 3-5 April 2014, 2282-2291.

[9] Morcous, G. and Lounis, Z. (2005) Maintenance Optimization of Infrastructure Networks Using Genetic Algorithms. *Automation in Construction*, **14**, 129-142. http://dx.doi.org/10.1016/j.autcon.2004.08.014

[10] Haupt, R. and Haupt, S. (2004) Practical Genetic Algorithms. 2nd Edition, John Wiley and Sons, Inc., New York.

[11] Weyers, R.E., Prowell, B.D., Sprinkel, M.M. and Vorster, M. (1993) Concrete Bridge Protection, Repair, and Rehabilitation Relative to Reinforcement Corrosion: A Methods Application Manual. SHRP-S-360, Strategic Highway Research Program, Washington DC.

[12] Highways Agency (1999) Serviceable Life of Highway Structures and Their Components. Final Report, Project Number 970530.

[13] Pearson, S. and Cuninghame, J.R. (1997) Water Management for Durable Bridges. Project Report PR/CE/91/97, Transport Research Laboratory, Berkshire.

[14] Kepler, J.L., Darwin, D. and Locke, C.E. (2000) Evaluation of Corrosion Protection Methods for Reinforced Concrete Highway Structure. Structural Engineering and Engineering Materials SM Report No. 58, University of Kansas Center for Research, Inc., Lawrence.

[15] Krauss, P.D., Lawler, J.S. and Steiner, K.A. (2009) Guidelines for Selection of Bridge Deck Overlays, Sealers and Treatments. Wiss, Janney, Elstner Associates, Inc., Northbrook.

[16] Tilly, G.P. (1996) Principles of Whole Life Costing. *Proceedings of Conference on Safety of Bridges*, ICE, Thomas Telford, London, 138-144.

[17] Tantele, E.A., Onoufriou, T. and Mulheron, M. (2005) Effectiveness of Preventative Maintenance for Reinforced Concrete Bridges—A Stochastic Approach. *Proceedings of the* 5*th International Conference on Bridge Management*, Surrey, 11-13 April 2005, 443-451.

[18] Treasury, H.M. (2003) The Green Book: Appraisal and Evaluation in Central Government: Treasury Guidance. TSO, London.

[19] Li, C.Q. (2003) Life-Cycle Modelling of Corrosion—Affected Concrete Structures: Propagation. *Journal of Structural Engineering*, **129**, 753-761. http://dx.doi.org/10.1061/(ASCE)0733-9445(2003)129:6(753)

[20] BS EN 1990 (2002) Eurocode: Basis of Structural Design. British Standards Institution, London.

[21] JCSS (2000) Probabilistic Model Code, Part 1—Basis of Design. Joint Committee on Structural Safety, JCSS-OSTL/DIA/VROU-10-11-2000.

[22] Val, D.V. and Stewart, M.G. (2003) Life-Cycle Cost Analysis of Reinforced Concrete Structures in Marine Environments. *Structural Safety*, **25**, 343-362. http://dx.doi.org/10.1016/S0167-4730(03)00014-6

[23] OECD (1992) Bridge Management, Road Transport Research. Paris.

[24] BS 5400 (1998) Steel, Concrete and Composite Bridges—Part 1: General Statement. British Standards Institution, London.

Open Journal of Civil Engineering, 2014, 4, 353-360
Published Online December 2014 in SciRes. http://www.scirp.org/journal/ojce
http://dx.doi.org/10.4236/ojce.2014.44030

A Study on Health Monitoring of Structural Damages for Two Stories Model by Using Vibration Test

Toshikazu Ikemoto, Reza Amiraslanzadeh, Masakatsu Miyajima

School of Environmental Design, College of Science and Engineering, Kanazawa University, Kanazawa, Japan
Email: tikemoto@t.kanazawa-u.ac.jp, r.amiraslanzadeh@stu.kanazawa-u.ac.jp, miyajima@se.kanazawa-u.ac.jp

Received 26 September 2014; revised 20 October 2014; accepted 18 November 2014

Abstract

Many structures in Japan were built after the war at a revival term or rapid economic growth. These structures have been reached a life in recent years and it is economically not affordable to conduct repair and reconstruct these structures only with a possibility of being damaged. This paper presents an approach to detect the structural damages for two degrees of freedom (2DOF) model. In this study, we conducted Microtremor measurement, free vibration test and vibration test. The 2DOF model was demonstrated the feasibility of using the proposed approach to damage detection of structural member.

Keywords

Health Monitoring, Structural Damage, Vibration Test, Microtremor Measurements

1. Introduction

After a large earthquake, detection of damages in structures such as hospitals, bridges, and fire stations is very important. Therefore it is vital to conduct health monitoring to prevent secondary disaster. Numerous techniques have been presented in the literature on health monitoring of structures. Each researcher has applied different techniques to a different structure therefore it is difficult to compare merits, drawbacks and limitations of these various methodologies [1]-[4].

The ASCE task group recently developed structural health monitoring technique [5]. Structural health monitoring allows the engineer to use sensing of the structural responses in conjunctions with appropriate data analysis and modeling techniques to monitor the condition of a structure.

This paper presents an approach to detect structural damage for two degrees of freedom (2DOF) model. We

How to cite this paper: Ikemoto, T., Amiraslanzadeh, R. and Miyajima, M. (2014) A Study on Health Monitoring of Structural Damages for Two Stories Model by Using Vibration Test. *Open Journal of Civil Engineering*, **4**, 353-360.
http://dx.doi.org/10.4236/ojce.2014.44030

conducted microtremor measurement, free vibration test and forced vibration test for health monitoring of the model. The forced vibration test simply consisted of a low amplitude vibration imposed by an electro-shaker that has been installed at the roof level.

The proposed method is a three-step approach. In the first step, we estimated change of the natural frequency of damaged structural models comparing with that of the undamaged one. The change of natural frequency could be assigned as one of the prevalent damage detection method in health structural assessment techniques. When a damage exists in a structure, the stiffness is reduced and as a result, the natural frequency starts decreasing. One of the most advantages of this detection technique is that frequency measurements can be quickly and easily conducted. Moreover, experimental techniques used for the determination of resonant frequencies are classical vibrational measurement techniques; thus allowing the vibrational measurements to be extensive with a great number of measurement points and a very cheap experimental procedure [6]-[10].

Any undamped system vibrating at one of its natural frequencies can be reduced to the simple problem of a mass m attached to a spring of stiffness k (Equation (1))**.** The lowest natural frequency of such a system is:

$$f = \frac{1}{2\pi}\sqrt{\frac{k}{m}} \tag{1}$$

Specific cases require specific values for m and k. They can often be estimated with sufficient curacy to be useful in approximate modeling. In the second step, dynamic properties of the floors were analyzed by using response acceleration records on each floor level. Observed data for floors were analyzed in the frequency domain. The ratio of Fourier spectrum has considered in order to study the characterization and change of amplification between two floors. The ratio of Fourier spectrum between the first floor level and the second one indicates the damaged floor. In the third step, the strain was measured at specified locations on column members. We defined the maximum strain ratio of the damaged member to the undamaged member. As defined below, the ratio of extension to original length is called strain it has no units as it is a ratio of two measured lengths (Equation (2)).

$$\text{Strain} = \frac{\Delta L}{L} \tag{2}$$

where ΔL is the measured extension in metric units and L is original length measured in the same unit. This strain ratio was used to detect damaged member of the model structure.

2. Description of the Model

A 3D steel frame model with two stories and single span was designed and built. According to the old codes roof in Japan structures is made by light materials, and based on the said assumption the model was structured without roof, and only columns and beams were considered. The model was 2.4 m tall with a span width of 1.2 m and 1.2 m height for each story. Whole size of the model as well as sizes of the all profiles was in an approximate scale of 1:3. The connections were carried out through the blots without joints and the model assumed as a rigid-free-condition model. Each beam and column member restrained between two joints has the length of 1.2 m with I-shape cross section and height and width of 10 and 5 cm, respectively.

3. Configuration Cases

The measurements were performed for twelve test configuration cases. All test configurations were conducted at the full amplitude forced vibration levels. Furthermore, 1/3 amplitude was applied in the work, but the obtained strain was not satisfactory for the considered 1/3 scale and 1/3 amplitude, thus we believe that full amplitude forced vibration could give us more clear results, thus despite of 1/3 scale, full amplitude is considered. In addition to the forced vibration test, free vibration test and microtremor measurement were performed for each case. The damage in each case was introduced by cutting a fracture on the elements or disconnecting beam-column or base-column bolted connections. The damage pattern of column is shown in **Figure 1**. Experimental cases are presented in **Figure 2**.

The configuration cases shown in **Table 1** are as follow:

Case 1: The configuration of the frame model for the first case was an undamaged structure. The undamaged steel frame was measured for microtremor measurement, free vibration and the full amplitude for forced vibration.

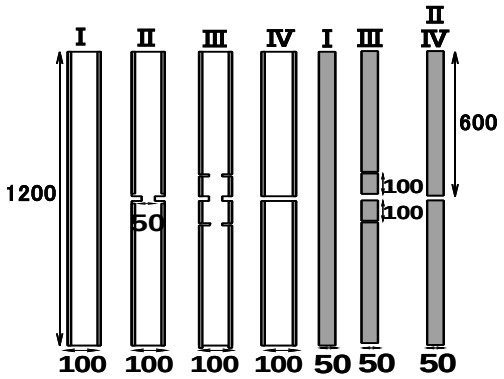

Figure 1. Damage pattern (Unit: mm).

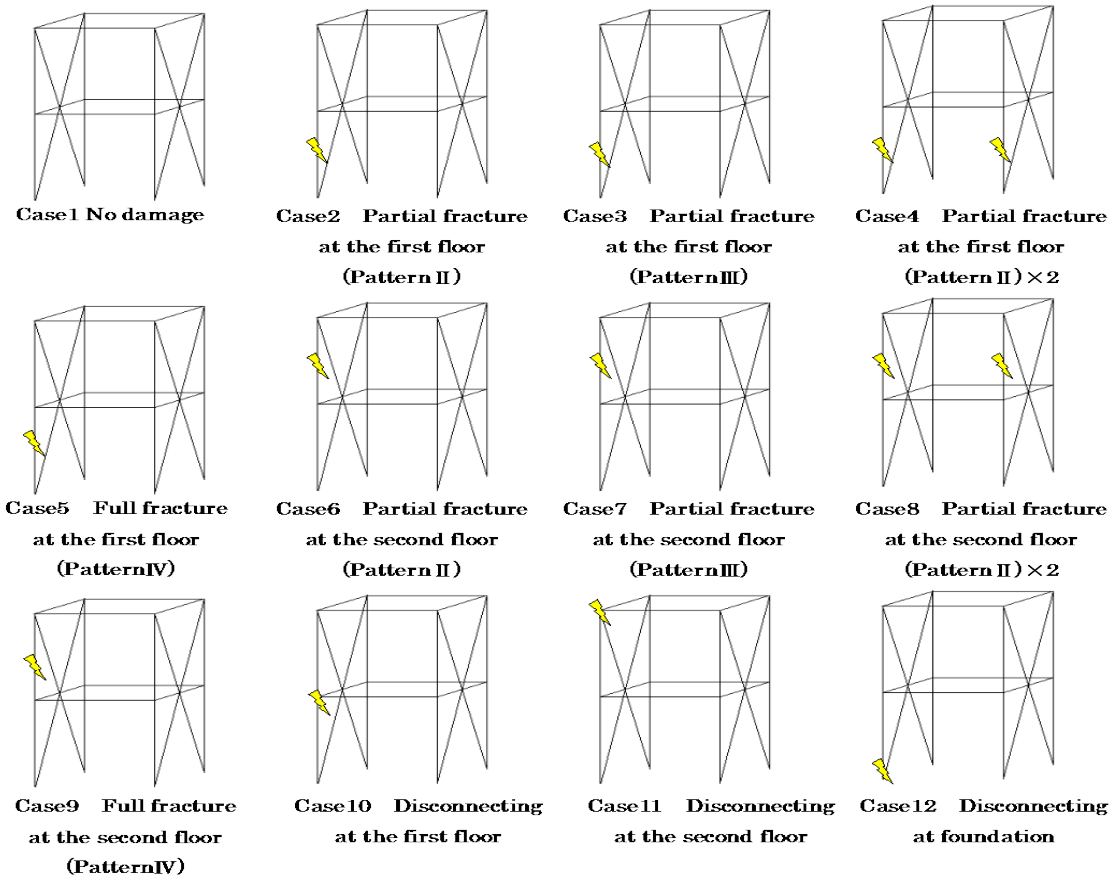

Figure 2. Damage cases.

Case 2: The damage was introduced to the frame by cutting a fracture on the middle of the profile up to 50% width of the both sides. The damaged column was considered at the first floor and as shown in **Figure 2**, indicated with number 2 of the damage pattern.

Case 3: The damage level in this case was larger than Case 2. In this case damage was introduced to the frame by cutting three fractures on the middle of the profile up to 1/3 width of the both sides in the first floor.

Case 4: The damage was introduced to the frame by same as Case 2. But two damaged columns were considered at the first floor.

Case 5: The damage was introduced to the frame by a complete cut at the middle of the column. The damaged column was attached to the first floor such as Case 2.

Table 1. Configuration of damage cases.

No.	Damage case	Damage pattern of column
1	No damage	-
2	Small partial fracture at the first floor	2
3	Large partial fracture at the first floor	3
4	Small partial fracture at the first floor ×2	2 × 2
5	Full fracture at the first floor	4
6	Small partial fracture at the second floor	2
7	Large partial fracture at the second floor	3
8	Small partial fracture at the second floor ×2	2 × 2
9	Full fracture at the second floor	4
10	Disconnecting at the first floor	-
11	Disconnecting at the first second	-
12	Disconnecting at the foundation	-

Cases 6-9: The damage was as same as Cases 2-5 but in the second floor.

Case 10: In this case damage condition was introduced to the frame by disconnecting the beam-column connection in the first floor. The disconnected connection is indicated with the sign in **Figure 2**.

Cases 11: The damage was similar to Case 10 but the locations were in the second floor.

Case 12: In this case damage condition was introduced to the frame by disconnecting the base-column connection at the foundation.

4. Experimental Studies

In this study three kinds of measurements were performed: Microtremor measurement, free vibration test and vibration test by using the shaking machine. These three methods are described as follows.

4.1. Microtremor Measurements

One of the disadvantages of the shaking table measurements is the scale of structures which means that we cannot put desired structures on the shaking table, thus microtremor would be a handy method in order to measure dominant waves and amplifications. Microtremor measurement was performed by using six Microtremor-meters. The meters were set up in 2 directions on the beam of the second floor, first floor and the base level. **Figure 1** shows a typical meter layout of the locations and directions on each floor level.

4.2. Free Vibration and Vibration Test

Free vibration test was performed to evaluate dynamic properties of the model structures. Free vibration was made by applying and then sudden releasing of a static force on the beam of the roof level by the manpower [11]-[13]. **Figure 3** also shows locations layout of accelerometers and directions of accelerometers.

Shaking machine was installed at the roof, on top of a steel plate. Weight of the machine used in vibration test was about 200N. The shaking level was maximum magnitude of the shaker force. Applied load at roof level was approximately 900N. Measurements were taken in three locations on each floor. Measurements for two directions were taken in one location at the base level.

4.3. Natural Frequency

The natural frequency in the lateral direction was estimated using the microtremor measurements and vibration tests [14]. The data was analyzed in the frequency domain by using FFT analyses [14]-[17]. The results of natural frequency for all damage cases in the free vibration test and microtremor measurement are shown in **Figure 4**. This figure shows the natural frequencies of undamaged and damaged steel frame. The natural frequencies of

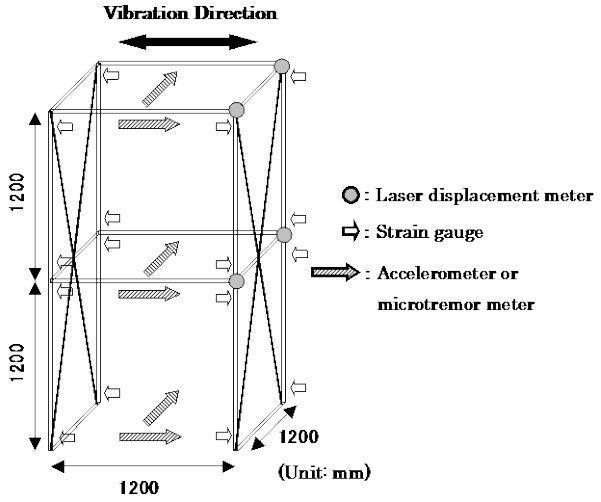

Figure 3. Experimental model.

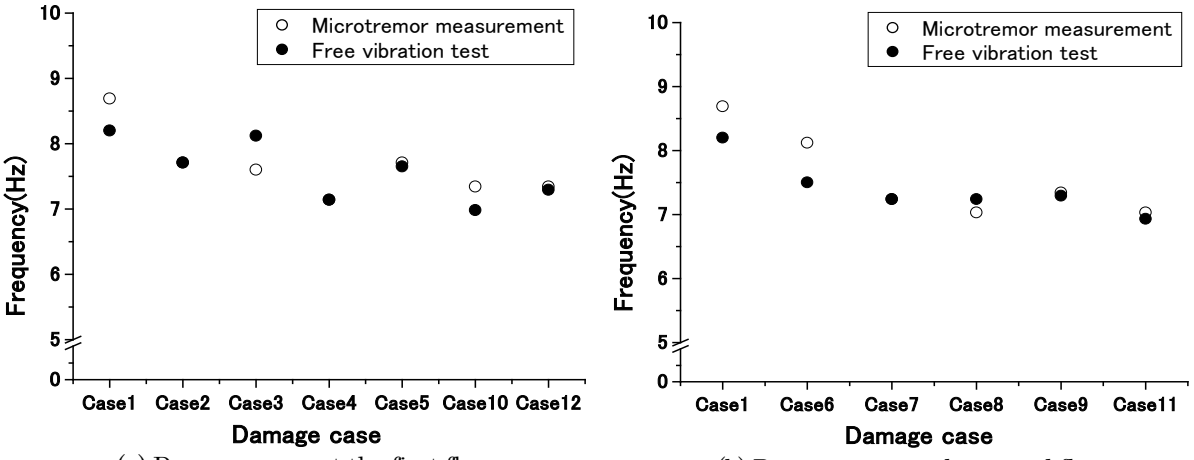

(a) Damage cases at the first floor.

(b) Damage case at the second floor.

Figure 4. Relationships between damage cases and natural frequency.

microtremor measurements of the structure are same as those obtained by the free vibration test. This figure was categorized by the results at the first floor and the second floor. The values of natural frequencies of damage cases decrease in comparing with undamaged one. As mentioned above, it is possible to have an estimation of the sensitivity in the model and member properties. As a result we can say that, damage evaluation of the whole model from natural frequency is possible. However, it is obvious that damage evaluation of model in details is difficult.

In the next step, we estimate the floor position of the damaged structure. Amplitude of microtremor wave is a few microns and the signal of the laser sensor is very small. Therefore, we measured displacement at each floor level by using vibration tests.

The ratio of relative displacement in the first and second floors was defined as the index to detect the damaged floor. **Figure 5** shows the comparison between these values with damage cases. As we can see in case of the first floor, the ratios become low according to the fracture scale of the frame (Cases 2, 5, 10). In the second floor same as the first floor, the ratio also increases according to the fracture scale of the frame (Cases 6, 9). However, in the damage cases by disconnecting the beam-column connection in the second floor in Case 11 and the base-column connection in Case 12, we cannot find damage detection by using this presented ratio because, it is difficult to evaluate the change of dynamic behavior by disconnecting the connection.

In order to detect the damage, the ratio was calculated. In the third step, the maximum strain ratio of damaged

frame to undamaged frame was used to detect the member of damaged frame. The relationship between the ratios and damage cases in the forced vibration tests was shown in **Figure 6**. The tendency in the results has a characteristic in which strain of the column with damage becomes small. The location and number of the strain gauges and the calculation method of the strain ratio were shown in **Figure 7**. The difference of the maximum strain ratio in two columns become large as damage grade becomes larger. The maximum strain ratio of the undamaged frames is close to 1. The similar trend also was appeared at the second floor. In the disconnection cases, the ratio of No. 8/6 located at the base level becomes low, if the damage occurs at another member of the frame. Therefore, this method was used as benchmark for comparison the damaged model to detect the damage.

A method has been conducted in the area of damage evaluation based on changes in dynamic properties of the structure. This method can be classified into three levels according to their performance.

Level I: The method that just identifies damage if it occurs.

Level II: The method that identifies damage if it occurs and determine the floor of the damage.

Level III: The method that identifies damage if it occurs and determines the location and estimates severity of the damage.

To detect the damage which was created to the frame, the presented method was applied to model structure. A non-destructive damage evaluation technique was performed in this study by using the results from the forced vibration test.

5. Conclusion

As mentioned above, by using three steps of the health monitoring techniques, changes in the natural frequency and maximum strain ratio showed that the damage evaluation of structure models was possible. As a future subject, this technique will be applied to an actual structure. Also more damage patterns like bending and buckling cases should be considered.

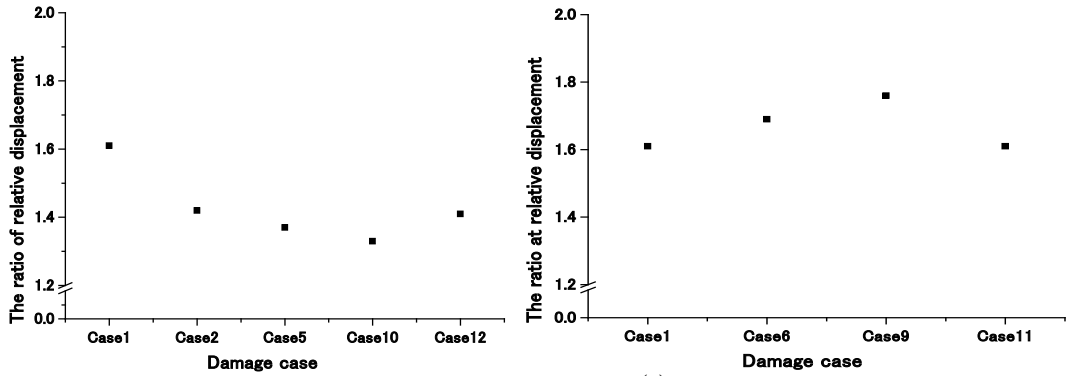

(a) Damage case at the first floor. (b) Damage case at the second floor.

Figure 5. Relationships between damage cases and the ratio of relative displacement.

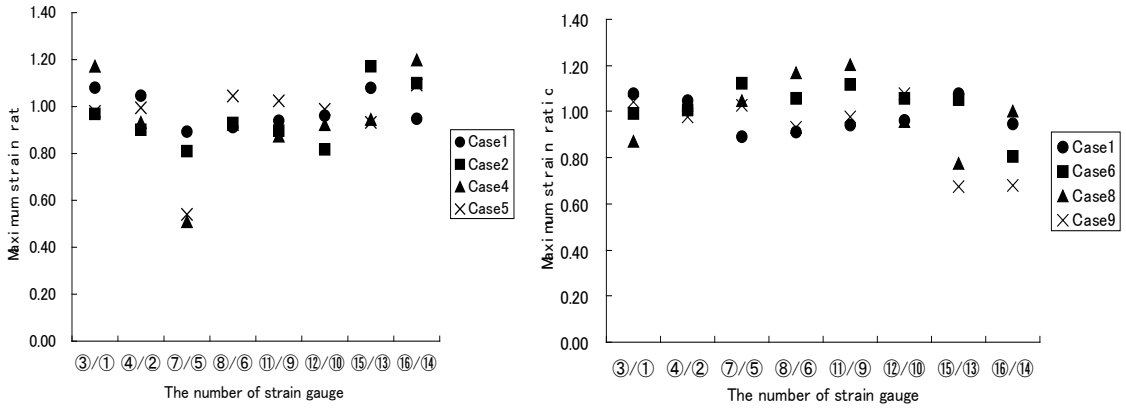

Figure 6. Relationships between damage cases and maximum strain ratio.

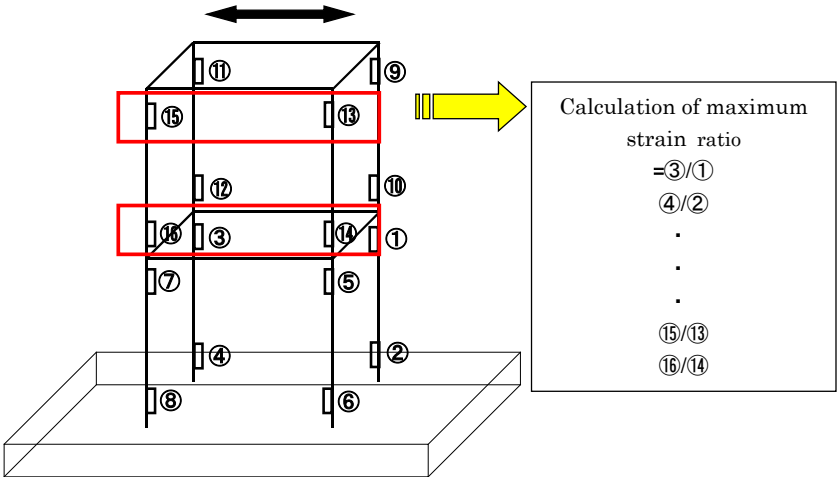

Figure 7. Location of strain guage.

Acknowledgements

The measurements were conducted with the assistance of participating students of Kanazawa University. A part of the expense of the study was supported by a Grant-in-Aid for research from the Ministry of Education, Science and Culture of Japan.

References

[1] Loh, C.H. and Tou, I.C. (1995) A System Identification Approach to the Detection of Changes in Both Linear and Non-Linear Structural Parameters. *Journal of Earthquake Engineering and Structural Dynamics*, **24**, 85-97. http://dx.doi.org/10.1002/eqe.4290240107

[2] Sone, A., *et al.* (1995) Estimation of Cumulative Damage of Building with Hysteretic Restoring Force by Using Wavelet Analysis of Strong Response Records. *Journal of Structural and Construction Engineering, AIJ*, No. 476, 67-74.

[3] Kitagawa, Y., *et al*. (2003) The Study on Diagnostic System of Structural Damage and Degradation. *Journal of Structural Engineering*, **49B**, 57-62.

[4] Sutoh, A. and Hoshiya, M. (1996) Optimization of Steel Structural System under Earthquake Excitation. *Proceeding of* 11*th World Conference on Earthquake Engineering*. CD-ROM.

[5] Ventura, C.E., *et al.* A Study on Damage Detection Using Output-Only Modal Data. http://vbn.aau.dk/files/12774317/A_Study_on_Damage_Detection_Using_Ouput-Only_Modal_Data

[6] Salawu, O. (1997) Detection of Structural Damage through Changes in Frequency: A Review. *Engineering Structures*, **19**, 718-723. http://dx.doi.org/10.1016/S0141-0296(96)00149-6

[7] Lifshitz, J. and Rotem, A. (1969) Determination of Reinforcement Unbonding of Composites by a Vibration Technique. *Journal of Composite Materials*, **3**, 412-423. http://dx.doi.org/10.1177/002199836900300305

[8] Hearn, G. and Testa, R. (1991) Modal Analysis for Damage Detection in Structures. *Journal of Structural Engineering*, **117**, 3042-3062. http://dx.doi.org/10.1061/(ASCE)0733-9445(1991)117:10(3042)

[9] Hasan, W. (1995) Crack Detection from the Variation of the Eigenfrequencies of Abeam on Elastic Foundation. *Engineering Fracture Mechanics*, **52**, 409-421. http://dx.doi.org/10.1016/0013-7944(95)00037-V

[10] Sinou, J.-J. (2007) Numerical Investigations of a Robust Identification of Crack Location and Size in Beams Using Only Changes in Ratio Pulsations of the Cracked Beams. *Structural Engineering Mechanics*, **25**, 691-716.

[11] Caron, J.N., DiComo, G.P. and Nikitin, S. (2011) Generation of Ultransound in Materials Using High Power Fiber Lasers. *Optics Letters*, 37830-37832.

[12] Staszewski, W.J., Lee, B.C. and Traynor, R. (2007) Fatigue Crack Detection in Metallic Structures with Lamb Waves and 3D Laser Vibrometry. *Measurement Science and Technology*, **18**, 727-739. http://dx.doi.org/10.1088/0957-0233/18/3/024

[13] An, Y.-K. and Sohn, H. (2011) Instantaneo Crack Detection under Varying Temperature and Static Loading Conditions. *Structural Control & Health Monitoring*, **17**, 730-741. http://dx.doi.org/10.1002/stc.394

[14] Ruzzene, M. (2007) Frequency-Wavenumber Domain Filtering for Improved Damage Visualization. *IOP Publishing, Smart Material and Structures*, **16**, 2116-2129. http://dx.doi.org/10.1088/0964-1726/16/6/014

[15] Giurgiutiu, V. (2005) Tuned Lamb Wave Excitation and Detection with Piezoelectric Wafer Active Sensor of Structural Health Monitoring. *Journal of Intelligent Material Systems and Structures*, **16**, 291-305. http://dx.doi.org/10.1177/1045389X05050106

[16] An, Y.-K., Park, B. and Sohn, H. (2013) Complete Noncontact Laser Ultrasonic Imaging for Automated Crack Visualization in a Plate. *Smart Material and Structures*, **22**, 1-10. http://dx.doi.org/10.1088/0964-1726/22/2/025022

[17] Raghavan, A. and Cesnik, C.E.S. (2007) Review of Guided-Wave Structural Health Monitoring. *Shock & Vibration Digest*, **39**, 91-114. http://dx.doi.org/10.1177/0583102406075428

Open Journal of Civil Engineering, 2014, 4, 361-372
Published Online December 2014 in SciRes. http://www.scirp.org/journal/ojce
http://dx.doi.org/10.4236/ojce.2014.44031

A Study on the Seismic Isolation Systems of Bridges with Lead Rubber Bearings

Woo-Suk Kim, Dong-Joon Ahn, Jong-Kook Lee*

School of Architecture, Kumoh National Institute of Technology, Gumi, Republic of Korea
Email: kimw@kumoh.ac.kr, djahn@kumoh.ac.kr, *ljk@kumoh.ac.kr

Received 12 September 2014; revised 8 October 2014; accepted 28 October 2014

Abstract

This study consists of the development and presentation of example of seismic isolation system analysis and design for a continuous, 3-span, cast-in-place concrete box girder bridge. It is expected that example is developed for all Lead-Rubber Bearing (LRB) seismic isolation system on piers and abutments which placed in between super-structure and sub-structure. Design forces, displacements, and drifts are given distinctive consideration in accordance with Caltrans Seismic Design Criteria (2004). Most of all, total displacement $\left(D_{\mathrm{TM}}=457\ \mathrm{mm}\right)$ on design for all LRBs case is reduced comparing with combined lead-rubber and elastomeric bearing system $\left(D_{\mathrm{TM}}=533\ \mathrm{mm}\right)$. Therefore, this represents substantial reduction in cost because of reduction of expansion joint. This presents a summary of analysis and design of seismic isolation system by energy mitigation with LRB on bridges.

Keywords

Seismic Isolation System, Bridge, Lead Rubber Bearing (LRB), Energy Mitigation

1. Introduction

Seismic isolation systems are the separating of structures (such as bridge, building, railway, road, airport, harbor, dam, and tunnel etc.) from ground motions generated by earthquakes which could induce damage to the structures. Among various seismic isolation systems, lead-rubber bearing (LRB) which has innovative mechanism can lead to increased effective stiffness and is accommodating force in reinforced concrete (RC) structures. LRB is a novel apparatus based on the combination of laminated layers rubber bearing using lead plugs (Constantinou, *et al*. (2006) [1]). In this research, a bridge was selected to demonstrate the application of analysis and bearing

*Corresponding author.

How to cite this paper: Kim, W.-S., Ahn, D.-J. and Lee, J.-K. (2014) A Study on the Seismic Isolation Systems of Bridges with Lead Rubber Bearings. *Open Journal of Civil Engineering*, **4**, 361-372. http://dx.doi.org/10.4236/ojce.2014.44031

design procedures for seismic isolation system. The bridge was used as an example of bridge design without an isolation system in the Federal Highway Administration (FHWA) Seismic Design Course, Design Example No. 4, prepared by Berger/Abam Engineers (1996) [2]. The bridge is a continuous, three-span, cast-in-place concrete box girder structure with a 30-degree skew. The two intermediate bents consist of two round columns with a crossbeam on top. The geometry of the bridge, section properties and foundation properties are assumed to be the same in the original bridge in the FHWA example (2000) [3]. It is presumed that the original bridge design is sufficient to sustain the loads and displacement demands when seismically isolated as described herein. Only minor changes in the bridge geometry were implemented in order to facilitate seismic isolation.

2. Description of Bridge

Figures 1-3 show, respectively, the plan and elevation, the abutment sections and a section at an intermediate bent. In **Figure 3**, the bent is shown at the skew angle of 30 degrees, whereas for the box girder the section is perpendicular to the longitudinal axis. The actual distance between the column centerlines is 7.92 m (**Figure 1**).

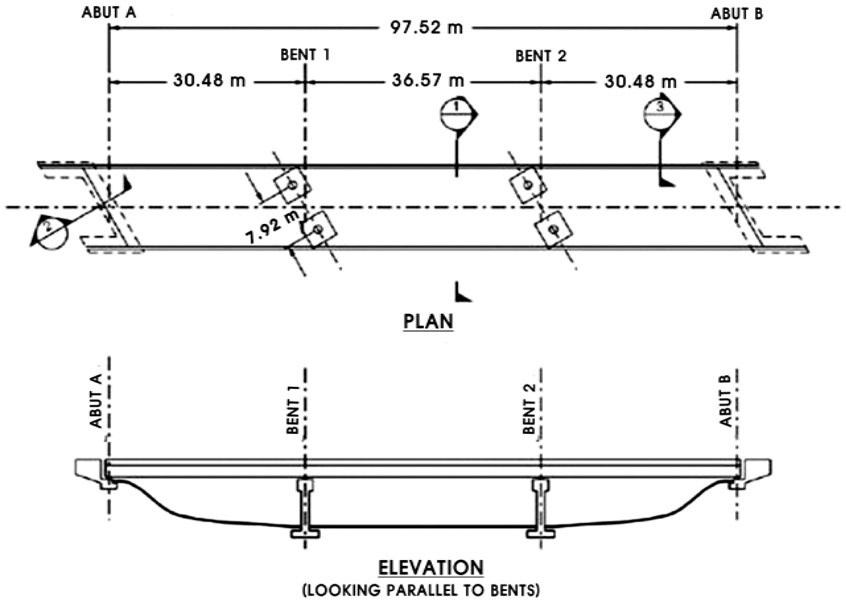

Figure 1. Bridge plan view and elevation.

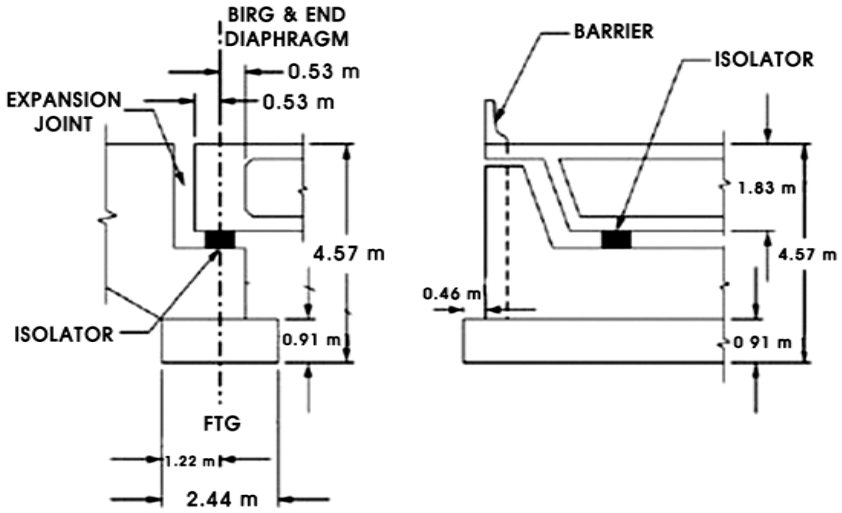

Figure 2. Section at abutment.

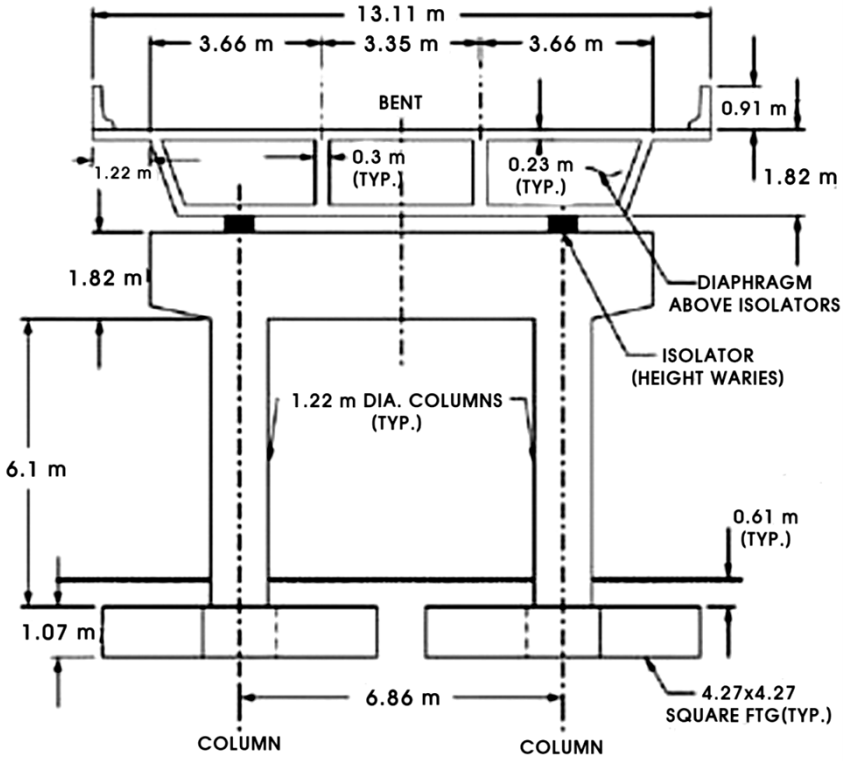

Figure 3. Cross section at intermediate bent.

The bridge is isolated with two multi-directional seismic isolators at each abutment and pier location for a total of eight multi-directional seismic isolators with lead rubber bearings. The isolators are directly located above the circular columns. The plan views of the isolated bridge are shown in **Figure 4**.

The bridge is isolated with two isolators at each abutment and pier location for a total of eight isolators. The isolators are directly located above the circular columns. The use of two isolators versus a larger number is intentional for the following reasons:

- With elastomeric bearings it is possible to achieve a larger period of isolation (more mass per bearing).
- The distribution of load on each isolator is accurately calculated. The use of more than two isolators per location would have resulted in uncertainty in the calculation of the axial load in vertically stiff bearings.
- Reduction in construction cost.

For better distribution of load to the bearings, diaphragms are included in the box girder at the abutment and pier locations above the isolators. An additional 596 kN weight at each diaphragm location is introduced by the addition of these diagrams. The bridge is considered to have three traffic lanes. Loadings were determined based on AASHTO LRFD Specifications (2001) [4] with live load consisting of truck, lane and tandem and wind load being representative of typical sites in the Western United States.

Figure 5 shows a model for the analysis of the bridge. The model may be used in static and multimode analysis.

The cross sectional properties of the bridge and weights are presented in **Table 1**. The modulus of elasticity of concrete is $E = 24.82$ GPa . Foundation spring constants are presented in **Table 2**.

2.1. Analysis of Bridge for Dead, Live, Brake and Wind Loadings

The weight of the seismically isolated bridge superstructure is 22,650 kN. The difference is due to the presence now of diaphragms at the abutment and pier locations in order to transfer loads to the bearings. Kim (2007) [5] presents calculations for the bearing loads and rotations due to dead, live, braking and wind forces. **Table 3** presents a summary of bearing loads and rotations. On the basis of the results in **Table 3**, the bearings do not experience uplift or tension for any combination of dead and live loadings.

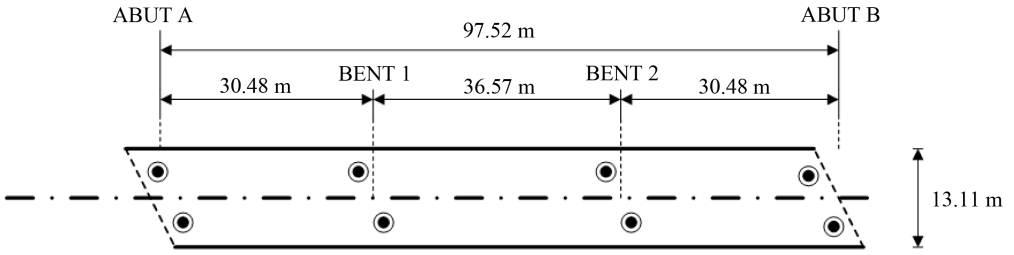

Figure 4. Plan view of bridge isolated with lead-rubber bearings.

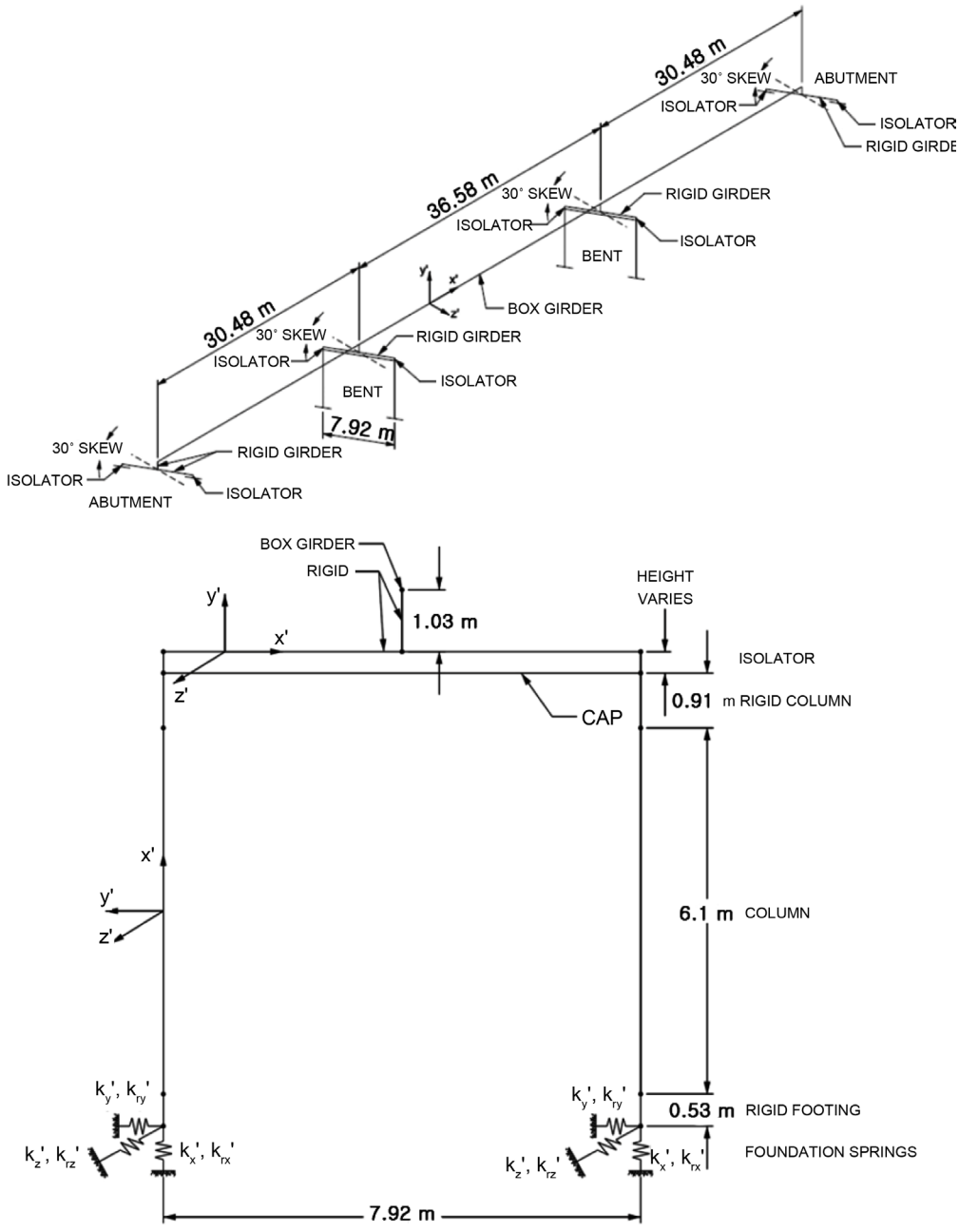

Figure 5. Model of bridge for single- and multimode analysis.

Table 1. Cross sectional properties and weights in bridge model.

Element Property	Box Girder	Bent Cap Beam	Column	Rigid Girder	Rigid Column	Rigid Footing
Area A_x^* (m^2)	6.76	2.23	1.17	18.58	18.58	18.58
Shear Area A_Y^* (m^2)	2.25	2.23	1.17	18.58	18.58	18.58
Shear Area A_Z^* (m^2)	5.30	2.23	1.17	18.58	18.58	18.58
Moment of Inertia I_Y (m^4)	82.82	0.27	0.08**	854.07	854.07	854.07
Moment of Inertia I_Z (m^4)	3.42	0.61	0.08**	854.07	854.07	854.07
Torsional Constant I_X (m^4)	15.12	0.64	0.21	854.07	854.07	854.07
Weight (kN/m)	207.9***	76.8	27.6	0	0	858.4****

*: Coordinates *X*, *Y* and *Z* refer to the local member coordinate system; **: Cracked section properties (0.7 I_g); ***: Add 596 kN concentrated weight at each bent and abutment location; ****: Total weight of footing divided by length of 0.53 m.

Table 2. Foundation spring constants in bridge model.

Constant	$K_{X'}$ (kN/m)	$K_{Y'}$ (kN/m)	$K_{Z'}$ (kN/m)	$K_{rX'}$ (kN-m/rad)	$K_{rY'}$ (kN-m/rad)	$K_{rZ'}$ (kN-m/rad)
Description	Vertical stiffness	Transverse stiffness	Longitudinal stiffness	Torsional stiffness	Rocking stiffness about *Y'*	Rocking stiffness about *Z'*
Value	1,391,158	1,517,895	7,517,895	1.57×10^7	9.7×10^6	9.7×10^6

Table 3. Bearing loads and rotations due to dead, live, brake and wind loads.

Loading	Abutment Bearings (per bearing)		Pier Bearings (per bearing)	
	Reaction (kN)	Reaction (rad)	Reaction (kN)	Reaction (rad)
Dead Load	V + 1497	0.00149	V + 4166	0.00006
Live Load (Truck, Tandem or Lane)	V + 610 V − 69	0.00057	V + 1101 V − 84	0.00040
HL93 (Live + IM + BR)	V + 835 V − 119	0.00090	V + 1550 V − 139	0.00064
Braking (BR)	V + 14 V − 14	0.00006	V + 18 V − 18	0.00004
Wind on Load (WL)	V + 11 V − 11 T 10	Negligible	V + 31 V − 31 T 29	Negligible
Wind on Structure (WS)	V + 12 V − 12 T 28	Negligible	V + 40 V − 40 T 90	Negligible
Vertical Wind on Structure (WV)	V − 142	Negligible	V − 458	Negligible

V: Vertical reaction; T: Transverse reaction; +: Compressive force; −: Tensile force.

2.2. Seismic Loading

Seismic loading is defined per Caltrans Seismic Design Criteria (2004) [6] to be the 5%-damped response spec-

trum of Magnitude 7.25, 0.7 g acceleration and soil profile C. The horizontal response spectra for acceleration and displacement are shown in **Figure 6**. This earthquake is considered to be the Maximum Earthquake. Calculations are performed only for this earthquake level and isolator safety checks are performed on the basis of the calculated response at this level. The vertical earthquake is assumed to be described by the spectra of **Figure 6** after multiplication by factor 0.70.

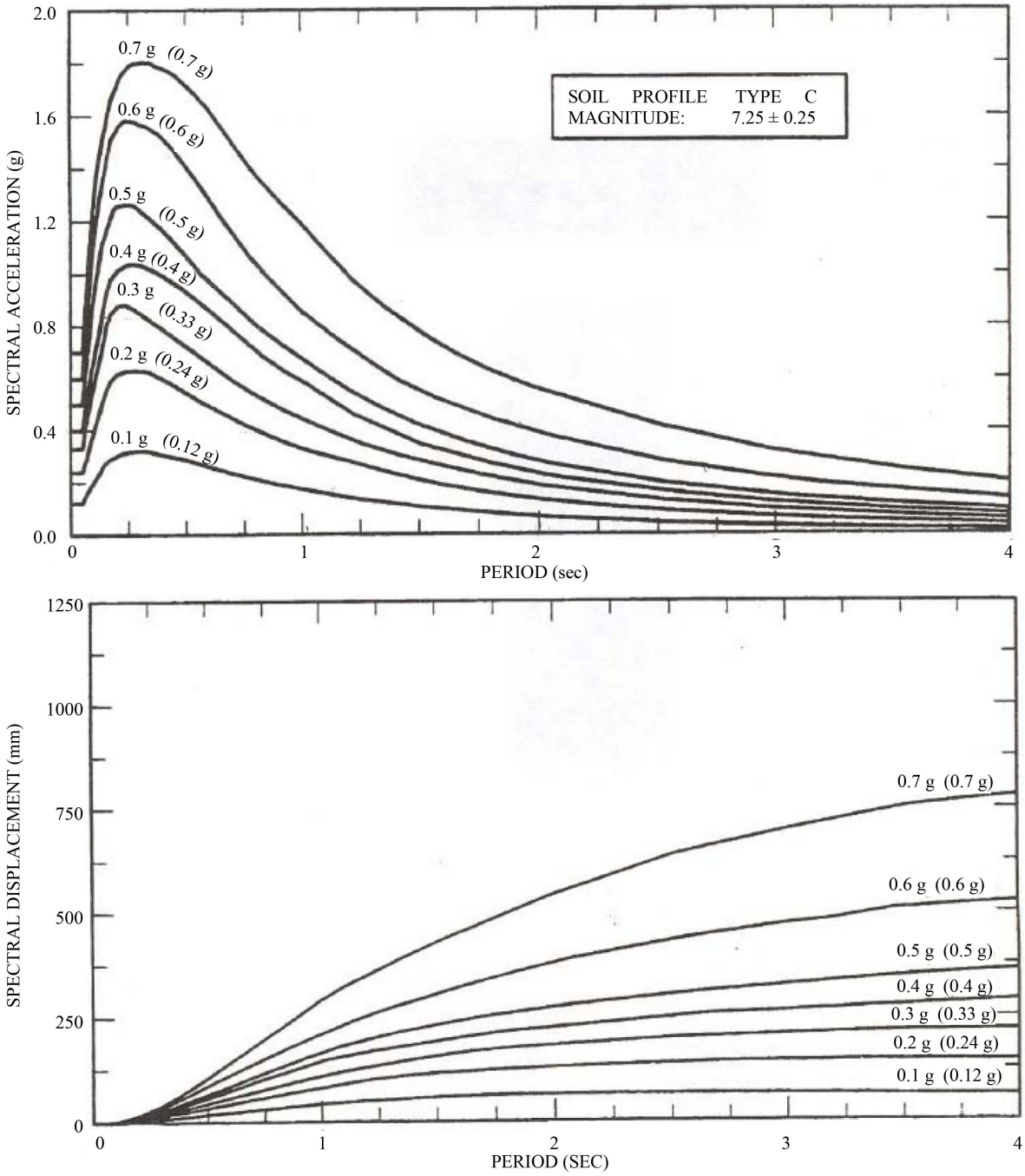

Note: Peak ground acceleration values not in parentheses are for rock (Soil Profile Type B) and peak ground acceleration values in parentheses are for Soil Profile Type C.

Figure 6. Horizontal 5%-damped response spectra for earthquake of magnitude 7.25 and soil profile type C (Adapted from Clatran Seismic Design Criteria (2004) [6]).

3. Design Analysis of Lead-Rubber Isolation System

This case study is developed as an alternative to the combined lead-rubber and elastomeric bearing isolation system (Constatinou, *et al*., 2007 [7]). The combined system may not be desirable because two different isolator types are used in an application with only eight bearings. An all lead-rubber bearing system is simpler and requires less testing.

3.1. Single Mode Analysis

Criteria for applicability of single mode analysis are presented in **Table 4**. Kim (2007) [5] presents the calculations for the analysis and safety check of the isolation system. The all pier abutment and pier bearings are lead-rubber bearings with 200 mm diameter lead core. All bearings are of identical construction and of identical materials. Drawing of the bearings is shown in **Figure 7**. The bearings need not be installed pre-deformed in order to accommodate displacements due to post-tensioning and shrinkage. The bearings are safe for a service displacement of 75 mm (includes shrinkage and post-tensioning effects) and 455 mm seismic displacement.

Table 5 presents a summary of the calculated displacement and force demands, the effective properties of the isolated structure and the effective properties of each type of bearing. These properties are useful in response spectrum, multi-mode analysis. The effective stiffness was calculated using

$$K_{\text{eff}} = K_d + \frac{Q_d}{D_M} \tag{1}$$

where (a) for abutment bearing, $K_d = 1016$ kN/m and $Q_d = 234.85$ kN for lower bound and $K_d = 1439$ kN/m and $Q_d = 610.7$ kN for upper bound, and (b) for each pier bearing, $K_d = 1439$ kN/m and $Q_d = 313.1$ kN for lower bound and $K_d = 1439$ kN/m and $Q_d = 615.1$ kN for upper bound.

Table 4. Applicability criteria for methods of analysis.

Method of Analysis	Application Criteria
Single Mode	1) Soil profile type A, B, C or D. 2) Bridge without significant curvature, defined as having a subtended angle in plan not more than 30˚. 3) Effective period $T_{\text{eff}} \le 4.0$ sec . 4) Effective damping $\beta_{\text{eff}} \le 0.30$. Method may be used when $\beta_{\text{eff}} > 0.30$ but less than 0.50 provided that $\beta_{\text{eff}} = 0.30$ is used. 5) Distance from active fault is more than 10 km. 6) The isolation system does not limit maximum displacement to less than the calculated demand. 7) The isolation system meets the re-centering capability criteria of Section 3.4 (Constantinou, *et al*., 2007) [7].
Multimode	1) Soil profile type A, B, C or D. 2) Bridge of any configuration. 3) Effective period $T_{\text{eff}} \le 4.0$ sec . 4) Effective damping $\beta_{\text{eff}} \le 0.30$. Method may be used when $\beta_{\text{eff}} > 0.30$ but less than 0.50 provided that $\beta_{\text{eff}} = 0.30$ is used. 5) Distance from active fault >10 km. 6) The isolation system does not limit maximum displacement to less than the calculated demand. 7) The isolation system meets the re-centering capability criteria of Section 3.4 (Constantinou, *et al*., 2007) [7].
Response History	1) Applicable in all cases. 2) Required when distance to active fault is less than 10 km. 3) Required when soil profile type is E or F. 4) Required when $T_{\text{eff}} > 4.0$ sec or $\beta_{\text{eff}} > 0.50$. 5) Required when the isolation system does not meet there-centering capability criteria of Section 3.4 (Constantinou, *et al*., 2007) [6], but it meets the criterion that the period calculated using the tangent stiffness of the isolation system at the design displacement is less than 6.0 sec.

Table 5. Applicability criteria for methods of analysis.

Parameter	Upper Bound Analysis	Lower Bound Analysis
Maximum Displacement D_M (mm)[1]	269	396
Total Maximum Displacement D_{TM} (mm)[2]	N.A.	457.2
Base Shear/Weight	0.350	0.240
Abutment Bearing Seismic Axial Force (kN)[3]	813.14	784.22
Pier Bearing Seismic Axial Force (kN)[3]	2820.17	2786.81
Abutment Bearing Seismic Axial Force (kN)[4]	524.00	307.37
Pier Bearing Seismic Axial Force (kN)[4]	1124.96	1028.43
Effective Stiffness of Each Abutment Bearing K_{eff} (kN/m)	3730	1620
Effective Stiffness of Each Pier Bearing K_{eff} (kN/m)	3730	1810
Effective Damping	0.352	0.242
Damping Parameter B	1.800	1.660
Effective Period T_M (sec) (Substructure Flexibility Neglected)	1.76	2.58
Effective Period T_M (sec) (Substructure Flexibility Considered)	1.87	2.67

[1]Based on one-directional excitation in longitudinal bridge direction; [2]Based on three-directional excitation using 100% - 30% - 30% rule, and multiplying by Factor 1.1; [3]Value is for 100% vertical + 30% transverse + 30% longitudinal combination (maximum axial load); [4]Value is for 100% transverse + 30% vertical + 30% longitudinal combination (worst case for lead-rubber bearing safety check-combined with maximum bearing displacement).

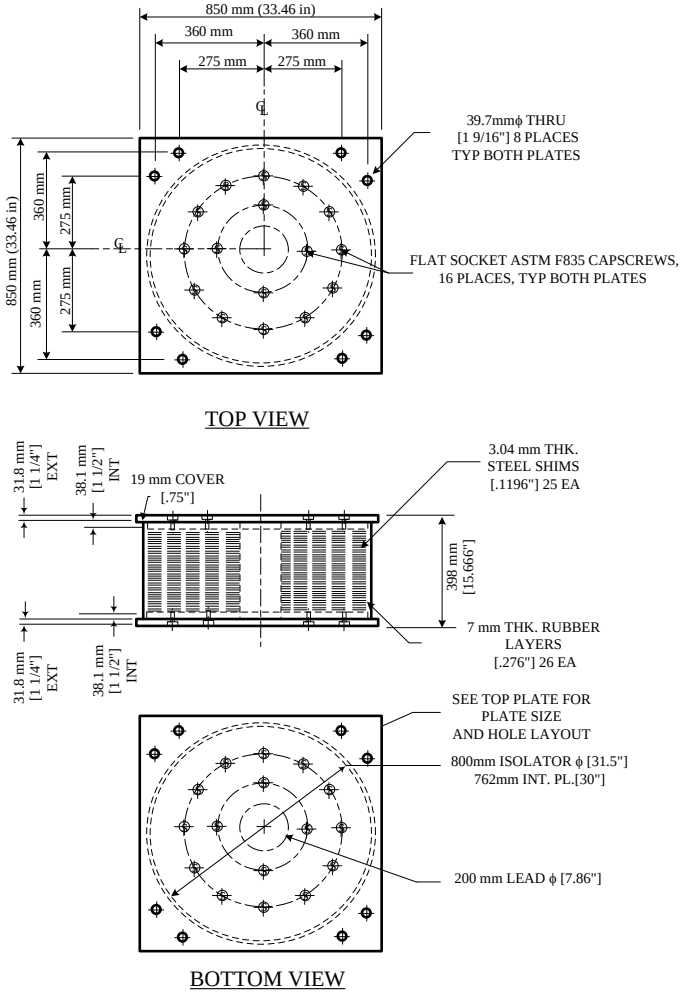

Figure 7. Principle structure and size of LRB for bridge example.

3.2. Multimode Response Spectrum Analysis

Figure 8 shows the bridge model used for response spectrum analysis. For this analysis, each isolator is modeled as a vertical 3-dimentional beam element-rigidly connected at its two ends-of length h, area A, moment of inertia about both bending axes I and torsional constant J. The element length is the height of the bearing, $h = 400$ mm (average height of bearings) and the area is calculated as described below in order to represent the vertical bearing stiffness. Note that the element is intentionally used with rigid connections at its two ends so that $P-\Delta$ effects are properly distributed to the top and bottom parts of the bearing. The vertical bearing stiffness was calculated using the theory presented in Section 9 of the report (Constantinou, *et al.*, (2007) [7]). Particularly, the vertical stiffness in the laterally un-deformed configuration is given by

$$K = \frac{A_r}{T_r}\left[\frac{1}{E_c} + \frac{4}{3K}\right]^{-1} \tag{2}$$

In Equation (2), T_r is total rubber thickness, T_r is the bonded rubber area (however adjusted for the effects of rubber cover by adding the rubber thickness to the rubber bonded diameter), K is the bulk modulus of rubber (assumed to be 2000 MPa). Moreover, E_c is the compression modulus given by

$$E_c = 6GS^2F \tag{3}$$

where G is the shear modulus of rubber, S is the shape factor and F is given by Equation (4) below with E_o and E_i being the outside and inside bonded diameters of the bearing. Note that for the calculation of the vertical stiffness of the lead-rubber bearing we consider that the lead core does not exist and treat the bearing as one without a hole for which parameter $F = 1$. Also, we used the nominal value of shear modulus G under static conditions in order to obtain a minimum value of vertical stiffness that can also be used in the bearing performance specifications.

$$F = \frac{\left(\frac{D_o}{D_i}\right)^2 + 1}{\left(\frac{D_o}{D_i} - 1\right)^2} + \frac{1 + \frac{D_o}{D_i}}{\left(1 - \frac{D_o}{D_i}\right)\ln\frac{D_o}{D_i}} \tag{4}$$

Torsional constant is set $J = 0$ or a number near zero since the bearing has insignificant torsional resistance. Moreover, shear deformations in the element are de-activated. The moment of inertia of each element is calculated by use of the following equation

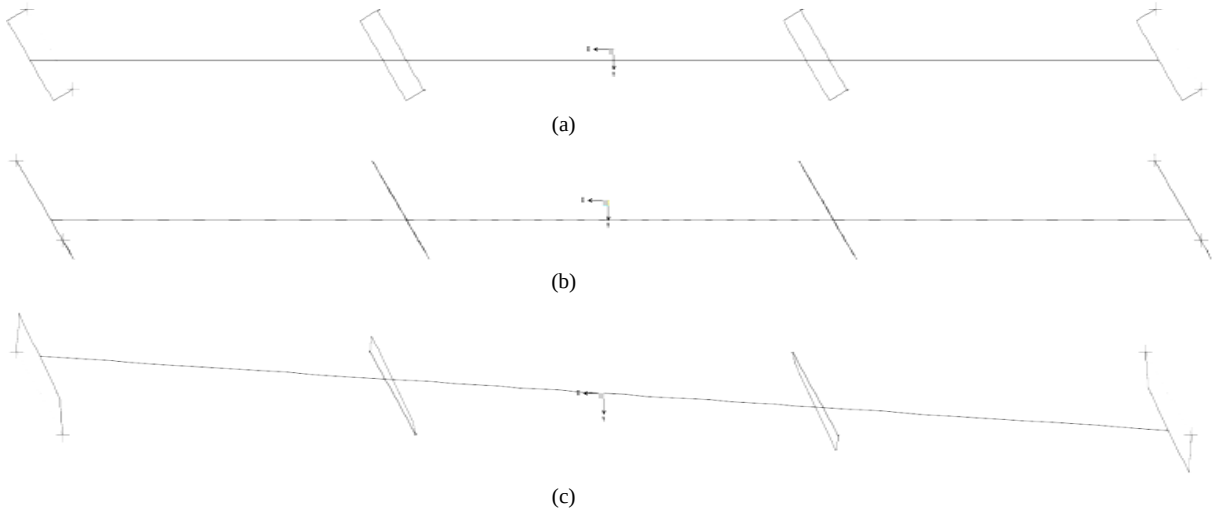

(a)

(b)

(c)

Figure 8. First three modes of vibration of isolated bridge with lead-rubber bearing system in lower bound analysis. (a) First mode: T_1 = 2.67 sec; (b) Second mode: T_2 = 2.61 sec; (c) Third mode: T_3 = 2.21 sec.

$$I = \frac{K_{\text{eff}} h^3}{12E} \tag{5}$$

Response spectrum analysis was performed using the response spectrum of **Figure 8** for 0.7 g which is 5%-damped spectrum after division by parameter B for periods larger or equal to 0.8 T_M, where T_M is the effective period and B is the parameter that relates the 5%-damped spectrum to the spectrum at the effective damping. Quantities T_M, B and the effective damping are presented in **Table 5**. It should be noted that these quantities are given in **Table 5** for the upper and lower bound cases, both of which are analyzed. Values of 0.8 T_M are 1.3 sec for upper bound analysis and 2.0 sec for lower bound analysis. Values of parameters used in response spectrum analysis of lead-rubber bearing isolation system are presented in **Table 6**. Besides, values of spectral acceleration used in the analysis are presented in **Table 7**.

Eigenvalue and response spectrum analysis were performed in program SAP2000 [8]. **Figure 8** presents the mode shapes of the first three modes of vibration of the isolated bridge in the lower bound analysis. They are two modes dominated by translational displacements in two orthogonal directions, and a third torsional mode of vibration. The results are qualitatively the same as those for the combined lead-rubber and elastomeric bearing system with the first mode characterized by deformation of both the isolators and the piers along the weak direction of the pier. The period matches nearly exactly the period that is calculated in simplified analysis accounting for the effects of substructure flexibility (T = 2.67 sec). The second mode is deformation along the strong axis of the pier and accordingly it consists primarily of isolator deformation. This period matches nearly the period calculated neglecting the effect of substructure flexibility (T = 2.58 sec).

Analysis was performed by separately applying the earthquake excitation in the longitudinal, transverse and vertical bridge directions. The vertical response spectrum was taken as a 70% portion of the horizontal 5%-damped spectrum without any modification for increased damping.

The results of these analyses are presented in **Table 8** in terms of the bearing displacements; isolation shear force and bearing axial forces (only part due to earthquake). **Table 8** presents a comparison of key response quantities obtained by the single and multimode-response spectrum methods of analysis. In each type of analysis, quantity D_{TM} was calculated as the vectorial sum of bearing displacements due to longitudinal and transverse earthquake components combined using the 100% - 30% rule and then multiplying by Factor 1.1. The results demonstrate very good agreement in the calculated bearing displacement demands and isolation shear forces between the two methods of analysis.

Axial bearing forces are underestimated by the single mode analysis method due, primarily, to neglect of the skew in the calculations. Consideration of the skew angle is not difficult but the underestimation in the calculation of loads to have any significance in the safety of the bearings. Calculations show that the bearings have capacity to sustain the calculated loads in the maximum earthquake.

Table 6. Values of parameters h, A, I and E used in response spectrum analysis of lead-rubber bearing isolation system.

Bearing Location	Parameter	Upper Bound Analysis	Lower Bound Analysis
Abutment	Effective Horizontal Stiffness K_{eff} (kN/m)	3730	1620
	Vertical Stiffness K_v (kN/m)	1,760,000	1,760,000
	Height h (mm)	398.8	398.8
	Modulus E (MPa)	99,963	99,963
	Area A (mm^2)	6987	6987
	Moment of Inertia I (cm^4)	19.5978	8.4982
Pier	Effective Horizontal Stiffness K_{eff} (kN/m)	3730	1810
	Vertical Stiffness K_v (kN/m)	1,760,000	1,760,000
	Height h (mm)	398.8	398.8
	Modulus E (MPa)	99,963	99,963
	Area A (mm^2)	6987	6987
	Moment of Inertia I (cm^4)	19.5978	8.4982

Table 7. Spectral acceleration values used in response spectrum analysis of isolated bridge with lead-rubber bearing system.

Period T (sec)	Spectral Acceleration for 5%-Damping (g)*	Spectral Acceleration for Upper Bound Analysis (g)	Spectral Acceleration for Lower Bound Analysis (g)
0	0.70	0.70	0.70
0.05	0.70	0.70	0.70
0.10	1.29	1.33	1.33
0.24	1.77	1.78	1.78
0.30	1.80	1.80	1.80
0.50	1.72	1.75	1.75
0.75	1.44	1.44	1.44
1.00	1.19	1.19	1.19
1.25	0.95	0.95	0.95
1.40	0.86	0.48	0.86
1.50	0.78	0.43	0.78
1.60	0.72	0.40	0.72
1.75	0.64	0.36	0.64
2.00	0.55	0.31	0.55
2.10	0.53	0.29	0.32
2.20	0.50	0.28	0.30
2.50	0.41	0.23	0.25
2.75	0.37	0.21	0.22
3.00	0.32	0.18	0.19
3.25	0.29	0.16	0.17
3.50	0.25	0.14	0.15
3.75	0.23	0.13	0.14
4.00	0.20	0.11	0.12

*Vertical excitation spectrum is 0.7 times the 5%-damped horizontal spectrum.

Table 8. Key response quantities obtained by multimode analysis isolated bridge with lead-rubber bearing system.

Parameter	Upper Bound Analysis		
	100% Longitudinal EQ	100% Transverse EQ	100% Vertical EQ
Maximum Bearing Displacement, D_M (mm)	231.1 (P); 289.6 (A)	43.6 (P); 48.5 (A)	-
Isolation Shear/Weight	0.347	0.351	-
Bearing Axial Force (kN)	105.9 (P); 133.9 (A)	362.1 (P); 391.0 (A)	3226.3 (P); 1217.9 (A)
Parameter	Lower Bound Analysis		
	100% Longitudinal EQ	100% Transverse EQ	100% Vertical EQ
Maximum Bearing Displacement, D_M (mm)	355.6 (P); 406.4 (A)	373.4 (P); 398.8 (A)	-
Isolation Shear/Weight	0.234	0.236	-
Bearing Axial Force (kN)	50.0 (P); 61.8 (A)	230.0 (P); 251.8 (A)	3226.3 (P); 1217.9 (A)

Note: (P) denotes the pier bearings and (A) denotes the abutment bearings.

4. Conclusions

The examples presented in this paper demonstrate that single-mode and multi-mode analysis methods, when properly implemented, provide results in close agreement. On the basis of the results obtained in this study, the single mode method of analysis is sufficiently accurate and conservative to be used in analysis and design.

Examples of specifications which are consistent with the assumptions made in the analysis have been presented in this study. **Table 9** presents a summary of key response quantities for the two example designs of this paper as obtained by the single mode method of analysis. These quantities are the total maximum dis-

Table 9. Comparison of key response quantities for two examples as obtained by single mode method of analysis (W = 22,650 kN).

System	Lower Bound Analysis				Upper Bound Analysis			
	D_{TM} (mm)	F/W	F_a/W	F_p/W	D_M (mm)	F/W	F_a/W	F_p/W_p
Lead-Rubber and Elastomeric Bearing*	533	0.250	0.098	0.152	318	0.308	0.095	0.213
Lead-Rubber Bearing	457	0.240	0.113	0.127	269	0.350	0.175	0.175

*Constantinou, *et al.* (2007).

placement D_{TM} in the lower bound analysis, the maximum displacement D_T in the upper bound analysis, the base shear F/W and the portions of shear transmitted to the abutments, F_a/W, and piers, F_p/W, all normalized by the bridge weight W = 22,650 kN. The results demonstrate that the displacement demands in the two systems are about 457 to 533 mm. Brief summaries are as follows.

1) Total displacement $\left(D_{\mathrm{TM}} = 457\ \mathrm{mm}\right)$ on design for all Lead-Rubber bearings case is reduced comparing with combined lead-rubber and elastomeric bearing system $\left(D_{\mathrm{TM}} = 533\ \mathrm{mm}\right)$. As a result, this represents substantial reduction in cost because of reduction of expansion joint.

2) In lower bound analysis, the benefit of all LRB versus Elastomeric bearing/LRB is almost 2% reduction in shear force at pier. When F_p/W ratio is reduced, the force at pier is reduced by increasing stiffness.

3) Furthermore, while previous design requires tests for two types of bearing, another benefit is that construction and testing is needed to only one type of bearing.

Acknowledgements

The authors would like to gratefully acknowledge Professor Michael C. Constantinou for his advice to this study. This research was supported by research fund, Kumoh National Institute of Technology.

References

[1] Constantinou, M.C., Whittaker, A.S., Kalpakidis, Y., Fenz, D.M. and Warn, G.P. (2006) Performance of Seismic Isolation Hardware under Service and Seismic Loading. Technical Report MCEER-07-0012, Multidisciplinary Center for Earthquake Engineering Research, State University of New York at Buffalo, Buffalo.

[2] Berger/Abam Engineers, Inc. (1996) Federal Highway Administration Seismic Design Course, Design Example No. 4. (Document Available through NTIS, Document No. PB97-142111).

[3] Federal Emergency Management Agency (2000) Prestandard and Commentary for the Seismic Rehabilitation of Buildings. FEMA 356, Washington DC.

[4] American Institute of Steel Construction (AISC) (2001) Manual for Steel Construction, Load and Resistance Factor Design. 3rd Edition, American Institute of Steel Construction-AISC, Chicago.

[5] Kim, W. (2007) Seismic Isolation of Bridges with Lead Rubber Bearings and Friction Pendulum Bearings with Viscous Dampers. State University of New York at Buffalo, Master Project Report, Buffalo.

[6] California Department of Transportation (2004) Caltrans Seismic Design Criteria. Version 1.3. California Department of Transportation, Sacramento.

[7] Constantinou, M.C., Whittaker, A.S., Fenz, D.M. and Apostolakis, G. (2007) Seismic Isolation of Bridges. Version 2, Report to Sponsor, California Department of Transportation, Sacramento.

[8] CSI (2002) SAP 2000 Analysis Reference Manual. Computers and Structures Inc., Berkeley.

Open Journal of Civil Engineering, 2014, 4, 373-385
Published Online December 2014 in SciRes. http://www.scirp.org/journal/ojce
http://dx.doi.org/10.4236/ojce.2014.44032

3D-Analysis of Soil-Foundation-Structure Interaction in Layered Soil

Mohd Ahmed[1*], Mahmoud H. Mohamed[2], Javed Mallick[3], Mohd Abul Hasan[4]

Civil Engineering Department, Faculty of Engineering, King Khalid University, Abha, KSA
Email: [*]moahmedkku@gmail.com

Received 26 September 2014; revised 22 October 2014; accepted 20 November 2014

Abstract

The analysis of building structure in contact with soil involves an interactive process of stresses and strains developed within the structure and the soil field. The response of Piled-Raft Foundation system to the structure is very challenging because there is an important interplay between the component of building structure and the soil field. Herein, soil-foundation-structure interaction of buildings founded on Piled-Raft Foundation is evaluated through 3D-Nonlinear Finite Element Analyses using PLAXIS3D FOUNDATION code. The soil settlements and forces demand of the high-rise building structures and foundation is computed. The parametric study affecting the soil-foundation-structure response has been carried out. The parameters such as construction phasing, sequential loading, building aspect ratios, soil failure models and thickness proportion of soil field stiff layer, are considered. It is concluded that the interaction of building foundation-soil field and super-structure has remarkable effect on the structure.

Keywords

Foundation, Piled-Raft Foundation, Soil Models, Soil Field, Finite Element Method, Sequential Loading, Construction Phase

1. Introduction

The analysis of Piled-Raft Foundation is very challenging because the load in the piled-raft structures is transferred to the soil not only by the interaction between the soil and the piles but also by the interaction between foundation structure and superstructure. In this interaction, deformations in the soils are the key factor which will affect forces and deformation in foundation and superstructure. The soils below the ground level are heterogeneous and often found as layered system, *i.e*. layer wise varying properties below the ground. The combined

[*]Corresponding author.

How to cite this paper: Ahmed, M., Mohamed, M.H., Mallick, J. and Hasan, M.A. (2014) 3D-Analysis of Soil-Foundation-Structure Interaction in Layered Soil. *Open Journal of Civil Engineering*, **4**, 373-385.
http://dx.doi.org/10.4236/ojce.2014.44032

piled-raft foundation penetrates deep into the foundation soil increasing its significant depth below the ground and affects the response of structure and soil. The method of analysis of foundation and structure also affects the response of structure and soil. The complex foundation system requires a reliable advance computational method that can simulate the 3D-non-linear soil behavior and structure-foundation system interaction. Considerable attention has been paid to analyze, design and construction of combined piled-raft foundation (CPRF) system. The survey of various analytical methods and numerical methods used to model the behavior of geomechanics has been presented by [1]. The various aspects contributed in reference to piled-raft foundation design have been compiled by Hemsley [2]. Ahmed *et al*. [3] has pointed out the recent advances in the piled-raft foundation system. Lin and Feng [4] have presented piled-raft analysis output for settlement, bending moment both in pile and raft, and effects of raft flexibility for vertical uniform loading in the subsoil. For the case of piled raft placed over soft clay layer, the contact pressure is merely 4% - 6%, whereas it is 15% - 25% if the piled raft resting on sand layer at ground surface. Rabiei [5] has carried out the parametric study on piled-raft foundation design. The parameter studied were pile length and spacing, number of piles, raft thickness, pile-soil and raft-soil stiffness ratio and pile-raft interaction. They concluded that by ignoring the interactions involved in the piled raft system, may lead to serious underestimates of settlement and also lead to inaccurate estimates of raft bending moments and pile loads. Singh and Singh [6] demonstrated that ignoring the interactions between the piled raft foundations elements may lead to a very serious over-estimate of the stiffness of the foundation. The case studies on optimized piled-raft foundation performance comprising of connected and non-connected piles using simple 2D analysis are presented by Eslami *et al*. [7]. A simplified procedure applicable has been presented by Kapackci and Ozkan [8] for estimation of piled-raft settlement. Nguyen *et al.* [9] has proposed a simplified design approach of piled-raft foundations under vertical load considering interaction effects. They compared the results of method with experimental and other numerical results and found good agreement between the results. The optimization study of piled-raft foundation systems has been carried out by Horikoshi and Randolph [10]. It is experimentally demonstrated that model rafts, founded on structurally disconnected pile reinforced sand, will have reduced settlement and bending moments [11]. Field measurements of the load observed for the raft and the piles of piled-raft foundation on stiff clays at working conditions are reported by Cooke [12]. They suggest that the ratio of load in the most heavily loaded piles in the perimeter of the group to that in the least heavily loaded pile near the centre could be about 2.5. A displacement based design procedure is proposed by Prakoso and Kulhawy [13] for piled-raft foundation based on the results of simplified linear elastic and nonlinear plane strain piled-raft finite element models. The effect of raft and pile group compression capacity was evaluated on the raft settlements, raft bending moments, and pile-raft load transfer ratio. Mahmood and Ahmed [14] have carried out the dynamic analysis of framed including the soil-structure interaction effects and concluded that the soil-structure interaction problem can have beneficial effects on the structural behavior when non-linear soil models and interface conditions are considered. Shayea and Zeedan [15] have presented a new approach for the design of raft foundation using 3-D modelling of each part of the whole structure (superstructure, raft and the soil) and considering the soil structure interaction. They developed charts to show the relationship between thickness of raft and number of design parameters including soil type.

From the literature survey it is clear that the interaction of the superstructure in the soil-foundation analysis has not been taken into consideration in most of the research work and load from the super structure in considered acting directly on the raft as a uniform or concentrated load. The effect of construction phase and mode of superstructure loading on the response of structure and foundation has not been given due attention. In this paper, complete soil-structure interaction of combined Piled-Raft Foundation with the foundation soil and superstructure of the building is evaluated through 3D-nonlinear Finite Element Analyses using PLAXIS3D foundation code [16]. The different parameters affecting the soil-foundation-structure response, such as building aspect ratios, mode of load application to foundation soil, soil failure criteria of soil field and proportional thickness ratio of stiff soil in two-layer soil stratum is studied. The displacements and load demands imposed on the high-rise building structures having piled-raft foundation are computed. The most of the previous studies on soil-piled-raft foundation analysis are based on direct loading of superstructure on raft and without considering interaction of superstructure and foundation. The foundation soil in piled-raft foundation-soil models without including super structure will be stiffer than models with the one-phase super structure loading or sequential super structure loading. The foundation structure and soil field response is significantly affected by different building structure shape and soil failure models. The soil field response in layered soil is also affected by presence of lesser stiff layer below the raft. It is also observed effect on deflection and forces of superstructure components due to inclusion of loading phases in piled-raft foundation interaction analysis.

2. Statement of the Problem

A 15-storey square/rectangular building having piled raft foundation in the two layered soil system is selected for the complete structure-foundation interaction analysis. The square building (aspect ratio = 1) has 4 bays in X-and Y-direction and the rectangular building (aspect ratio = 1.75) has 3 bays in X-direction and 6 bays in Y-direction as shown in **Figure 1**. Buildings have nearly the same plan area. The ground and typical floors are 6.0 m and 3.0 m high respectively. The structural system of all floors is a flat concrete slab type of 200 mm thickness subjected to a total uniform load of 15 kN/m^2. Dimensions of columns are listed in **Table 1**. The concrete raft is assumed to be at a depth 2.0 (m) beneath the ground surface and has 1.5 (m) thicknesses. The plan dimension of square raft is 25 m × 25 m with overhang of 2.5 m while the plan dimension of rectangular raft is 19.2 m × 33.6 m with overhang of 2.4 m. The estimated total vertical load on square and rectangular rafts is 138.8 MN. A total of 25 circular concrete piles of 0.75 m diameter are located under the raft for each building structure. Modulus of elasticity of concrete is assumed as 3.4 × 107 kN/m^2 while concrete Poisson's ratio and density is considered in structural models as 0.2 and 25 kN/m^3 respectively. The typical floor plans and foundation plans having raft with pile location of square and rectangular shaped building are shown in **Figure 1**.

The slenderness ratio (L/D) of piles is taken as 26.7 and end tip of the piles are considered resting on the bottom surface of top soil layer having hardening soil model for different aspect of building, mode of application

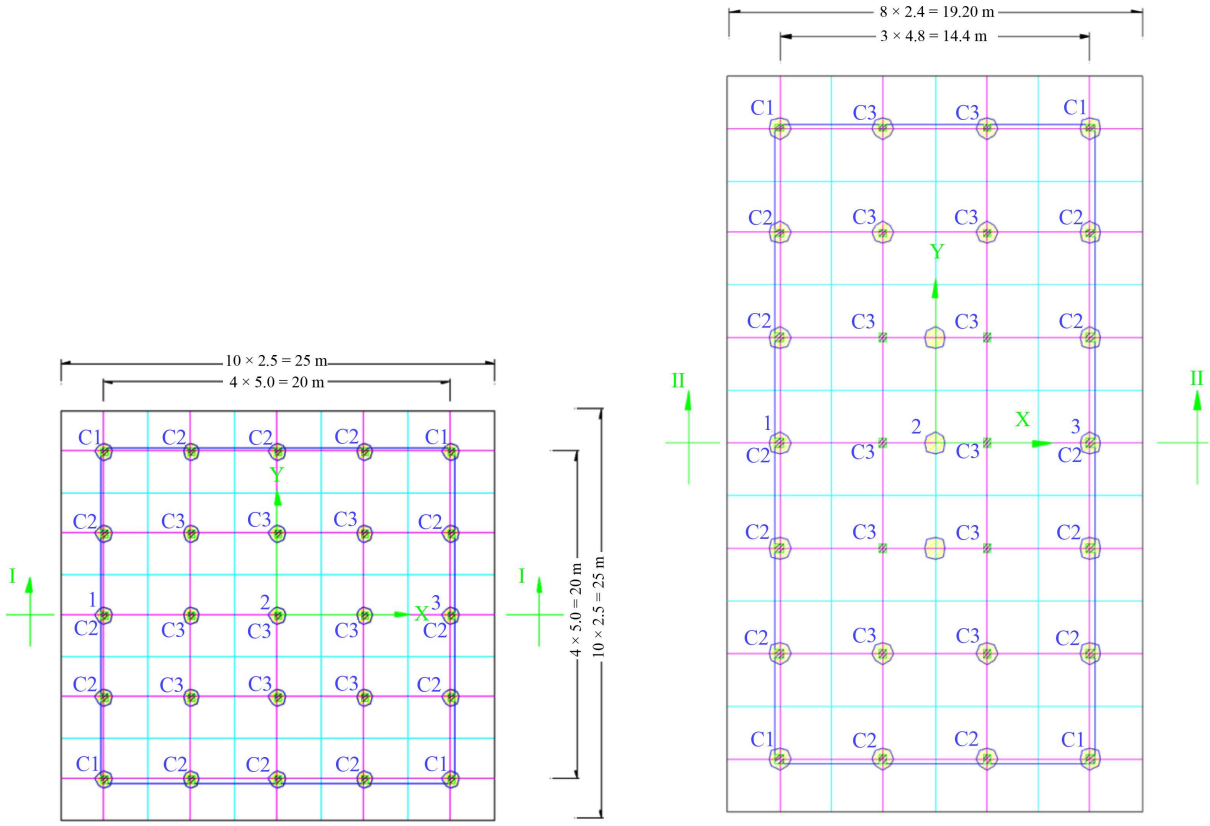

Figure 1. Typical floor and raft-pile plans of buildings.

Table 1. Dimension of columns in buildings.

Building Shape	Column Dimensions (m × m)		
	C1	C2	C3
Square	0.65 × 0.65	0.75 × 0.75	0.9 × 0.9
Rectangular	0.65 × 0.65	0.75 × 0.75	0.9 × 0.9

of structure loading on foundation and for different failure model of soils. Modulus of elasticity of pile material is taken as 2.35 × 107 kN/m^2 while its density is considered as 25 kN/m^3. The soil profile is of two layer systems with upper layer of loose sand and lower layer of dense sand (stiff soil). The different thickness of stiff soil is considered in the model to study the effect of stiff soil on the interaction analysis. Three thickness proportion of stiff soil namely 25%, 50% and 75% of total thickness are taken. The water level is assumed at the ground surface.

3. Soil Models

Soil is a complex material that behaves differently in primary loading, unloading and reloading. It exhibits non-linear behaviour well below failure condition with stress dependant stiffness [17]. The elastic-perfectly plastic models based on soil failure criteria namely, Mohr-coulomb (MC) and Mohr-coulomb incremental stiffness (MCI) with depth, are taken because of the most common used models. In the study, second order Hardening Soil (HS) model that considers shear hardening and compression hardening [17] and suitable to cohesion less soil is also used. The assigned soil parameters for the two layers soil field are given in **Table 2**.

4. Finite Element Modelling Methodology

The finite element method based on software PLAXIS 3D is used for three dimensional modelling of 15-storey building structure having piled-raft foundation in layered soil field. The columns and piles are modelled as frame elements with linear elastic properties. The interaction effect of pile and soil at the pile shaft is considered by means of Elasto-Plastic line-to-volume and point-to-volume interfaces [19] as an embedded pile model. The embedded pile model consisting of beam elements with non-linear skin and tip interfaces. There is no need for mesh refinement around piles as 3D mesh is not distorted by introducing embedded pile model [19]. The floor slab and raft is discretized using 6-node triangular plate elements with linear elastic properties. The soil field with two layers of non-cohesive soils namely loose and dense sand is modelled as 15-node wedge triangular continuum elements. The total number of elements in the discretized mesh for square building structure including soil field are 35,785 while for rectangular building structure including soil field, number of elements are 24,785. As the mesh discretization has no significant effect on piled-raft analysis result [20], mesh sensitivity has not been examined and mesh generated automatically by PLAXIS code is used for the analysis. The 3D finite elements structural models of square (aspect ratio = 1) and rectangular (aspect ratio = 1.75) shaped buildings with piled-raft foundation are shown in **Figure 2**. The cross-section of 3D finite elements soil field models are shown in **Figure 3**.

Table 2. Soil parameters for different soil models.

Parameters	Soil model	Soil layer	
		Loose sand	Dense sand
Unsaturated weight (γ_{unsat}), kN/m^3	All models	17	19
Saturated weight (γ_{sat})	All models	20	21
Stiffness (E_{50}^{ref}), kN/m^2	HS [9]	20,000	60,000
Stiffness (E_{oed}^{ref}), kN/m^2	HS [9]	20,000	60,000
Stiffness (E_{ur}^{ref}), kN/m^2	All models	100,000	180,000
Rate of increase of E with depth (ΔE) kN/m^2	MCI [18]	4720	31,470
Power (m)	HS	0.65	0.55
Poisson's ratio (ν)	All models	0.2	0.2
Dilatancy (ψ), degree	All models	2	8
Friction angle (φ), degree	All models	32	38
Cohesion (c_{ref}), kN/m^2	HS	0.1	0.1

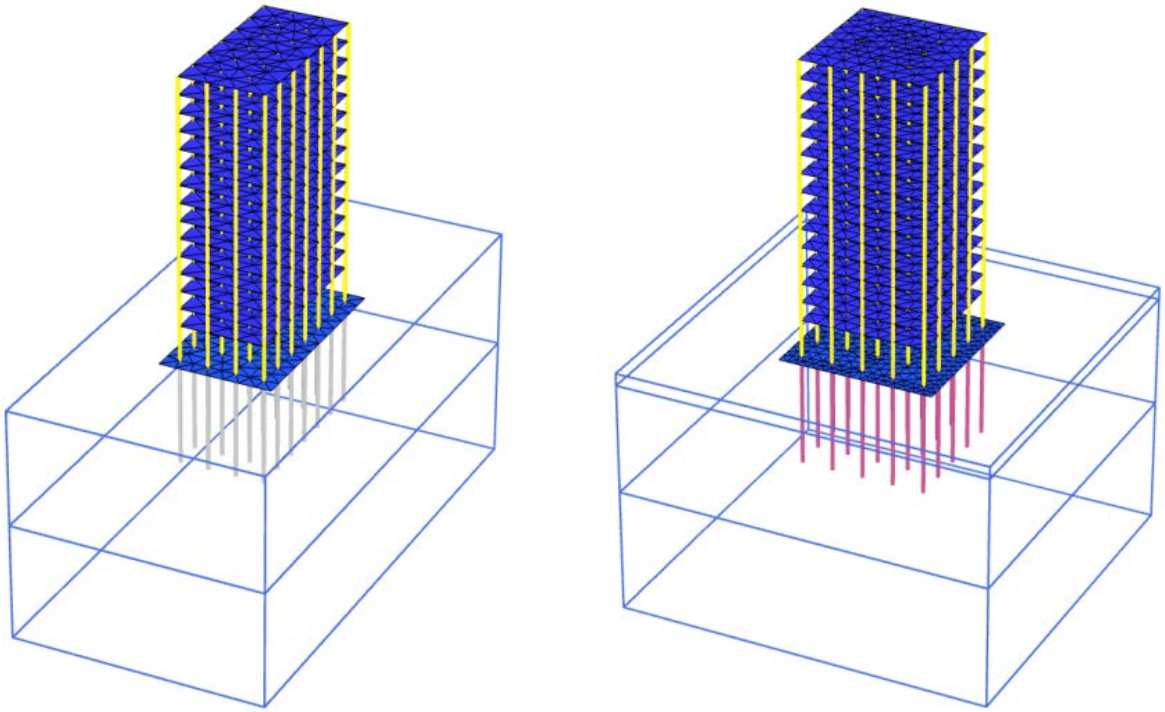

Figure 2. 3D model of buildings with piled-raft foundation.

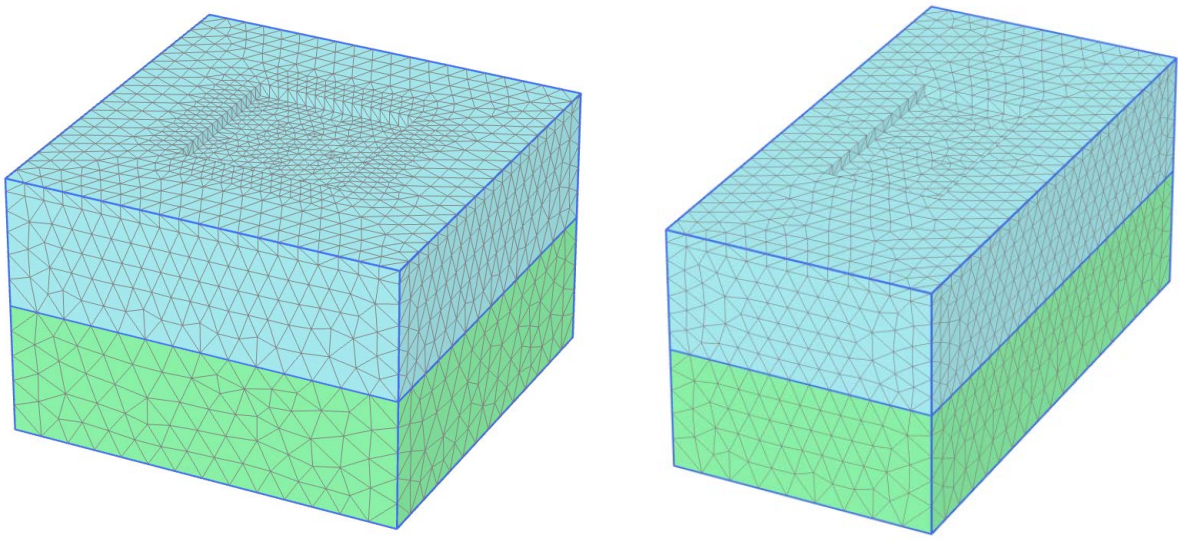

Figure 3. 3D finite elements foundation soil models of square and rectangular shaped buildings.

5. Results and Discussion

5.1. Foundation-Structure Interaction Effect on Soil Field

The results of interaction of building foundation-structure with different aspect ratio of building and different soil models on the soil are given in **Table 3**. The results are presented at three locations below the ground level, *i.e*. 2 m (below raft level), 10 m and 20 m below the ground. It is evident from the results that there is noteworthy effect of interaction of building aspect ratio and soil failure models on the soil response. The predicted amount of soil settlement is different with different aspect ratio of building. The soil settlement decreases with

Table 3. Maximum soil settlement with different soil models and building aspect ratio.

Soil Models	Location		Maximum Soil Settlement (cm)
Hardening Model (Aspect Ratio = 1.0 & 1.75)	Below the raft, 2 m below GL	Aspect Ratio = 1.0	23.19
		Aspect Ratio = 1.75	22.0
	10 m below GL	Aspect Ratio = 1.0	11.74
		Aspect Ratio = 1.75	11.30
	Below the pile, 20 m below GL	Aspect Ratio = 1.0	3.22
		Aspect Ratio = 1.75	3.05
Mohr-Coulomb Incremental Model (Aspect Ratio = 1.0)	Below the raft, 2 m below GL		26.83
	10 m below GL		14.37
	Below the pile, 20 m below GL		4.16
Mohr-Coulomb Incremental Model (Aspect Ratio = 1.0)	Below the raft, 2 m below GL		12.97
	10 m below GL		4.43
	Below the pile, 20 m below GL		1.23

the increase of aspect ratio of building. This may due to the reason that the load is distributed on a larger area in one direction of the building. The use of different soil failure model for soil field has also predicted dissimilar soil settlement. The behavior of soil at various levels also varies under different failure models of soil. The soil settlement is predicted highest using Mohr-coulomb failure criteria (MC) and predicted least by Mohr-coulomb incremental stiffness model (MCI). The soil settlements of a square building (aspect ratio = 1) at raft level are 26.83 cm, 12.97 cm and 23.19 cm respectively in Mohr-coulomb (MC) model, Mohr-coulomb incremental stiffness (MCI) model and hardening soil (HS) model while, the settlements at pile end are 4.16 cm, 1.23 cm and 3.22 cm. For the rectangular structure (aspect ratio = 1.75), the soil settlement is concentrated in the shorter direction of the building structure. The contours of soil settlements along vertical cross-section of the soil field for building aspect ratios and soil failure criteria are depicted in **Figure 4** and **Figure 5**.

Table 4 presents the soil settlements variation with proportional depth of loose sand layer of the building foundation soil. The contours of soil settlements along vertical and horizontal cross-section of the soil field are shown in **Figure 6**. It is evident from the results that the maximum soil settlements go on increasing with the increase of depth of loose sand layer below the ground level. The soil settlements are also increases with the increase of loose sand layer at same level below the ground level. The maximum soil settlements with different proportional depth of loose sand layer are 18.46 cm, 23.19 cm and 23.95 cm respectively at loose sand depth 25%, 50% and 75% of total depth, while with similar proportional depth of loose sand layer, the settlements at bottom pile end are 2.76 cm, 3.22 cm and 6.0 cm. For different proportional depth of loose sand layer, settlement dissipates along the raft sides towards the outer edges of soil field. The change in soil settlement is observed with lesser stiff layer thickness up to the pile length and more thickness of lesser stiff layer will not affect the soil behavior in piled-raft foundation.

Table 5 shows the predicted soil settlements with the mode of super structure loading to the foundation soil. The contours of soil settlements along the vertical and horizontal cross-section of the soil field are shown in **Figure 7**. It is evident from the results that there is clear interaction of building structure with the foundation soil. The analysis of piled-raft foundation-soil models with super structure will indicate foundation soil to be more rigid than model without the super structure. The maximum soil settlements will decreases when loading is applied through the construction phasing of the building structure or sequential loading. The maximum soil settlements will increase when loading is applied through the vertical elements tributary area method of the structure. The maximum soil settlements are 23.19 cm 23.45 cm and 22.74 cm respectively at loading through the super structure, loading directly to footing and through sequential loading while on similar conditions of loading, the soil settlements at bottom pile end are 3.22 cm, 3.25 cm, and 3.16 cm.

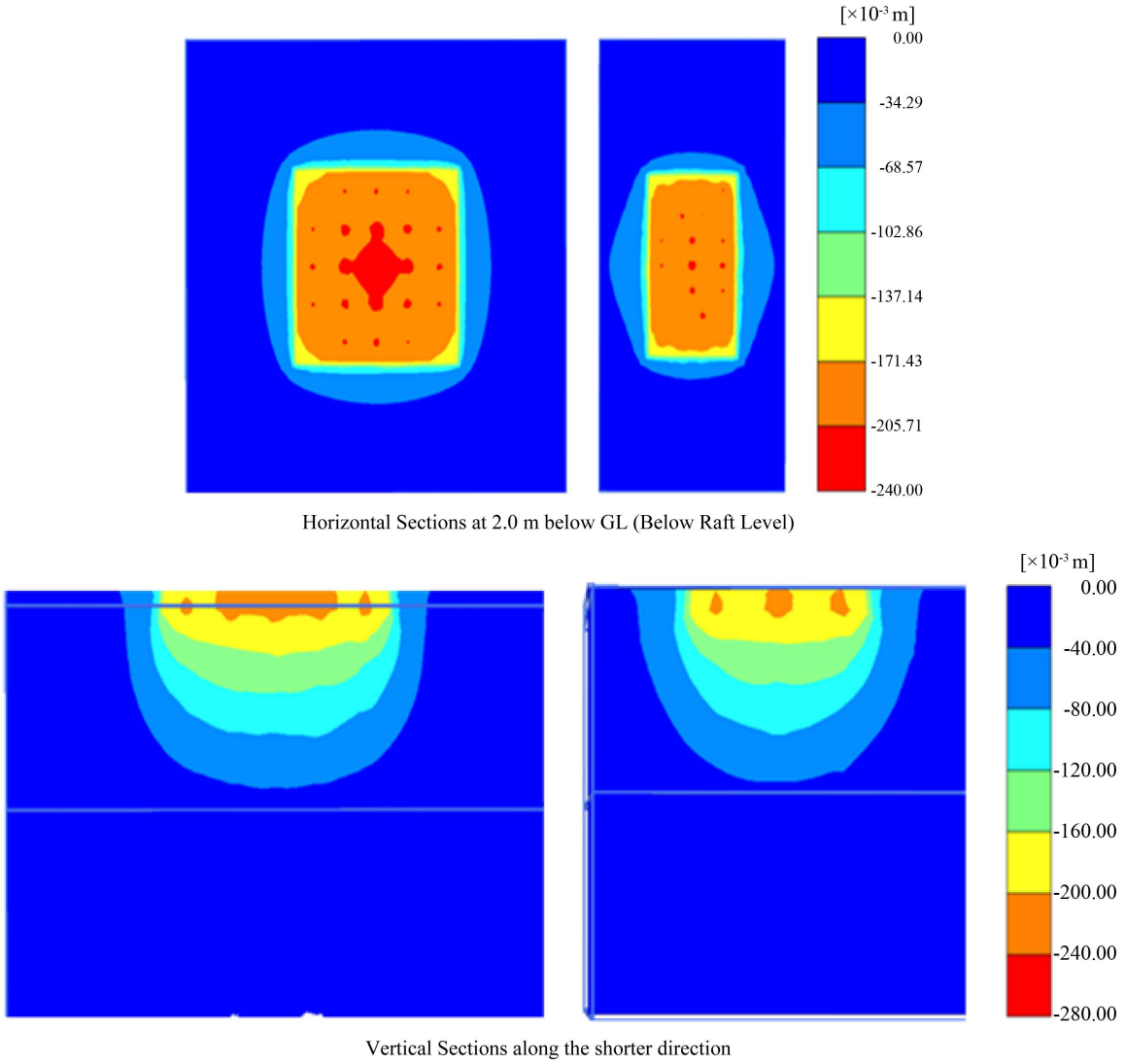

Figure 4. Contours of soil settlements on horizontal and vertical section of square (aspect ratio = 1.0) and rectangular buildings (aspect ratio = 1.75).

Table 4. Maximum soil settlement of square structure building with loose sand layer (HS) proportional depth.

Soil Models	Location	Maximum Soil Settlement (cm)
Top Loose Sand—−25% of total depth	Below the raft, 2 m below GL	18.46
	10 m below GL	5.49
	Below the pile, 20 m below GL	2.76
Top Loose Sand—−50% of total depth	Below the raft, 2 m below GL	23.19
	10 m below GL	11.74
	Below the pile, 20 m below GL	3.22
Top Loose Sand—−75% of total depth	Below the raft, 2 m below GL	23.95
	10 m below GL	13.89
	Below the pile, 20 m below GL	6.0

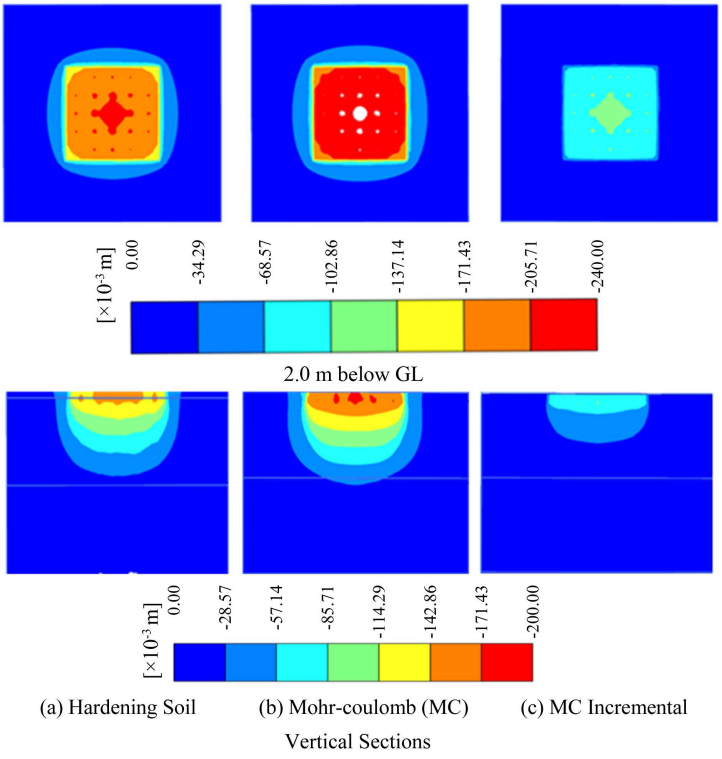

Figure 5. Contours of soil settlements on horizontal and vertical section of square buildings with soil models.

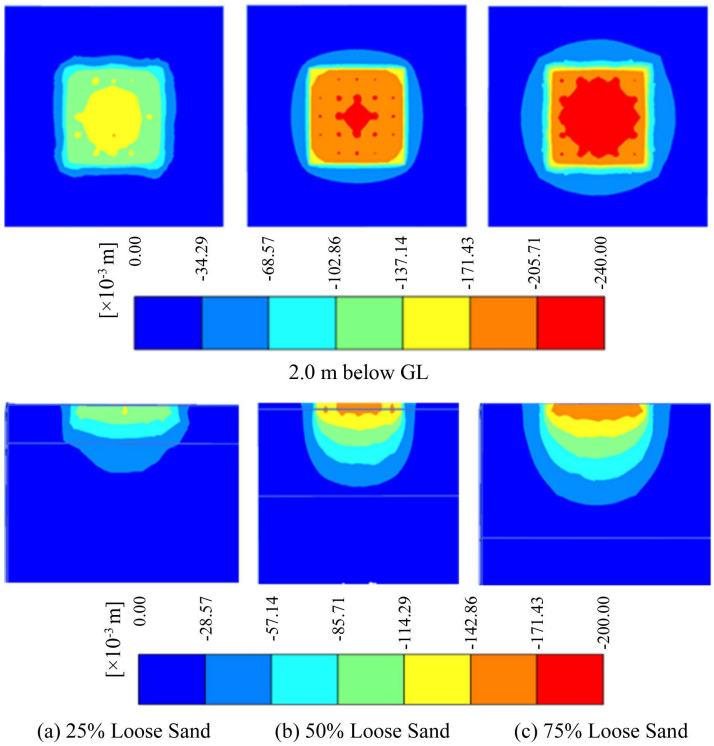

Figure 6. Contours of soil settlements on horizontal and vertical section of square buildings with proportional depth of loose sand (HS) layer.

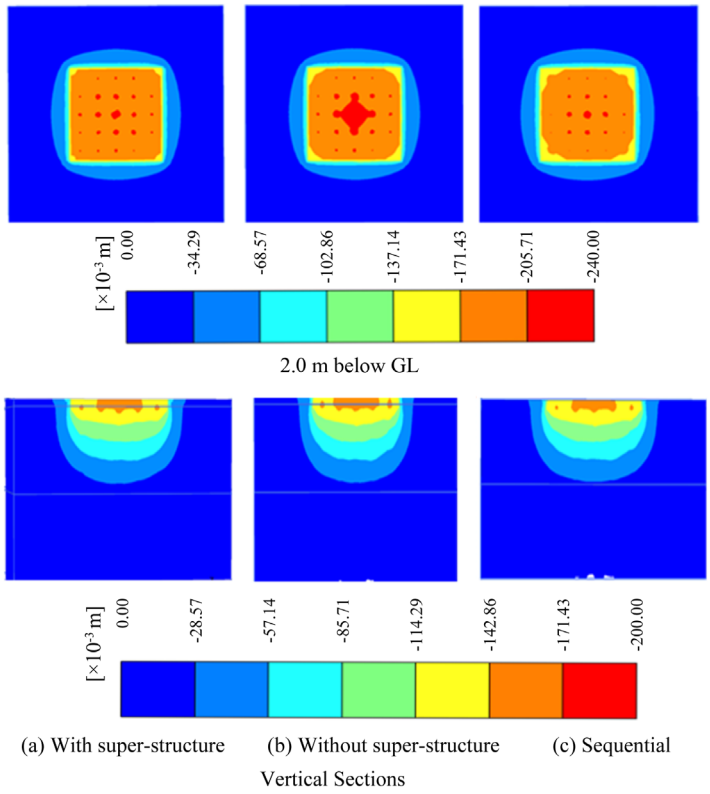

Figure 7. Contours of soil settlements on horizontal and vertical section of squarebuildings with mode of super structure loading.

Table 5. Maximum soil settlement of square structure building with mode of super structure loading.

Soil Models	Location	Maximum Soil Settlement (cm)
Loading through super structure	Below the raft, 2 m below GL	23.19
	10 m below GL	11.74
	Below the pile, 20 m below GL	3.22
Loading without super structure	Below the raft, 2 m below GL	23.45
	10 m below GL	11.6
	Below the pile, 20 m below GL	3.25
Sequential loading through super structure	Below the raft, 2 m below GL	22.74
	10 m below GL	11.47
	Below the pile, 20 m below GL	3.16

5.2. Foundation-Structure Interaction Effect on Piled-Raft Footing

Table 6 shows the analysis results of interaction of building foundation-structure on the component of piled-raft footing. The table shows the computed settlements of raft and total static load transferred from the upper structure to the raft of building with different aspect ratios and soil failure models. The forces developed in the raft are also presented in this table. The results of analysis depicts that the amount of raft maximum and differential settlement vary with different aspect ratio of buildings and failure models of soil. The differential settlement and raft forces decrease with the increase of aspect ratio of the building structure. The predicted differential settlement of the raft is highest using Mohr-coulomb failure criteria of soil field and it is least in Mohr-coulomb incremental stiffness model. The least value of maximum positive and negative moment in the raft is computed

Table 6. Differential settlement, moments and forces in the raft with different soil models and building structure aspect ratio.

Building Aspect Ratio	Settlements/Max. Moments/Max. Shear Force/Vertical Load	Soil Models		
		Hardening Model	Mohr Coulomb (MC) Model	MC Incremental Model
Aspect Ratio = 1.0 (Square)	Differential Settlement (cm)	7.3	7.8	6.37
	Positive Moment (kN·m/m)	4850	5092	4455
	Negative Moment (kN·m/m)	130	121	120
	Shear Force (kN)	4852	4986	4916
	Total Vertical Load (kN)	138,801	138,801	137,014
Aspect Ratio = 1.75 (Rectangular)	Differential Settlement (cm)	6		
	Positive Moment (kN·m/m)	2562		
	Negative Moment (kN·m/m)	213		
	Shear Force (kN)	1401		
	Total Vertical Load (kN)	138,812		

with Mohr-coulomb incremental stiffness (MCI) failure criteria. The computed value of raft maximum positive moments are (4850, 5092, 4455 kN·m/m), raft maximum negative moments are (130, 121, 120 kN·m/m), and raft maximum shear force are (4852, 4986, 4916 kN) using hardening soil (HS) model, Mohr-coulomb (MC) model and Mohr-coulomb incremental stiffness (MCI) model respectively. The maximum positive moment, maximum negative moment and maximum shear force in the raft obtained from the interaction analysis are 2563 kN·m/m, 213 kN·m/m and 1401 kN respectively for building aspect ratio of 1.75.

Table 7 and **Table 8** show the differential settlement and forces developed in the raft with proportional depth of loose sand and mode of loading to the foundation soil. The results of analysis concluded that the amount of raft maximum and differential settlement varies with different proportional depth of loose sand and mode of loading to the foundation soil. The differential settlement of the raft decreases with the increase of proportional depth of loose sand. The raft forces decreases with the increase of aspect ratio of the building structure. The predicted differential settlement of the raft is highest using Mohr-coulomb failure criteria of soil field and it is least in Mohr-coulomb incremental stiffness model. The lowest value of maximum negative moment in the raft is computed with lower thickness of loose sand layer while the lowest value of maximum shear in the raft is obtained with highest thickness of loose sand layer. The computed value of raft maximum positive moments are (5129, 4850, 4809 kN·m/m), raft maximum negative moments are (117, 130, 129 kN·m/m), and raft maximum shear force are (2390, 4852, 2295 kN) using 25%, 50% and 75% proportional thickness of loose sand layer respectively.

The analysis results of piled-raft foundation model, developed without the superstructure and loading directly to structure based on tributary area of columns and loading through super-structure with or without phasing of construction, is shown in the **Table 8**. The results of piled-raft foundation model with and without the superstructure indicate a clear interaction between the foundation-soil and the super structure. The bending moments and shear force due to loading and differential settlements in the raft are lesser in case of piled-raft foundation-soil model without the building super structure. The developed raft bending moments is maximum when is loading is transferred to footing is sequential manner. There is no noticeable interaction effect on differential settlements of the raft with different mode of application of loading to the foundation. The maximum and differential settlements of soil field due to piled-raft foundation with different mode of loading to foundation are (23.19 cm, 7.3 cm) and (23.45 cm, 6.76 cm), (22.74 cm, 7.32 cm) respectively due to loading through building super structure, loading directly to footing and due to sequential loading of the super structure. The maximum positive moments and negative moments, and maximum shear force in the raft are (4850 kN·m/m, 130 kN·m/m, 4852 kN), (3916 kN·m/m, 170 kN·m/m, 3626 kN) and (4850 kN·m/m, 131 kN·m/m, 4992 kN) respectively due to loading through building super structure, loading directly to piled-raft footing and due to sequential loading of

Table 7. Settlement, moments and forces in the raft with proportional depth of loose sand (HS) layer.

Settlements/Max. Moments/Max. Shear Force/Vertical Load	Proportional Depth of Loose Sand (HS) Layer		
	25% Loose Sand	50% Loose Sand	75% Loose Sand
Differential Settlement (cm)	9.26	7.3	7.26
Positive Moment (kN·m/m)	5129	4850	4809
Negative Moment (kN·m/m)	117	130	129
Shear Force (kN)	2390	4852	2295
Total Vertical Load (kN)	138,759	138,801	138,767

Table 8. Settlement, moments and forces in the raft with mode of super structure loading.

Settlements/Max. Moments/Max. Shear Force/Vertical Load	Mode of Super Structure Loading		
	Single Phase Super-Structure Loading	Without Super-Structure-Direct Loading	Sequential Loading
Maximum Settlement (cm)	23.19	23.45	22.74
Differential Settlement (cm)	7.3	6.76	7.32
Positive Moment (kN·m/m)	4850	3916	4856
Negative Moment (kN·m/m)	130	170	131
Shear Force (kN)	4852	3626	4992
Total Vertical Load (kN)	138,801	138,808	138,804

the super structure.

5.3. Foundation-Structure Interaction Effect on Super-Structure

Table 9 and **Table 10** show the results of interaction of building foundation-structure on the component of super-structure (*i.e.* columns and slabs) due to phasing of construction. The side sways (deflections) and axial loads in the columns are given in **Table 9**. The axial loads in columns of building are affected by the different mode of loading applied to the foundation soil. The maximum axial loading in the column increases while minimum axial loading decreases due to application of loading in sequential way. The maximum side sway or deflection of the column is increased when applied loading considers the construction phasing. The maximum top side sway in x and y directions for sequential loading to the building structure are 95 mm and 207 mm while deflections for one phase loading to the foundation are 12.2 mm and 43.3. The interaction of the super structure with the raft-foundation-soil will affect the maximum and minimum axial load of the columns. The maximum and minimum axial loads of the columns, obtained by incorporating the super-structure mode of loading to piled-raft foundation-soil model, are (9938 kN, 1768 kN) and (10,244 kN, 1740 kN) for one phase loading and for sequential loading to the building structure respectively while based on the column tributary area, the maximum and minimum axial load of the columns are 7556 kN and 2268 kN.

Table 10 depicts the maximum deflections and moments in slab at first, eighth floor and roof of the super structure with sequential loading to the foundation. The floor slab deflections and slab forces are different with different mode of loading of the building super structure. There is clear interaction effect on different floor of the building with phase loading of construction. The maximum deflection of the first floor slab is observed highest due to loading of super structure applied in sequential manner but observed decreasing on upper floors of building structure while deflection observed is more or less same if super structure loading is applied in single phase. The maximum deflection produced in the floor slabs of roof, eighth and first floor of the building super structure with different mode of loading to the foundation are (38.6 cm, 37.5 cm, 34.6 cm) and (16.1 cm, 24.0 cm, 38.8 cm) respectively due to loading in one phase through building super structure and due to sequential loading of the super structure. The moments developed in the roof slab are observed more after application of sequential loading of super structure than the other floor slabs and go on increasing on others floors of building structure. The maximum positive moments and negative moments in the roof slab, eighth and first floor of the

Table 9. Columns deflection and axial loads with mode of super structure loading.

Top Deflection (mm)/Axial Load (kN)	Mode of Super Structure Loading		
	Super-Structure Loading	Sequential Loading	Without Super-Structure Model
Top Deflection (x-dir.)	23.19	23.45	22.74
Top Deflection (y-dir.)	7.3	6.76	7.32
Axial Load (max.)	4850	3916	4856
Axial Load (min.)	130	170	131

Table 10. Maximum deflection and moments in the floors of square building structure with different mode of super structure loading.

Storey Level	Max. Slab Deflection/Max. Moments	Mode of Super Structure Loading	
		Single Phase Super-Structure Loading	Sequential Loading
First Floor	Deflection (mm)	34.6	38.8
	Positive Moment (kN·m/m)	64	64
	Negative Moment (kN·m/m)	97	97
Eighth Floor	Deflection (mm)	37.5	24.0
	Positive Moment (kN·m/m)	65	63
	Negative Moment (kN·m/m)	95	100
Roof	Deflection (mm)	38.6	16.1
	Positive Moment (kN·m/m)	66	61
	Negative Moment (kN·m/m)	94	106

building are respectively (66 kN·m/m, 94 kN·m/m), (65 kN·m/m, 95 kN·m/m) and (64 kN·m/m, 97 kN·m/m) due to loading through building super structure and while these forces respectively are (61 kN·m/m, 106 kN·m/m), (63 kN·m/m, 100 kN·m/m) and (64 kN·m/m, 97 kN·m/m) due to sequential loading of the super structure.

6. Conclusions

The analysis of combined piled-raft foundation of multi-storey building is very challenging because of complexities involved in the interaction between the components of building structure and soil field. The analysis of the tall building structure with complex foundation system in non-uniform (layered soil) soil field should include the interaction of structure-foundation-soil. In this study, the finite element 3D interaction analysis of building structure having piled-raft foundation in two layered non-cohesive soil field is carried out using PLAXIS 3D foundation code. The complete interaction among the soil field depth, soil layer type with foundation and foundation with super-structure with different aspect ratio and loading mode has been evaluated. The available literatures on soil-piled-raft foundation analysis are based on direct loading of superstructure on raft and without considering interaction of superstructure and foundation. The foundation soil in piled-raft foundation-soil models without including super structure will be stiffer than models with the one-phase super structure loading or sequential super structure loading.

The foundation structure and soil field response is significantly affected by different building structure shape and soil failure models. The foundation soil settlement and raft differential settlement is highest using Mohr-coulomb (MC) failure criteria of soil field among the HS, MC and MCI failure criteria. The soil field response in layered soil is also affected by presence of lesser stiff layer below the raft. The soil behavior in piled-raft foundation is not much affected by lesser stiff layer having thickness more than the pile length. A clear foundation-structure interaction effect is observed on the building superstructure components behavior with application of construction loading sequentially. The wide variability of deflection and moments of the floor slab is also observed due to loading of super structure applied in sequential manner which is not observed when super structure loading is applied as a single phase. The deflection and moments of the first floor slab is observed highest due to

loading of super structure applied in sequential manner but observed decreasing on upper floors of building structure.

References

[1] Bobet, A. (2010) Numerical Methods in Geo-Mechanics. *The Arabian Journal for Science and Engineering*, **35**, 27-48.

[2] Hemsley, J.A. (2000) Design Applications of Raft Foundations. Thomas Telford Ltd., London.

[3] Ahmed, M., Mahmoud, H. and Mallick, J. (2013) Advances in Piled-Raft Foundation System. *Recent Trends in Civil Engineering and Technology*, **3**, 1-8.

[4] Lin, D.G. and Feng, Z.Y. (2006) A Numerical Study of Piled Raft Foundations. *Journal of the Chinese Institute of Engineers*, **29**, 1091-1097. http://dx.doi.org/10.1080/02533839.2006.9671208

[5] Rabiei, M. (2010) Piled Raft Design for High Rise Building. *Electronic Journal of Geotechnical Engineering*, **15**, 495-505.

[6] Singh, N.T. and Singh, B. (2008) Interaction Analysis for Piled Rafts in Cohesive Soils. 12*th International Conference of International Association for Computer Methods and Advances in Geo-Mechanics* (*IACMAG*), Goa, 1-6 October 2008, 3289-3296.

[7] Eslami, A., Veiskarami, M. and Eslami, M.M. (2012) Study on Optimized Piled-Raft Foundations (PRF) Performance with Connected and Non-Connected Piles-Three Case Histories. *International Journal of Civil Engineering*, **10**, 100-110.

[8] Kapackci, V. and Ozkan, M.Y. (2012) A Simplified Approach Applicable to the Settlement Estimation of Piled-Raft. *ACTA Geo-Technica Slovenica*, **1**, 77-84.

[9] Nguyen, D.D.C., Jo, S.B. and Kim, D.S. (2013) Design Method of Piled-Raft Foundations under Vertical Load Considering Interaction Effects. *Computers and Geotechnics*, **47**, 16-27. http://dx.doi.org/10.1016/j.compgeo.2012.06.007

[10] Horikoshi, K. and Randolph, M.F. (1998) A Contribution to Optimum Design of Piled Rafts. *Geotechnique*, **48**, 301-317. http://dx.doi.org/10.1680/geot.1998.48.3.301

[11] Cao, X.D., Wong, M.F. and Chang, M.F. (2004) Behavior of Model Rafts Resting on Pile-Reinforced Sand. *Journal Geotechnical Engineering*, **130**, 129-138.

[12] Cooke, R.W. (1986) Piled Raft Foundations on Stiff Clays: A Contribution to Design Philosophy. *Geotechnique*, **36**, 169-203. http://dx.doi.org/10.1680/geot.1986.36.2.169

[13] Prakoso, W.A. and Kulhawy, F.H. (2001) Contribution to Piled Raft Foundation Design. *Journal Geotechnical Engineering*, **127**, 17-24.

[14] Mahmood, M.N. and Ahmed, S.Y. (2007) Nonlinear Dynamic Analysis of Framed Structures including Soil-Structure Interaction Effects. *The Arabian Journal for Science and Engineering*, **33**, 45-64.

[15] Al-Shayea, N. and Zeedan, H. (2012) A New Approach for Estimating Thickness of Mat Foundations under Certain Conditions. *The Arabian Journal for Science and Engineering*, **37**, 277-290. http://dx.doi.org/10.1007/s13369-012-0178-5

[16] PLAXIS Version 2012.02 (2012) Scientific Manual, Delft University of Technology & PLAXIS, The Netherlands, A. A. Balkema, PUBLISHERS. http://www.plaxis.nl/

[17] Ti, K.S., Huat, B.B.K., Noorzaei, J., Jaafar, M.S. and Sew, G.S. (2009) A Review of Basic Soil Constitutive Models for Geotechnical Application. *Electronic Journal Geotechnical Engineering*, **14**, 1-18.

[18] US Department of Transportation (2006) Federal Highway Administration. Publication No.: FHWA NHI-06-088.

[19] Engin, H.K. and Brinkgreve, R.B.J. (2009) Investigation of Pile Behavior Using Embedded Piles. *Proceedings of the* 17*th International Conference on Soil Mechanics and Geotechnical Engineering*. In: Hamza, M., *et al*., Eds., *Alexandria*, Millpress, Amsterdam.

[20] Lebeau, J.S. (2008) FE-Analysis of Piled and Piled Raft Foundations. Ph.D., Institute for Soil Mechanics and Foundation Engineering, Graz University of Technology, Graz.

Open Journal of Civil Engineering, 2014, 4, 386-396
Published Online December 2014 in SciRes. http://www.scirp.org/journal/ojce
http://dx.doi.org/10.4236/ojce.2014.44033

Using GIS for Time Series Analysis of the Dead Sea from Remotely Sensing Data

Maher A. El-Hallaq[1], Mohammed O. Habboub[2]

[1]Surveying and Geodesy, Civil Engineering Department, The Islamic University of Gaza, Gaza, Palestine
[2]GIS, IT Department, The University College of Applied Science, Gaza, Palestine
Email: mhallaq@iugaza.edu.ps, mhabboub@ucas.edu.ps

Received 22 September 2014; revised 20 October 2014; accepted 15 November 2014

Abstract

Developed tools of Remote Sensing and Geographic Information System are rapidly spread in recent years in order to manage natural resources and to monitor environmental changes. This research aims to study the spatial behavior of the Dead Sea through time. To achieve this aim, time series analysis has been performed to track this behavior. For this purpose, fifteen satellite imageries are collected from 1972 to 2013 in addition to 2011-ASTGTM-DEM. Then, the satellite imageries are radiometrically and atmospherically corrected. Geographic Information system and Remote Sensing techniques are used for the spatio-temporal analysis in order to detect changes in the Dead Sea area, shape, water level, and volume. The study shows that the Dead Sea shrinks by 2.9 km^2/year while the water level decreases by 0.65 m/year. Consequently, the volume changes by −0.42 km^3/year. The study has also concluded that the direction of this shrinkage is from the north, northwest and from the south direction of the northern part due to the nature of the bathymetric slopes. In contrast, no shrinkage is detected from the east direction due to the same reason since the bathymetric slope is so sharp. The use of the Dead Sea water for industrial purposes by both Israel and Jordan is one of the essential factors that affect the area of the Dead Sea. The intensive human water consumption from the Jordan and Yarmouk Rivers for other usages is another main reason of this shrinkage in the area as well.

Keywords

Dead Sea, Time Series Analysis, Remote Sensing, GIS

1. Introduction

Understanding changes in wetlands, land-uses, seashores and vegetation areas over time is essential to many as-

How to cite this paper: El-Hallaq, M.A. and Habboub, M.O. (2014) Using GIS for Time Series Analysis of the Dead Sea from Remotely Sensing Data. *Open Journal of Civil Engineering*, **4**, 386-396. http://dx.doi.org/10.4236/ojce.2014.44033

pects of engineering, geographic and planning researches. Interpretation and analysis of remotely sensed imagery require an understanding of the processes that determine the relationships between the property the sensor actually measures and the surface properties we are interested in identifying and studying [1].

Changes of the earth's surface are becoming more and more important in monitoring the local, regional and global resources. Large collection of past and present remote sensing imagery makes it possible to analyze the spatio-temporal pattern of environmental elements and impact of human activities in past decades [2]. Reference [3] defines change detection as the process of identifying differences in the state of an object or phenomenon by observing it at different time. Another definition of change detection is a technology ascertaining the changes of specific features within a certain time interval. It provides the spatial distribution of features, qualitative and quantitative information of features changes [4]. Simply, US Department of Defense defines change detection as an image enhancement technique that compares two images of the same area from different time periods. Identical picture elements are eliminated, leaving signatures that have undergone change.

Change detection algorithms analyze multiple images of the same scene—taken at different times—to identify regions of change [5]. Reference [3] classifies change detection methods into two types, namely, classification comparison and direct comparison. Reference [6] proposes a classification of three categories, including pixel-based, feature-based and object-based change detection. Reference [7] generalizes the change detection methods into seven types, namely, arithmetic operation, transformation, classification comparison, advanced models, GIS integration, visual analysis and some other methods. Reference [8] summarizes change detection methods in general terms and proposes a classification of direct difference, statistical hypothesis testing, predictive models, shading model, and background modeling and so on.

Reference [2] classifies change detection from its approaches, namely, bi-temporal change detection and temporal trajectory analysis. The former measures changes based on a "two-epoch" timescale, *i.e*. the comparison between two dates. The latter analysis the changes based on a "continuous" timescale, *i.e*. the focus of the analysis is not only on what has changed between dates, but also on the progress of the change over the period. Reference [5] classifies change detection algorithms as algorithms based on pixel amplitude, both the magnitude and phase, or on transformed pixel values. Reference [9] classifies change detection methods based on history since the algebra techniques such as image differencing or image rationing were the first techniques used to characterize changes in digital imagery then more complex techniques were developed since then with the improvement of processing capacities but also with the development of new theoretical approaches.

2. Research Problem

According to [10], the decrease of inflow into the Dead Sea is causing its shoreline to undergo very fast and to change dynamically in its area. The area of the Dead Sea surface—at the end of the 1950's—was about 1000 km^2 of which about 757 km^2 where located in the northern part and 240 km^2 in the southern part. Other studies state that the water level of the Dead Sea is dropping by an average of 0.9 m per year [11], while [12] illustrates that the Dead Sea has been experiencing a severe drop in level since 1978 with an average of 0.7 m/year.

3. The Study Area

The Dead Sea is located on 31˚30'N, 35˚30'E, WGS84 reference datum, bordering Jordan to the east, historical Palestine and the West Bank to the west. The Dead Sea is considered as the lowest point on the Earth's surface at about −400 m [13]. The east and west shores of the Dead Sea are bounded by towering fault escarpments that form part of the African-Syrian rift system. The valley slopes gently upward to the north along the Jordan River, and to the south along the Wadi Araba. Since 1978, the Dead Sea has retreated, and the sea body turned into two basins: The principal northern one that is about 308 m deep (in 1997), and the shallow southern one with the Lisan (or Lashon) Peninsula and the Lynch Straits in between, which has a sill elevation of about 400 m below the sea level [14].

4. Methodology

The following points describe the methodology followed by the researchers:

1) Satellite imageries are collected based on the criteria shown in the next section;

2) All the imageries are pre-processed and normalized by converting Digital Number (DN) to spectral radiance.

Then, atmospheric effects are removed. After that, the resulted image is converted to reflectance. Finally, the black gaps are removed if exist;
3) Supervised classification is implemented;
4) Change detection techniques are conducted to study the changes in the area, shape, water level, and volume of the Dead Sea;
5) Results and discussion.

4.1. Imagery Selection

In this research, ASTGTM-DEM for 2011 and the Landsat imageries are downloaded from USGS website. The first criterion in data collection is to download even-year imageries including the oldest and newest Landsat archived imageries, 1972 and 2013. The second criterion is to give TM imagery a priority over ETM+ and/or MSS since TM sensor life span is longer than ETM+ (approx. 20 years) so consistent data will be collected. In contrast, Landsat ETM+ imageries have the problem of the Scan Line Corrector Failure (SLC-off) which presents in black gaps. Moreover, Landsat ETM+ has the only advantage of the panchromatic band existence. However, the resolution in the multispectral bands in ETM+ is the same of TM, 30 m. The third criterion is reducing the preprocessing by downloading all imageries in the same date; the month of October is chosen to avoid clouds in the scene. In the case of the October imagery did not match the listed criteria, the closest imagery to October matching the criteria is downloaded. The fourth criterion is downloading full-bands imagery in a Geostationary Earth Orbit Tagged Image File Format (Geo TIFF). The fifth criterion is downloading free clouds scenes, at least above the water-body. Based on these criteria, fifteen imageries were downloaded as illustrated in **Table 1**. The only exception was 1975 imagery which is an odd-year imagery. It was preferred to use it because of the lack of satellite imageries from 1973 to 1983.

4.2. Image Pre-Processing and Normalization

Since digital sensors record the intensity of electromagnetic radiation from each spot viewed on the Earth's surface as a Digital Number (DN) for each spectral band, the exact range of DN that a sensor utilizes depends on its radiometric resolution. For example, a sensor such as Landsat MSS measures radiation on a 0 - 63 DN scale even as Landsat TM and ETM+ measure it on a 0 - 255 scale [15]. Therefore, normalizing image pixel values for differences in sun illumination geometry, atmospheric effects and instrument calibration is necessary specially because a time series of Landsat imageries will be used, from 1972 to 2013, and compared to each other. The radiometric correction is used to restore the image by using sensor calibration concerned with ensuring uniformity of output across the face of the image, and across time.

Using the Cosine of the Solar Zenith Angle (COST) method, the DN is transformed to reflectance as discussed above. Atmospheric correction using Dark Object Subtraction (DOS) is also included in this method [16]-[19].

4.3. Supervised Classification

In this research, supervised classification was used since the Areas of Interest (AOI) are known and clear to be

Table 1. Imagery data set used in this research.

Year	Imagery Type	Year	Imagery Type
Sep 15, 1972	MSS	Oct 04, 2000	TM
Jun 29, 1975	MSS	Oct 18, 2002	TM
Sep 06, 1984	TM	Jun 17, 2004	ETM+
Sep 28, 1986	TM	Oct 13, 2006	ETM+
Dec 30, 1988	TM	Oct 18, 2008	ETM+
Aug 30, 1990	TM	Dec 03, 2010	TM
Aug 3, 1992	TM	Jun 03, 2013	OLI
Oct 15, 1998	TM		

distinguished (the water-body). The spectral signatures of the sea body and the land around are developed and then the software assigned each pixel in the image to the type to which its signature is most similar. The steps performed for supervised classification area are as follows:

- Identifying Training sites;
- Creating spectral signatures for each of the cover types;
- Classifying the entire image pixel by pixel, according to identified signatures.

In term of evaluation how similar signatures are to each other, there are several different statistical techniques that can be used; minimum distance, maximum likelihood classifier and parallelepiped classifier. In this research the maximum likelihood method is used since Reference [20] recommends that if the training sites are well defined—as in the Dead Sea Area—the Maximum Likelihood classifier should produce the best results.

Figure 1 represents the image pre-processing and normalization while **Figure 2** represents the image supervised classification process. Finally, removing black gaps in Landsat 7 ETM+ imageries (SLC-off data-contains black gaps, DN = 0). This type of gaps has been minimized by taking two ETM+ scenes, radio metrically corrected, and then combines them for more complete coverage [21].

4.4. Change Detection Analysis

In this stage, area, shape, water level and volume change detection analysis are done using ArcGIS tools. Reference [22] [23] describes a volume estimating method of a watershed by considering it as a bowl. Its volume can be found by delineating a plane across its rim and its curved inner surface. A capping surface can be constructed by connecting a set of points located along the divide, while the inner surface is the modern topography represented by the ASTGTM-DEM. The volume is simply the difference between the cap elevation and topography.

5. Results and Analysis

5.1. The Change in Area over Time

Historical studies tell that the Dead Sea was separated into two basins in 1978, unfortunately, the earliest im-

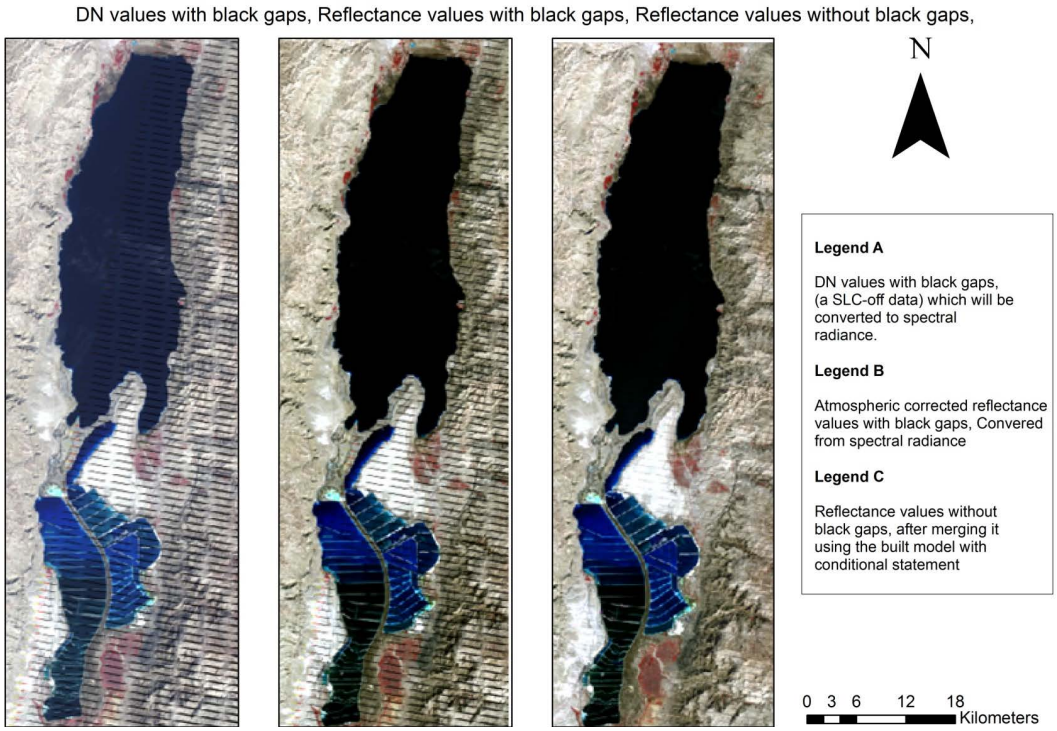

Figure 1. Image pre-processing.

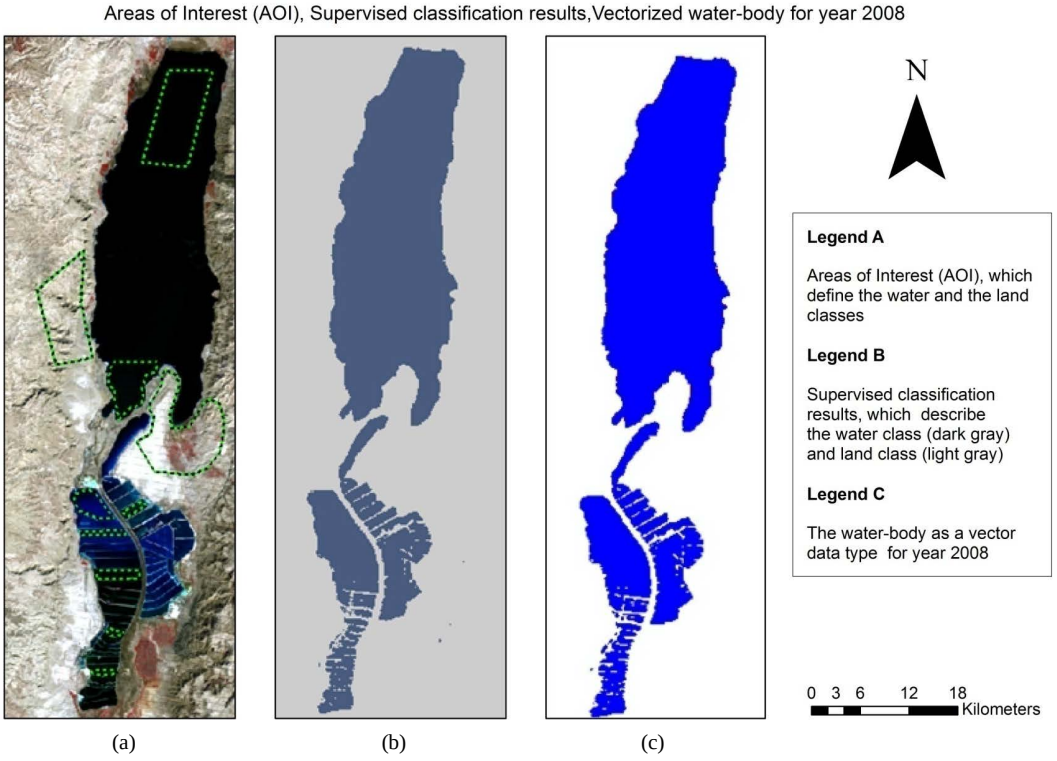

Figure 2. Supervised classification and victorization.

agery which is convenient to the data collection criteria is in 1984, so from this date, it was preferred to distinguish between the two parts with focusing on the northern part since southern part was turned to manmade basins. The general trend of the area of the northern part is decreasing as shown in **Table 2**. It illustrates that from 1984 to 2013 the area of the northern part decreases in a percentage of 12.4%.

The behavior of this trend is nonlinear and it is noticeable that in 2000, 2004 and 2010 the level increases a little bit if compared with previous and later years. This increasing has been making such a cycle, however this cycle can't be identified accurately due to the lack of imageries from 1992 to 1998. Worthy to say, that the decrease between 1984 and 1992 (8 years) reaches 7.98% while this percentage decreases to 5% from 1992 to 2013 (21 years). This variation is due the amount used in the industry and the amount of inflow released from Jordan River. Perhaps this variation is also due to the period of time consumed to use the water from the southern part in industrial use. In other words, from 1978 to 1984 is the period needed to use the southern part water and to start compensating by northern part water. In terms of defining the minimum values, it's clear that the area reached the deck in 2013, 611.23 km^2. In general, the annual average area change is −2.98 km^2.

Figure 3 represents the change in shape of the water-body from 1972 to 1984. The change is detected in the eastern part of the south portion of the Dead Sea (before separation) and the bathymetry in the southern portion of the sea began to appear more clearly due to that shrinkage in the area. As discussed so far, this research focuses on the northern part of the Dead Sea since the southern part is converted to manmade evaporation basins. The shape change of the northern part water-body over 14 years, from 1984 to 1998, in general, is detected in two major directions; from the northern west and from the south. The change in area reached 3.7% in the first year. It is worthy to say that there is no remarkable change in the eastern side of the Dead Sea; this is because the depth of the water is so deep where the fault exists. Over the period from 2000 to 2008, the shrinkage happened in the same direction even though the magnitude of the shrinkages is just 3.7% which the same percent of shrinkage between 1984 and 1986. However, the area increases in 2010 by about 2% and decreases again in 2013.

Figure 4 gives the big picture of what happened from 1972 till 2013. It is worthy to say that the behavior of the water-body over time travels from north, northwest and south with no horizontal movement from the east which is very convenient to bathymetric nature. In fact, determining the exact reasons of this shrinkage in this

Table 2. Areas of the northern & southern parts of Dead Sea.

Year	Area (km^2)	Northern part (km^2)	Southern part (km^2)
1972	986.21	986.21	
1975	926.01	926.01	
1984	968.37	697.94	270.43
1986	911.65	672.08	239.57
1988	898.30	667.70	230.60
1990	892.10	661.50	230.60
1992	904.62	642.87	261.75
1998	887.99	639.35	248.63
2000	901.82	642.04	259.78
2002	859.80	639.57	220.23
2004	865.80	637.43	228.37
2006	837.99	624.69	213.30
2008	832.89	618.34	214.55
2010	844.47	631.27	213.21
2013	812.18	611.32	200.86

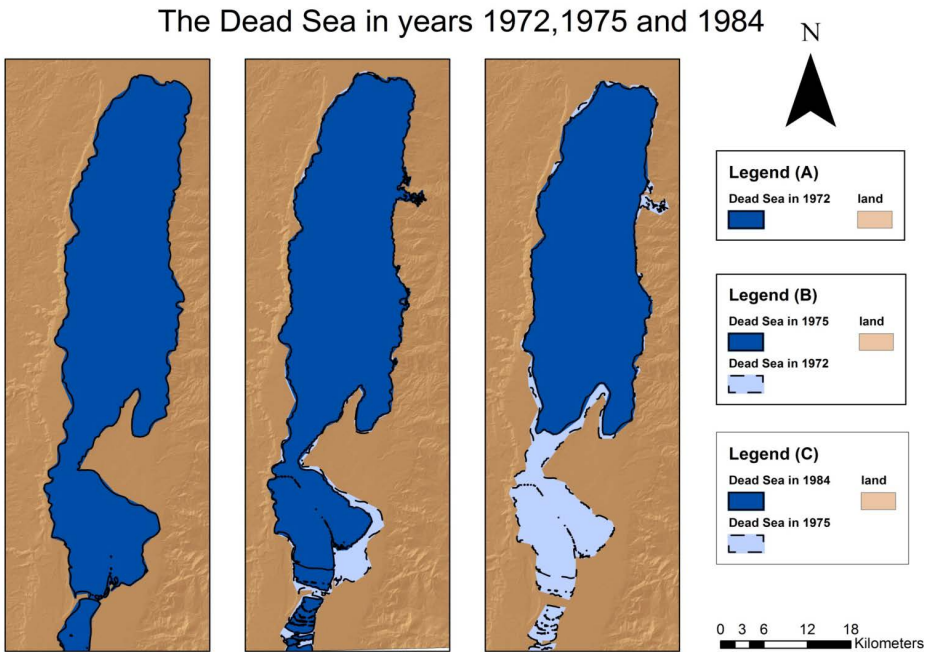

Figure 3. The Dead Sea in 1972, 1975 and 1984.

percentage is too hard and need lots of researches and a closed sea such as the Dead Sea reflects more than one factor. The use of Dead Sea water for the industry by both Israel and Jordan is one of the essential factors that affect the area of the Dead Sea. Moreover, these quantities are roughly estimated even in governmental reports. Climatic conditions play an important part of this behavior of the water body since this behavior is a result of the balance between water running into the sea from the tributary area and direct precipitation, minus water evaporation. In any case, the main reason causing this dramatic recession in the Dead Sea area is the intensive human water consumption from the Jordan and Yarmouk Rivers for other usages. Israel transfers huge quantities of

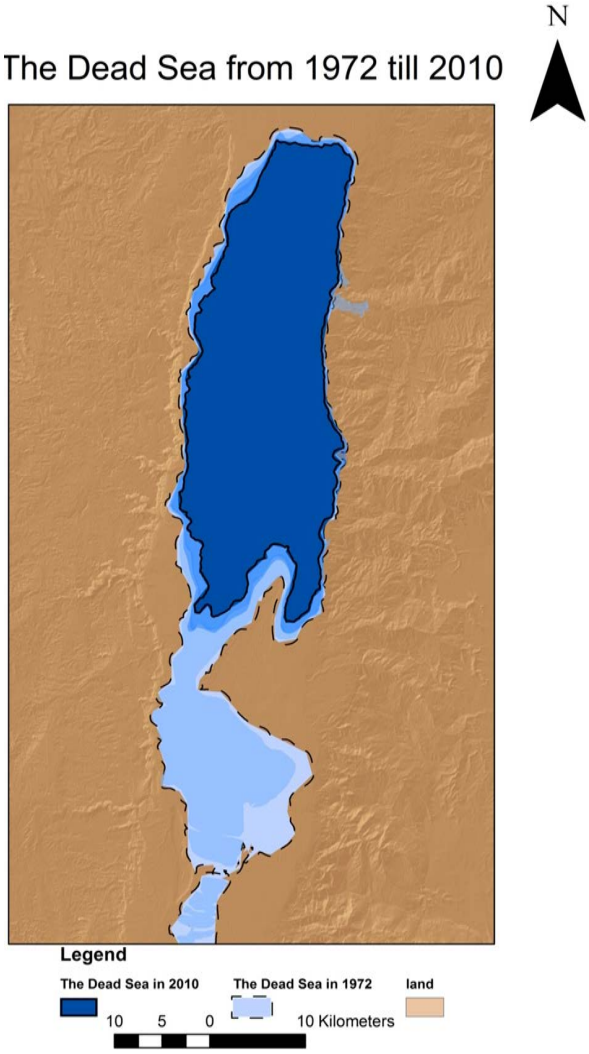

Figure 4. The Dead Sea from 1972 till 2013.

surface water through the National Water Carrier from Upper Jordan River to the Negev, where these quantities equal 420 MCM/year in addition to local consumption in the Tiberius Basin and the Huleh Valley. By studying the trend behavior of this decrease, a third degree polynomial could be derived from regression analysis as shown in **Figure 5** with $R^2 = 0.943$ which indicates that the derived equation is representative.

5.2. The Change in Water Level over Time

The derivation of the Dead Sea level is not a straight forward process even though the results are consistent with area changing as well as with previous studies, as will be discussed later. **Table 3** illustrates the average Dead Sea level derived using the satellite imageries in collaboration with ASTGTM-DEM raster data. The table shows the standard deviation representing the variance values of these derived points about the average. It is obvious that from 1984 to 2013 the water level of northern part decreased by about 25.83 m and this decrease reached more than this in 2006 and 2008. Since the behavior of this trend is nonlinear, it is noticeable that from 1975 to 1984 the Dead Sea level raised dramatically by 6.6 m, perhaps this is due to the separation as discussed in the area change detection section. However, there is no point in finding a relation between water level and area before and after the separation since the boundary conditions is totally changed. The change in water level between 1984 and 1986 could be justified by the changing in water-body area. In 2006 and 2008, the water levels reached the deck which corresponds to the change in the area in these years. In general, every year the average water

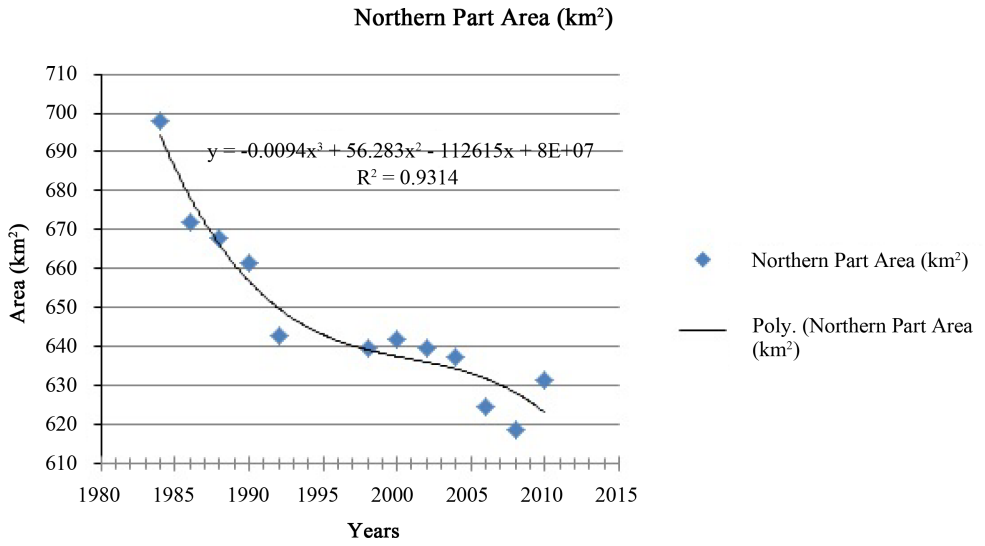

Figure 5. Regression analysis of the northern Dead Sea.

Table 3. The average Dead Sea level in meters.

Year	Area (km^2)	Standard Deviation
1972	−404.30	7.2
1975	−404.80	6
1984	−411.40	8
1986	−420.00	8
1988	−419.5	7.5
1990	−421.32	7.1
1992	−424.30	14
1998	−427.90	6
2000	−427.30	5
2002	−428.20	5.1
2004	−428.90	4.7
2006	−431.10	2.5
2008	−431.00	2.6
2010	−429.90	4.5
2013	−430.13	5.36

level change is −0.65 m. Reference [12] gets a close result in his research −0.7 m/year. By studying the trend behavior of this decrease, a third degree polynomial could be derived from regression analysis as shown in **Figure 6** with $R^2 = 0.9506$ which indicates that the derived equation is representative.

5.3. Area-Water Level Relationship

In order to find the relation between the Dead Sea area and its water level, regression analysis is used putting the areas on x-axis and corresponding water level on y-axis to get a linear equation with $R^2 = 0.9672$ which is considered a strong relation between both, see **Figure 7**. Therefore from this relation, the water level could be estimated without even ASTGTM-DEM, just by using satellite imageries.

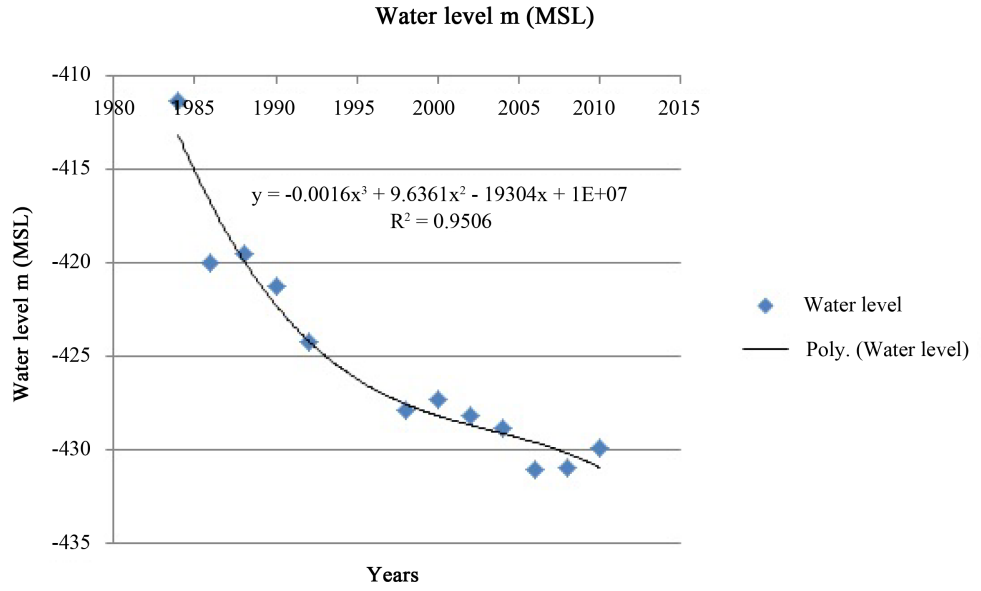

Figure 6. Water level through time.

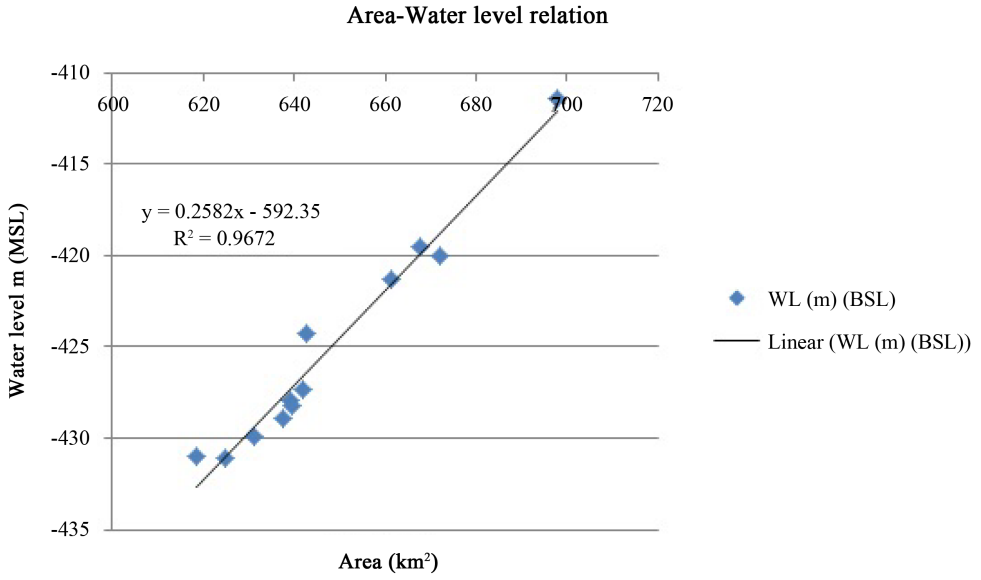

Figure 7. Area water level relation.

5.4. The Change in Volume over Time

Based on the area and water level derivations, the volume change could be calculated. **Figure 8** illustrates the volume changing from the referential year, 1984. In general, every year the average volume change is −0.42 km^3.

6. Conclusion

The area of the Dead Sea surface (at the end of the fifties) is about 1000 km^2. The altitude of the surface is around 350 m below sea level. Since 1978, the Dead Sea has retreated, and the sea body turned into two basins: the principal northern one that was about 631.27 km^2 with a water level of −430.13 m (in 2013), and the shallow southern one with the Lisan Peninsula and the Lynch Straits in between, which has a sill elevation of about 400 m below the sea level. The Dead Sea shrinks by 2.9 km^2/year while the water level decreases by 0.65 m/year. Consequently, the volume changes by −0.42 km^3/year. The direction of this shrinkage is from the north, north-

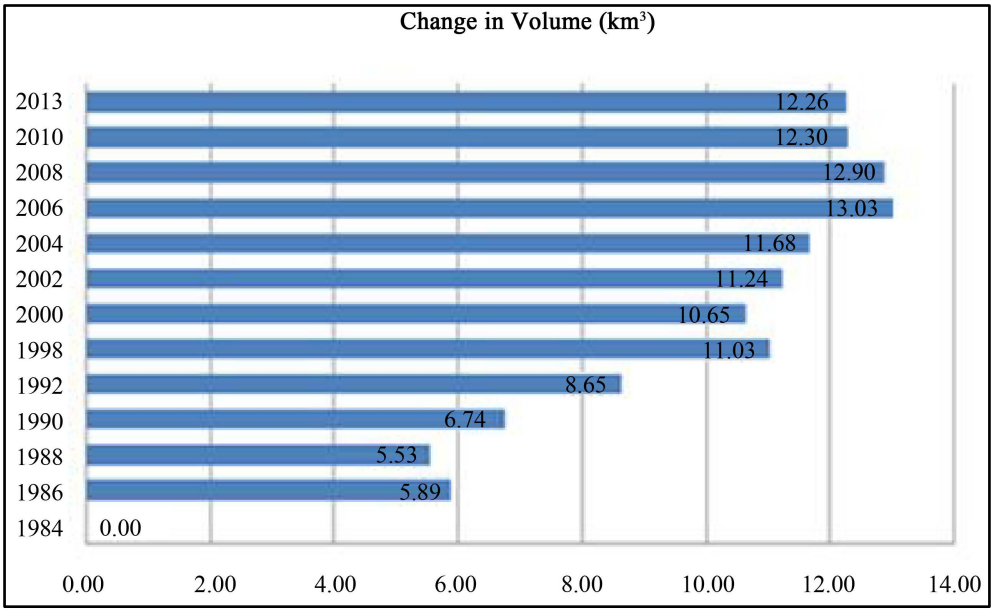

Figure 8. Volume change over time.

west and from the south direction of the northern part due to slopes of bathymetry. No shrinkage was considered from the east direction due to the same reason since the bathymetric slope is so sharp.

References

[1] Smith, R.B. (2012) Introduction to Remote Sensing. Lecture Notes.

[2] Gong, J.Y., *et al.* (2008) A Review of Multi-Temporal Remote Sensing Data Change Detection Algorithms. *The International Archives of the Photogrammetry, Remote Sensing and Spatial Information Sciences* (*Hong Kong*), **37**, 757-762.

[3] Singh, A. (1989) Digital Change Detection Techniques Using Remotely-Sensed Data. *International Journal of Remote Sensing*, **10**, 989-1003.

[4] Kandare, K. (2000) The Time Series Change Detection Methods of Remote Sensing. ISPRS SC Newsletter, Vienna.

[5] AUG Signals (2012) Change Detection. AUG SIGNALS. (Online) http://www.augsignals.com/page.php?menu=14

[6] Deer, P. (1999) Digital Change Detection Techniques. Civilian and Military Application Published in the UK. Taylar & Francis Ltd., London.

[7] Lu, D., *et al.* (2004) Change Detection Techniques. Taylor & Francis Ltd., London.

[8] Richard, J., *et al.* (2005) Image Change Detection Algorithms. A Systematic Survey. *IEEE Transactions on Image Processing*, **14**, 294-307.

[9] Théau, J. (2012) Change Detection. In: Danko, D.M. and Kresse, W., Eds., *Springer Handbook of Geographic Information*, Springer, New York, 7.

[10] Omar, M. (1996) Shrinking of Dead Sea Raises Deep Environmental Concerns. Christian Information Centre, Jerusalem.

[11] Al-Zubaidy, R., Khaled, M. and Shambour, Y. (2011) Prediction of the Dead Sea Water Level Using Neural Networks. *4th International Symposium on Innovation in Information & Communication Technology*, Amman, 29 November-1 December 2011, 147-154.

[12] Abu Ghazleh, S., *et al.* (2010) Rapidly Shrinking Dead Sea Urgently Needs Infusion of 0.9 km 3/a from Planned Red-Sea Channel: Implication for Renewable Energy and Sustainable Development. **4**, 1995-6665.

[13] Morin, E., *et al.* (2009) Flash Flood Prediction in the Dead Sea Region Utilizing Radar Rainfall Data. *Journal of Dead-Sea and Arava Research*, **1**, 1066-1076.

[14] US Geological Survey (1998) Overview of Middle East Water Resources: Water Resources of Palestinian, Jordanian and Israeli Interest. Water Data Bank Project, Executive Action Team, New York, 41.

[15] Green, E.P., *et al.* (2000) Remote Sensing Handbook for Tropical Coastal Management. UNESCO, Paris.

[16] Chavez, Jr. (1996) Image-Based Atmospheric Corrections—Revisited and Improved. *Photogrammetric Engineering and Remote Sensing*, **62**, 1025-1036.

[17] Wen, W. (2008) Wetland Change Prediction Using Markov Cellular Automata Model in Lore Lindu National Park Central Sulawesi Province. Master Thesis, BOGOR Agricultural University, Indonesia.

[18] Ramsey, R.D. (2013) Image Standardization. RS/GIS Laboratory. (Online) http://earth.gis.usu.edu/imagestd/

[19] Irons, J. (2013) Chapter 11. Landsat Hand Book. NASA. (Online) http://landsathandbook.gsfc.nasa.gov/data_prod/prog_sect11_3.html

[20] Chinea. J.D. (2013) Supervised Classification. Universidad de Puerto Rico, Recinto Universitario de Mayagüez. (Online) http://www.uprm.edu/biology/profs/chinea/gis/lectesc/tut4_3.pdf

[21] USGS (2008) Landsat Update. Landsat Update.

[22] Akin, E. and Cooley, S. (2013) Lake Basin Volume. GIS 4 Geomorphology. (Online) http://gis4geomorphology.com/lake-basin-volume/#more-1239

[23] Cooley, S. (2013) Minimum Eroded Volume. GIS 4 Geomorphology. (Online) http://gis4geomorphology.com/calculate-basin-volume/#more-8

Open Journal of Civil Engineering, 2014, 4, 397-405
Published Online December 2014 in SciRes. http://www.scirp.org/journal/ojce
http://dx.doi.org/10.4236/ojce.2014.44034

Present Assessment of Public Traffic System Based on GIS in Kitakyushu

Kazuyuki Watari[1,2], Weijun Gao[1]

[1]Faculty of Environmental Engineering, The University of Kitakyushu, Kitakyushu, Japan
[2]Geo Cluster Co. LTD, Japan
Email: gaoweijun@me.com

Received 18 September 2014; revised 10 October 2014; accepted 2 November 2014

Abstract

With increasing of serious environment problems and the coming of the aging society, new traffic systems should be urgently rebuilt. It is necessary to evaluate the traffic service level by utilizing new technique and tool. This paper takes Kitakyushu city as case study to carry out an evaluation of urban traffic system. The concept of accessibility and mobility is used to evaluate the present condition of existing public traffic system based on GIS technology, and then establishment of new route is discussed according to the evaluation results. Additionally, this paper established GIS database and illustrated the relationship between the public traffic and population density. The regions without enough existing traffic were identified. Moreover, the essential terms and considerations were put forward to simulate a new route of public traffic line.

Keywords

Urban Public Traffic, GIS Technology, Kitakyushu, Japan

1. Introduction

Advanced urban traffic system needs to be adjusted due to urgent demand of national/city's government. Therefore, it is important for urban traffic management department to put forward an improvement measure. Meanwhile, with increasing of serious environment problems (energy circumstances and urban traffic) and the coming of the aging society, new traffic systems should be urgently rebuilt. Moreover, the urban traffic plan needs to be further examined. So, it is necessary to evaluate the traffic service level by utilizing new technique and tool.

There are many researches with the traffic system. Thong [1], developed a GIS database with consideration of efficient data input and retrieval process in a way that is most useful to transportation planners for network travel demand projection and evaluation purposes. Arampatzis [2] presented a decision support system (DSS) inte-

How to cite this paper: Watari, K. and Gao, W.J. (2014) Present Assessment of Public Traffic System Based on GIS in Kitakyushu. *Open Journal of Civil Engineering*, **4**, 397-405. http://dx.doi.org/10.4236/ojce.2014.44034

grated in a geographical information system (GIS) for the analysis and evaluation of different transport policies. Suzanne Mavoa [3] calculated a public transit and walking accessibility index for Auckland, New Zealand. SUN [4] investigated the inherent principles of spatial-temporal evolution of traffic congestion based on Shenzhen floating car data (FCD) and geo-simulation platform. Charlotte Wahl [5] studied public participation in Swedish municipal traffic planning with the focus onto what extent and how municipalities and consultants interact with participants in traffic-planning processes. Lee [6] proposed a wiki-like collaborative real-time traffic information collection, fusion and sharing framework, which includes user-centric traffic event reacting mechanism, and automatic agent-centric traffic information aggregating scheme.

This paper takes Kitakyushu city as a case study to carry out an evaluation of urban traffic system. The concept of accessibility and mobility is used to evaluate the present condition of existing public traffic system based on GIS spatial technology, and then establishment of new urban traffic route is discussed according to the evaluation results. Then, the paper establishes the region item and discusses new routes and their profit.

2. Study Area

Kitakyushu (33˚52'N, 130˚49'E) locates in Fukuoka prefecture, Kyushu, Japan. Its total area is 486.81 km^2, population is 976,800 in 2013 [7], and population density is 2040.80 per km^2 (**Figure 1**). In the view of topographical features, topographic relief in Kitakyushu is bigger, sea extent elevation reaches to above 900 meters, mid-mountain and low-mountain accounting for 35% of total region area is main topographic types. Kitakyushu borders on the main islands of Japan across Kanmon Strait and is adjacent to several other Asian countries, and particularly it is conveniently located at the straight line connecting two largest cities, Tokyo in Japan and Shanghai in China. Meanwhile, the eastern and northern Kitakyushu has long coast line. It is one of the most active areas in Kitakyushu and enjoys the fastest economic development. In the 2013, GDP is JPY 3,523,636 million, travel people is 1220 ten thousand.

3. Investigation of Public Traffic Service

Firstly, this study extracts blank and inconvenient areas of public traffic service in Kitakyushu as research objectives on the basis of GIS database.

Secondly, operating route and attained profit in these areas are evaluated.

Finally, feasibility of the new public traffic system is discussed according to the evaluation results.

Case analysis flows based on GIS technology are seen in **Figure 2**. The six cases are seen in **Figure 3**.

The cases area assumed as follow to evaluate the traffic blank area:

The inconvenient where operation new route to the bus stop is lower than 1 are extracted. The street where one-way lines are lower than 16 from am 6 to pm 10 is considered. Seen from **Figure 4**, the traffic blank area is outside the buffer, and the traffic inconvenient area is inside the buffer. The repeated points of each data are deleted by manual operation. The center of each terminal in the six cases is set the center of a circle, a distance is taken as radius, the resulting circle is considered to blank and inconvenient areas. The inconvenient area in-

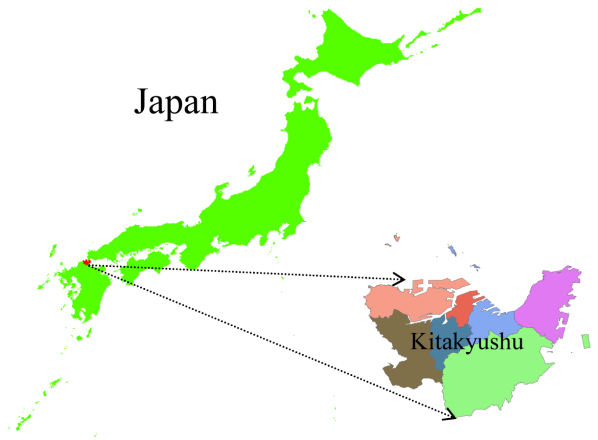

Figure 1. Study area.

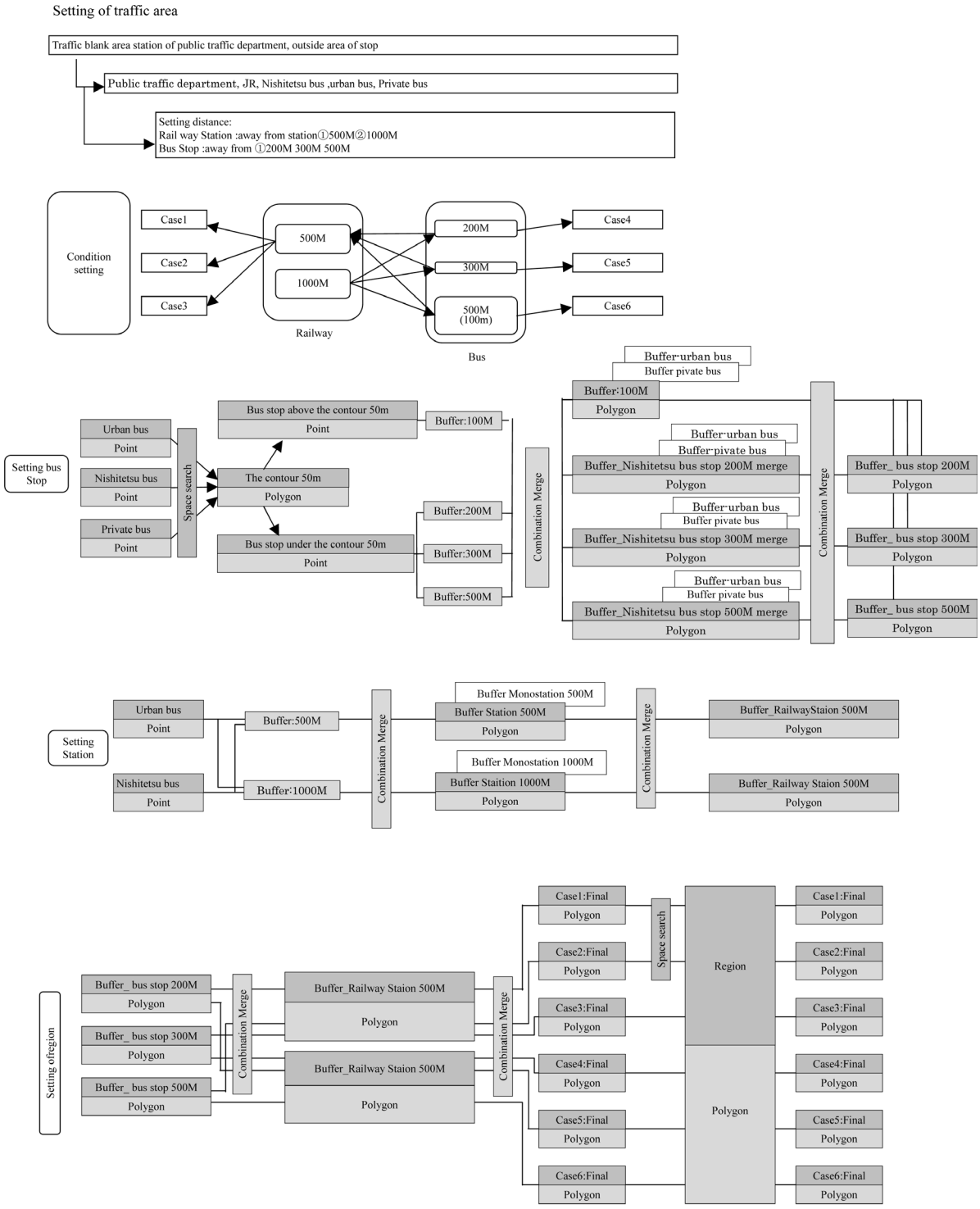

Figure 2. Case analysis flow based on GIS technology. ① 500 m away from railway and 200 m away from bus stop; ② 500 m away from railway and 300 m away from bus stop; ③ 500 m away from railway and 500 m away from bus stop; ④ 1000 m away from railway and 200 m away from bus stop; ⑤ 1000 m away from railway and 300 m away from bus stop; ⑥ 1000 m away from railway and 500 m away from bus stop.

creases according to the extraction data (500, 300 and 200 m away from bus stop). According to investigation results, population without access to traffic will increase with the distance away from bus stop.

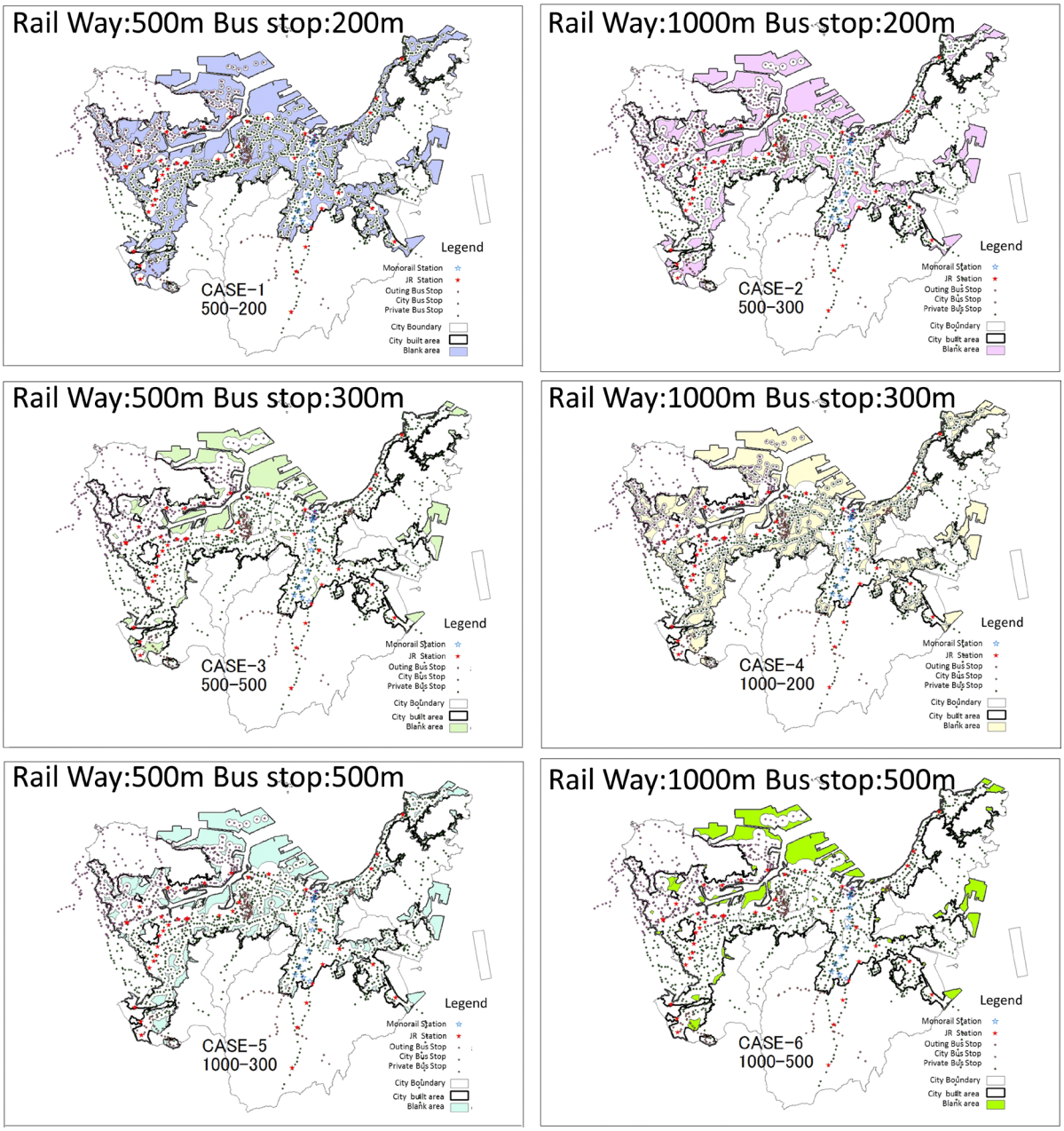

Figure 3. Case analysis.

4. Establishment of Region Item

According to the extracted elementary school, this paper selects some school areas where there are more than 2000 people and more than 500 elders as research objectives, and then neighborhoods with 1 km radius around the research objective are considered as the same areas to carry out case studies. The case studies contain CASE2 and CASE5. The number of the extraction was as follows: CASE2: 26 districts (**Figure 5**); CASE5: 11 districts (**Figure 6**). In order to discuss new route setting of target district, the following conditions need to be proposed. In CASE 2, inconvenient area is extracted to take as research objective. In the adjacent circumstances, if an area is longed to other elementary schools, but the area is situated in the 1 kilometer radius around the research objective, we think it as the same region. The requested area of government is taken as a research object.

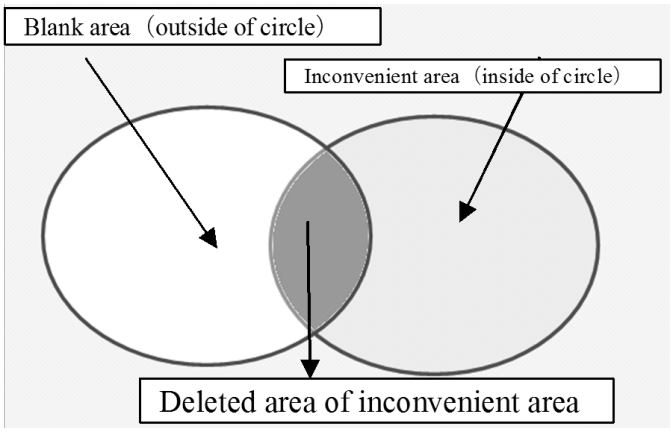

Figure 4. Blank area and inconvenient area.

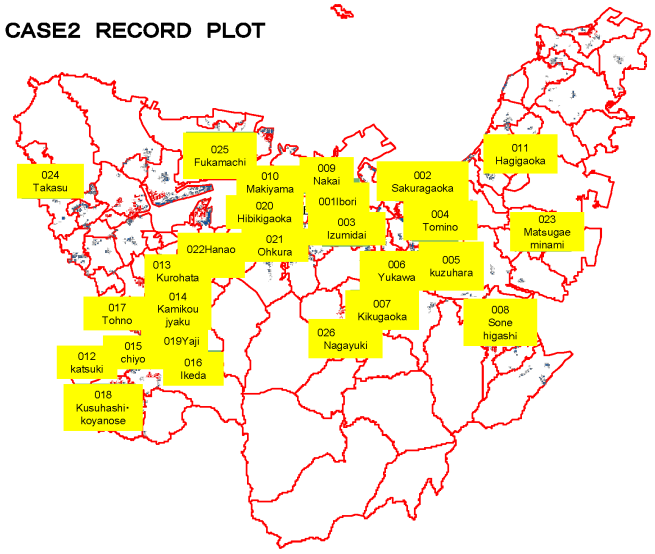

Figure 5. CASE2 26 districts.

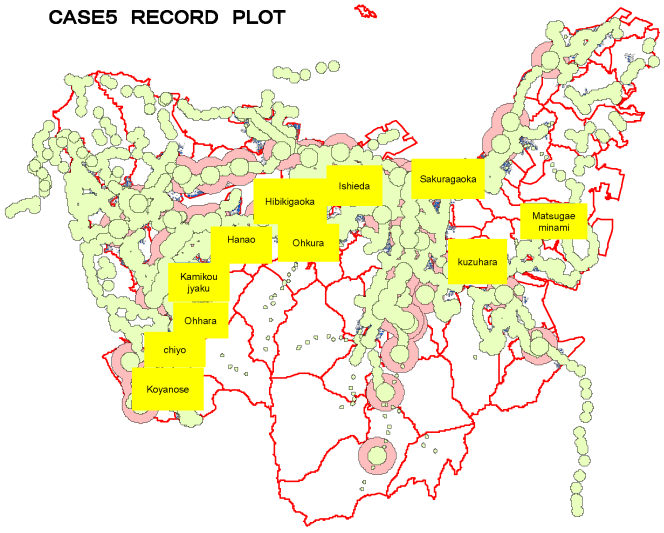

Figure 6. CASE5 11 districts.

5. Result and Discussion

5.1. Discussion of New Route

At present, bus users are inclined to decreasing. There are two reasons, on the one hand, traffic jam of the highway becomes more and more serious because of the concentration of the increasing cars; on the other hand, timing system of bus is bad. Meanwhile, there are many residents in the suburbs area. However, development balance of public bus is not adjusted, which result in that buses do not pass through the suburbs area. Until now, there aren't bus routes in the many places. Therefore, it is necessary to set up the community bus routes in the inconvenient area of public traffic. The system with short distance, small quantity, frequent transportation and the circulation type should be firstly discussed to offer comfortable mobility for every people in the narrow roads of the public transport blank (inconvenient) area (**Figure 7**).

It is easy to go to the urban center by operating the route linking with busy streets, the main facilities and the traffic blank zones. In addition, circulation bus of the one way will be operated; it only takes 30 - 60 minutes to run a round. So the number of bus should be increased. Since the larger route bus doesn't pass the narrow road of the residential area, if minibus is applied, the bus stops become nearer.

If the mobility of the public blank (inconvenience) area is improved, communication of local people will be activated; community will be brought up; increasing of elder's outgoing opportunities will be promoted; activation of the social participation will be supported. It is anticipated to improve the access to central town and to activate the people's communication. Importantly, the system will help the urban traffic away from seriously

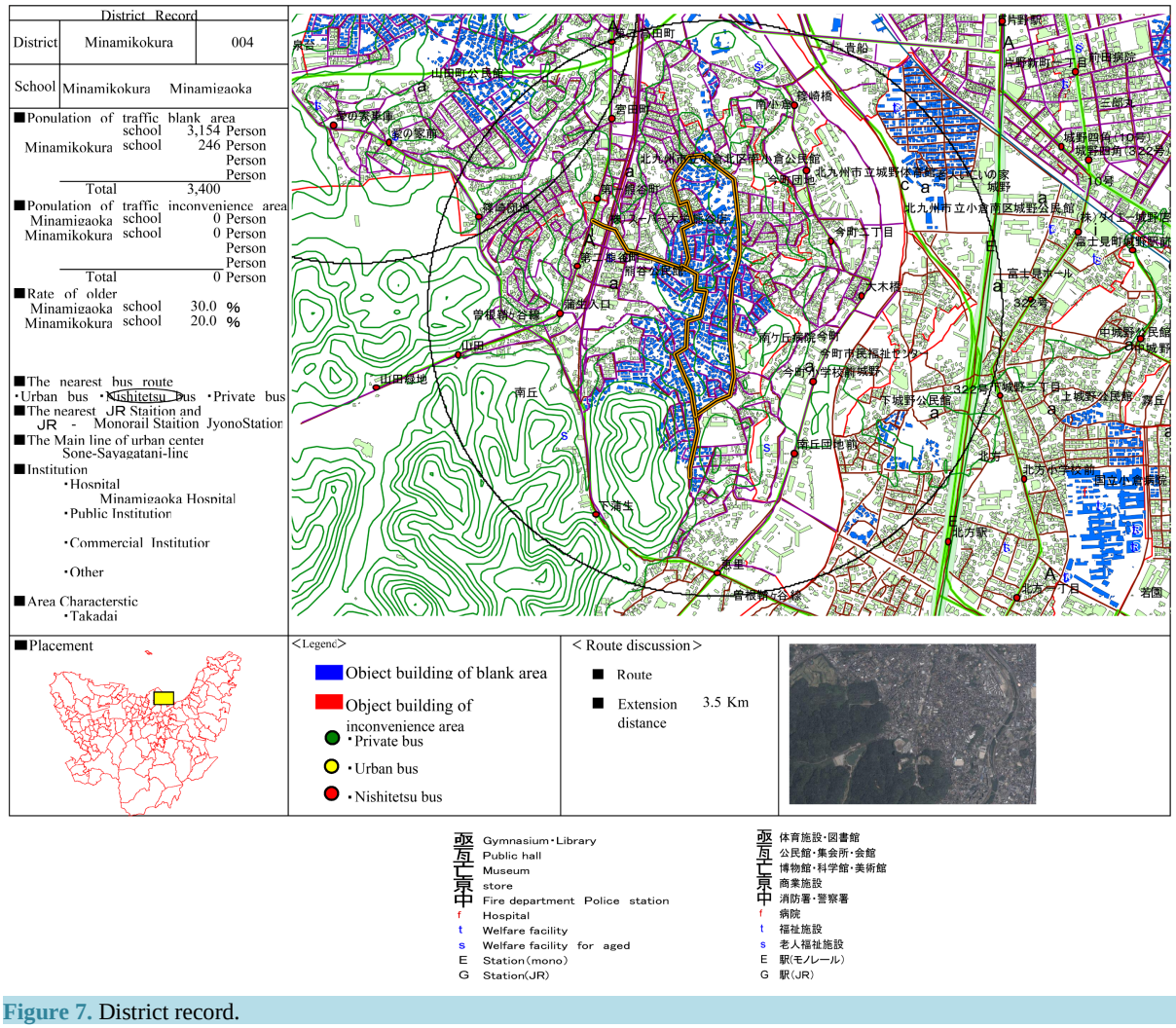

Figure 7. District record.

depending on the private cars.

5.2. Discussion of Profit

There are many irregular areas and ramps in the suburb; on the other hand, streets in the resident area are adjusted in the process of management. The jamming in some parts of arterial streets will make it difficult for bus to run on the dot. Even in the central area, landform and street structure still limit the convenience of traffic. Due to the willing of traveling, the amount of traveling elders has been increasing. Among the traffic ways, walking and taking bus occupy a large percent, especially, bus is usually applied in everyday life. However, some complaints are arisen against the problems when taking bus, for example, climbing up and down, receiving the message, distance to the station, bus intermediate, noisy and services.

The target people of the system are those elders who reside in the traffic-lagging areas. They use the bus in many occasions of everyday life, such as, shopping, going to hospital, and so on. The system covers the traffic-lagging areas, areas with high elder percent and central town. The route will be regulated to single-direction circulation through the narrow streets in the period of 30 - 60 minutes. The system will provide the people with amenity and mobility; moreover, some valuable suggestions will be zealously discussed and be introduced into the system. The distance of two bus stations is set to 200 m; additionally, waiting places are constructed under the considerations of accumulating snow. Especially, the existing establishment will be neatly made the best use.

Here about the calculation of the profit.

We assumed enterprise (investment) cost as $C_{\text{enterprise}}$ and the value of enterprise cost based on the data from the bus company.

We estimated the number of users P for the target area according to the population and age by

P = population of area × a_p (person)

Here, a_p = the use rate of people at the kind of age (based on the data from the bus company).

The income of the bus area C_{gain} can be predicted by

$$C_{\text{gain}} = sum\ \left(g \times P\right)\left(JPY\right)$$

Here g is the income for one bus line including financial aid and advertisement support (*JPY*/Person).

If the income of the bus area C_{gain} is larger than the $C_{\text{enterprise}}$, the project gets the profit and we say this line is "OK", otherwise we say the line is "OUT".

All the simulation was calculated in the GIS platform.

5.3. Discussion of New Traffic Service

Service time: 5 days one week, 8 hours one day, 250 days one year. Eight percent of elders (older than 65 ages) of target area will use the new traffic service, according to the data statistic of Bus Company.

Charge of standard service: 23,400 Yen; Charge of subvention: 20,500 Yen; Charge of advertisement sponsorship: 20,100 - 16,500 Yen. According to the assumed conditions, profit of the new route in 2015 is simulated based on GIS technology (**Table 1**). "Out" means no profit under the designated condition. Therefore, in Iwai-machi area, there is no profit even with financial aid or advertisement support due to the lack of population. Profit of the 10th route under the assumed conditions is estimated by using amount of 2nd route by the 2015 will be increased because of increasing of elder's percent, which indicates that 12th route will obtain more profit. If charge of other routes can be sponsored by the advertisement agencies, possibility of getting profit will be ensured (**Figure 7**).

6. Conclusions

In this paper, we try to present a method to verify the traffic blank and inconvenient area in Kitakyushu city.

The six cases were selected to evaluate the traffic system. Based on the data of registered permanent residence, timetables of railway and road, urban management information of Kitakyushu, this study established the GIS database and illustrated the relationship between the public traffic departments and population divisions. Additionally, the regions without enough existing traffic establishments were identified. Moreover, the essential terms and considerations were put forward to simulate the verifying methods for new routes of public traffic

Table 1. Profit of new route in 2015.

No.	2015 Element school name	Running hour 8/week 5 days	Standard case	Financial aid case	Advertisement support case									
		250 days			100,000	200,000	300,000	400,000	500,000	600,000	700,000	800,000	900,000	1,000,000
		200JPY	23,400	20,500	20,100	19,700	19,300	18,900	18,500	18,100	17,700	17,300	16,900	16,500
1	Ibori	52,614	OK	OK	OK	OK	OK	OK	OK	OK	OK	OK	OK	OK
2	Nakai	27,408	OK	OK	OK	OK	OK	OK	OK	OK	OK	OK	OK	OK
3	Izumidai	27,958	OK	OK	OK	OK	OK	OK	OK	OK	OK	OK	OK	OK
4	Minamigoka	20,551	OUT	OK	OK	OK	OK	OK	OK	OK	OK	OK	OK	OK
5	Tomino	19,133	OUT	OUT	OUT	OUT	OUT	OK	OK	OK	OK	OK	OK	OK
6	Kuzuhara	31,365	OK	OK	OK	OK	OK	OK	OK	OK	OK	OK	OK	OK
7	Yukawa	24,528	OK	OK	OK	OK	OK	OK	OK	OK	OK	OK	OK	OK
8	Kikugaoka	30,602	OK	OK	OK	OK	OK	OK	OK	OK	OK	OK	OK	OK
9	Sone	34,461	OK	OK	OK	OK	OK	OK	OK	OK	OK	OK	OK	OK
10	Makiyama	56,668	OK	OK	OK	OK	OK	OK	OK	OK	OK	OK	OK	OK
11	Ookura	29,034	OK	OK	OK	OK	OK	OK	OK	OK	OK	OK	OK	OK
12	Iwaimachi	15,621	OUT	OUT	OUT	OUT	OUT	OUT	OUT	OUT	OUT	OUT	OUT	OUT
13	Kurohata	21,750	OUT	OK	OK	OK	OK	OK	OK	OK	OK	OK	OK	OK
14	Kamikojyaku	48,012	OK	OK	OK	OK	OK	OK	OK	OK	OK	OK	OK	OK
15	Chiyo	43,034	OK	OK	OK	OK	OK	OK	OK	OK	OK	OK	OK	OK
16	Hanao	24,806	OK	OK	OK	OK	OK	OK	OK	OK	OK	OK	OK	OK
17	Touno	17,705	OUT	OUT	OUT	OUT	OUT	OUT	OUT	OUT	OK	OK	OK	OK
18	Sarakura	4,660	OUT	OUT	OUT	OUT	OUT	OUT	OUT	OUT	OUT	OUT	OUT	OUT
19	Katsuki	15,467	OUT	OUT	OUT	OUT	OUT	OUT	OUT	OUT	OUT	OUT	OUT	OUT
20	Matsugaoka	8522	OUT	OUT	OUT	OUT	OUT	OUT	OUT	OUT	OUT	OUT	OUT	OUT
21	Hagigaoka	18,442	OUT	OUT	OUT	OUT	OUT	OUT	OUT	OK	OK	OK	OK	OK
22	Fukamachi	19,804	OUT	OUT	OUT	OK	OK	OK	OK	OK	OK	OK	OK	OK

departments. However, recently price of fuels has remarkably increased, which led to the considerations again and again on arranging the outlay. We selected 22 areas to predict the profit by introducing a new bus line and gave a judgment to establish a new bus line.

In the future, we will add some GIS databases concerning about the buildings and circulating destinations, and will investigate the relations among these data; meanwhile, it is necessary to emphasize the influencing factors in the research method of new routes.

Acknowledgements

This research was based on data from the project of Kitakyushu Transportation Bureau. We would like to express our thanks to Kitakyushu city.

References

[1] Thong, C.M. and Wong, W.G. (1997) Using GIS to Design a Traffic Information Database for Urban Transport Planning. *Computers, Environment and Urban Systems*, **21**, 425-443. http://dx.doi.org/10.1016/S0198-9715(98)00003-9

[2] Arampatzis, G., Kiranoudis, C.T., Scaloubacas, P. and Assimacopoulos, D. (2004) A GIS-Based Decision Support System for Planning Urban Transportation Policies. *European Journal of Operational Research*, **152**, 465-475.

[3] Mavoa, S., Witten, K., McCreanor, T. and O'Sullivan, D. (2012) GIS Based Destination Accessibility via Public Transit and Walking in Auckland, New Zealand. *Journal of Transport Geography*, **20**, 15-22. http://dx.doi.org/10.1016/j.jtrangeo.2011.10.001

[4] Sun, J. (Daniel), Liu, Q. and Peng, Z.R. (2011) Research and Analysis on Causality and Spatial-Temporal Evolution of Urban Traffic Congestions—A Case Study on Shenzhen of China. *Journal of Transportation Systems Engineering and Information Technology*, **11**, 86-93.

[5] Wahl, C. (2013) Swedish Municipalities and Public Participation in the Traffic Planning Process—Where Do We Stand? *Transportation Research Part A*: *Policy and Practice*, **50**, 105-112. http://dx.doi.org/10.1016/j.tra.2013.01.012

[6] Lee, W.-H., Tseng, S.-S. and Shieh, W.-Y. (2010) Collaborative Real-Time Traffic Information Generation and Sharing Framework for the Intelligent Transportation System. *Information Sciences*, **180**, 62-70. http://dx.doi.org/10.1016/j.ins.2009.09.004

[7] Kitakyushu City (2014) Population. http://www.city.kitakyushu.lg.jp/soumu/file_0373.html

Call for Papers

Open Journal of Civil Engineering

ISSN Print: 2164-3164 ISSN Online: 2164-3172
http://www.scirp.org/journal/ojce/

Open Journal of Civil Engineering (OJCE) is an international journal dedicated to the latest advancement of civil engineering. The goal of this journal is to provide a platform for scientists and academicians all over the world to promote, share, and discuss various new issues and developments in different areas of civil engineering.

Editor-in-Chief

Dr. Hwai-Chung Wu — Wayne State University, USA

Editorial Board

Prof. Alireza Afshari
Dr. Ayman Batisha
Prof. Fabio Bisegna
Prof. Christopher Chao
Dr. Carlos Chastre
Dr. Cristina Gentilini
Dr. Raja Rizwan Hussain
Prof. Jian Kang
Dr. Vojko Kilar
Prof. Kiyoshi Kobayashi
Dr. Triantafyllos Makarios
Prof. George C. Manos
Prof. Ali M. Memari
Prof. Low Sui Pheng
Prof. Miroslav Premrov
Prof. Nicola Pugno
Dr. Gian A. Rassati
Dr. Rehan Sadiq
Prof. Evangelos J. Sapountzakis
Prof. Mehdi Setareh
Prof. Wen-Pei Sung
Prof. Chong-Shien Tsai
Prof. Francesco Ubertini
Dr. Roberto Valentino
Dr. Heng Wei
Dr. I-Tung Yang
Prof. Ka-Veng Yuen
Prof. Jun Zhang

Subject Coverage

All manuscripts must be prepared in English, and are subject to a rigorous and fair peer-review process. Accepted papers will immediately appear online followed by printed hard copy. The journal publishes original papers including but not limited to the following fields:

- Assemblage and System
- Behavior of Structures
- Behavior of Structures under Seismic Loads
- Building and Environmental Acoustics
- Building Climate Systems
- Building Energy
- Civil and Environmental Engineering
- Coastal Engineering
- Composite Materials
- Concrete Structures
- Construction Economics
- Construction Engineering
- Design and Performance of Green Building
- Design Optimization of Structures
- Earthquake Engineering
- Energy Efficient Building Technology
- Energy Saving Building Materials
- Evaluation of Building Envelope Systems under Structural and Environmental Loads
- Evaluation of Glazing Systems for Energy Performance
- Fire Engineering
- Foundations Dynamics
- Geotechnical Engineering
- Health Monitoring and Life Prediction of Structures
- High Performance Concrete
- Hydraulic Engineering
- Life Cycle Engineering
- Materials and Durability
- Materials Engineering
- Mechanics and Materials Aspects of Advanced Construction Materials
- Municipal or Urban Engineering
- Nondestructive Testing and Evaluation
- Numerical Modelling of Structures
- Optimal Design of Structures
- Properties and Mechanics of Concrete
- Residential, Commercial, Industrial and Public Works
- Seismic Evaluation of Building Nonstructural Components
- Simulation Optimization and Risk Management
- Soil-Structure Interaction
- Structural Engineering
- Structural Evaluation of Panelized and Masonry Wall Systems
- Structural Reliability Analysis
- Surveying
- Sustainable Structures
- Transportation Engineering
- Ventilation and Indoor Air Quality
- Water Supply and Drainage

We are also interested in: 1) Short Reports—2-5 page papers where an author can either present an idea with theoretical background but has not yet completed the research needed for a complete paper or preliminary data; 2) Book Reviews—Comments and critiques.

Notes for Intending Authors

Submitted papers should not have been previously published nor be currently under consideration for publication elsewhere. Paper submission will be handled electronically through the website. All papers are refereed through a peer review process. For more details about the submissions, please access the website.

Website and E-Mail

http://www.scirp.org/journal/ojce **E-mail: ojce@scirp.org**

What is SCIRP?

Scientific Research Publishing (SCIRP) is one of the largest Open Access journal publishers. It is currently publishing more than 200 open access, online, peer-reviewed journals covering a wide range of academic disciplines. SCIRP serves the worldwide academic communities and contributes to the progress and application of science with its publication.

What is Open Access?

All original research papers published by SCIRP are made freely and permanently accessible online immediately upon publication. To be able to provide open access journals, SCIRP defrays operation costs from authors and subscription charges only for its printed version. Open access publishing allows an immediate, worldwide, barrier-free, open access to the full text of research papers, which is in the best interests of the scientific community.

- High visibility for maximum global exposure with open access publishing model
- Rigorous peer review of research papers
- Prompt faster publication with less cost
- Guaranteed targeted, multidisciplinary audience

Scientific Research

Website: http://www.scirp.org

Subscription: sub@scirp.org

Advertisement: service@scirp.org